STATUS OF THESIS

Title of thesis

Modeling and Simulation of CO_2 and H_2S Absorption from Methane using Aqueous Methyldiethanolamine Solution

I, **FARHATAMATUL HALIM**
hereby allow my thesis to be placed at the Information Resource Center (IRC) of Universiti Teknologi PETRONAS (UTP) with the following conditions:

1. The thesis becomes the property of UTP
2. The IRC of UTP may make copies of the thesis for academic purposes only
3. This thesis classified as

    ☐ Confidential

    ✓ Non-confidential

If the thesis is confidential, please state the reason:
_____
_____
_____

The contents of the thesis will remain confidential for _____ years.
Remarks on disclosure:
_____

<div align="right">Endorsed by</div>

_____   _____
    Signature of author   Signature of Supervisor
                          AP Dr Mohamed Ibrahim Abdul Muthalib

Taman Sari Atas
Gg Karya Bhakti No 33/59   Department of Chemical Engineering
Bandung, Indonesia   Universiti Teknologi PETRONAS
                          Bandar Seri Iskandar, Perak Malaysia

Date :   Date :

APPROVAL

<div style="border: 1px solid black;">

UNIVERSITI TEKNOLOGI PETRONAS

Approval by Supervisor

The Undersigned certify that they have read, and recommend to The Postgraduate Studies Programme for acceptance, a thesis entitled "**Modeling and Simulation of CO_2 and H_2S Absorption from Methane using Aqueous Methyldiethanolamine Solution**" submitted by **Farhatamatul Halim** for the fulfilment of the requirements for the degree of Master of Science in Chemical Engineering.

_____
Date

</div>

Signature   : _____

Main supervisor   : _____

Date   : _____

UNIVERSITI TEKNOLOGI PETRONAS

Modeling and Simulation of CO_2 and H_2S Absorption from Methane using

Aqueous Methyldiethanolamine Solution

By

Farhatamatul Halim

A THESIS

SUBMITTED TO THE POSTGRADUATE STUDIES PROGRAMME

AS A REQUIREMENT FOR THE DEGREE OF MASTER OF SCIENCE

IN CHEMICAL ENGINEERING PROGRAMME

BANDAR SERI ISKANDAR

PERAK

February 2010

DECLARATION

I hereby declare that the thesis is based on my original work except for quotations and citations which have been duly acknowledged. I also declare that it has not been previously or concurrently submitted for any other degree at UTP or other institutions.

Signature   : _____

Name   : <u>FARHATAMATUL HALIM</u>

Date   : _____

ACKNOWLEDGMENT

First and foremost, all praises thanks to Allah, the almighty God, for giving me the knowledge, the strength, and path to finish this thesis.

I am most grateful to my supervisor, AP Dr Mohamed Ibrahim Abdul Muthalib, for giving me an opportunity to pursue a master degree. Thank you for the patience and guidance during my study. Thank you for the motivation to keep me strong and enthusiastic to finish the work finely.

I would like express my gratitude to Dr Murni Melati, Dr Suhaimi Mahadzir, and En. Shahrul Azman Zainal Abidin for helping me evaluate the thesis.

Special thanks also to all my postgraduate fellows and Bandar U fellows for their support.

The most importantly, thank you for my family for their support. To my husband and my son, thank you for giving me strength and conviction during the study.

- For Kenzie Satria -

ABSTRACT

The acid gases (CO_2 and H_2S) removal process is very important in natural gas processing. The acid gases absorption process using methyldiethanolamine (MDEA) solvent has found increased application. Evaluation on the acid gases absorption process using MDEA solvent can be done using modeling and simulation on the system. Several attempts have been made on the modeling and simulation of the phase equilibrium and also the absorption column system. Some limitations were found in the attempts.

The aim of this study is to construct a rigorous simulation procedure of the acid gases absorption from methane using methyldiethanolamine solvent. The simulation of the contactor column is based on equilibrium modeling. The methane solubility that was not considered in the previous studies is accounted in this simulation. Part of the study is the development of phase equilibrium model to determine the solubility of acid gases in MDEA solvent. The ElecGC model is used for calculation of the activity coefficient of the components in the liquid phase. The non-ideality of the components in the gas phase is accounted using Peng-Robinson Equation of State. The Astarita representation introduced by Hoff (2003) is used to solve the set of reaction equilibrium and component balance equations and to calculate the liquid phase composition.

The study observed the solubility of CO_2, H_2S, CH_4, and mixture of CO_2 and H_2S in MDEA solvent. The predicted solubility was found to be in good agreement with published experimental data. Relatively large error (84.7%) was found on CO_2 partial pressure prediction at loading lower than 0.1 mole CO_2/mole MDEA. The absorption column simulation compared the CO_2 and H_2S separation from methane, for the similar specification of the feed gas (10 mole% acid gas) and solvent (45 wt% MDEA). The simulation result shows that H_2S composition in the product gas was lower than that of the CO_2 composition. For the 5 stages fixed to separate the acid gas, CO_2 purity in gas product is 0.085 mole%, while H_2S purity is 0.059 mole%. Parametric analysis was performed to evaluate the effect of changing the solvent flow rate and the solvent concentration to the acid gas composition in the sweet gas.

Key words: Absorption, Acid gases, Methyldiethanolamine

ABSTRAK

Proses penyerapan gas asid (CO_2 dan H_2S) adalah sangat penting dalam pengolahan gas asli. Proses penyerapan gas asid dengan menggunakan pelarut methyldiethanolamine (MDEA) telah menunjukkan peningkatan aplikasi. Proses penyerapan gas asid ini boleh dikaji menggunakan kaedah pemodelan dan simulasi. Beberapa percubaan telah dilakukan dengan kaedah pemodelan dan simulasi melibatkan keseimbangan fasa dan kesan keatas system penyerapan tersebut. Beberapa kelemahan telah ditemui di dalam percubaan-percubaan tersebut.

Tujuan kajian ini adalah untuk membangunkan prosedur simulasi yang lebih menyeluruh untuk penyerapan gas asid daripada metana dengan menggunakan pelarut MDEA. Kebolehlarutan metana telah tidak diambil kira dalam kajian sebelumnya. Sebahagian daripada kajian ini tertumpu kepada pembangunan model keseimbangan fasa untuk menentukan kelarutan gas asid di dalam pelarut MDEA. Model ElecGC digunakan untuk mengira pekali keaktifan daripada komponen-komponen dalam fasa cecair. Faktor ketidakunggulan komponen-komponen di dalam fasa gas diambil kira dengan menggunakan persamaan keadaan Peng-Robinson. "Astarita representation" yang diperkenalkan oleh Hoff (2003) digunakan untuk menyelesaikan serangkaian persamaan keseimbangan reaksi dan keseimbangan komponen bagi mengira komposisi fasa cecair.

Kajian ini mengamati kelarutan CO_2, H_2S, CH_4, dan campuran CO_2 dan H_2S dalam pelarut MDEA. Jangkaan kelarutan yang didapati daripada kajian menunjukkan persamaan dengan data yang didapati daripada kajian terdahulu. Ralat yang agak besar (84.7%) ditemui pada tekanan separa CO_2 dengan muatan yang lebih rendah daripada 0.1 mol CO_2/mol MDEA. Simulasi turus penyerapan gas asid yang dilakukan membandingkan penyerapan antara CO_2 dan H_2S daripada metana, untuk spesifikasi gas suapan (10 mol% gas asid) dan spesifikasi pelarut yang sama (45 wt% MDEA). Hasil simulasi menunjukkan bahawa kandungan H_2S yang terhasil lebih rendah daripada kandungan CO_2. Bagi 5 tahap pemisahan yang ditetapkan ke atas simulasi turus penyerapan, ketulenan CO_2 dalam gas produk adalah 0.085 mol%, sedangkan ketulenan H_2S adalah 0.059 mol%. Analisa parametrik dilakukan untuk menilai kesan daripada

perubahan kadar alir pelarut dan kepekatan pelarut kepada komposisi gas asid di dalam gas yang terhasil.

Kata kunci: Proses penyerapan, Gas asid, Methyldiethanolamine

TABLE OF CONTENT

LIST OF FIGURES

LIST OF TABLES

NOMENCLATURE

Latin Symbols

Symbol   Meaning

P_i	Partial pressure [Bar]
P	Total gas pressure [Bar]
K_i	Reaction equilibrium constant
$K_{\gamma,i}$	Reaction equilibrium constant in terms of the activity coefficients
$K_{x,i}$	Reaction equilibrium constant, mole fraction based (apparent equilibrium constant)
K_{abs}	Reaction equilibrium constant of overall reaction
x_i	Mole fraction of component in liquid phase
y_i	Mole fraction of component in gas phase
Υ	Degree of saturation
Υm	total concentration of chemically combined acid gas in the liquid phase [mol/L]
$c_w^{\;0}$	Density of water [mol/L]
$f_i^{\;V}$	Fugacity of component in gas phase [Bar]
$f_i^{\;L}$	Fugacity of component in liquid phase [Bar]
$P_i^{\;sat}$	Saturated pressure of component [Bar]
H_i	Henry's law constant [Bar]
$V_i^{\;sat}$	Saturation molar volume of component [m^3/mole]
$V_{i,S}^{\;\infty}$	Molar volume of component at infinite dilution [m^3/mole]
T	Temperature [Kelvin]
T_r	Reduced temperature
Z	Compressibility factor
z	Valence of ion
R_i	molecular van der Waals volumes
Q_i	molecular van der Waals surface areas
$v_k^{(i)}$	k group in component i (UNIFAC)
N	Number of stages in absorption column
N	number of species in the solution (MSA)

k	Boltzmann's constant = 1.38045 x 10^{-16} erg/K
e	electronic charge = 1.60206 x 10^{-19} coulomb
N_L	Avogadro number = 6.02214178 x 10^{23} mole $^{-1}$
C_i	ionic concentration [mole /m^3]
V_n	Flow rate of gas [mole /s]
L_n	Flow rate of liquid [mole /s]
$H_{G,n}$	Enthalpy of gas at stage n [J/mole]
$Cp_{L,n}$	Heat capacity of liquid at stage n [J/mole K]
Cp_G	Heat capacity of gas [J/mole K]
T_{ref}	Temperature reference [Kelvin]
Q_{abs}	Heat of absorption [J/mole]
Q_{H2O}	Heat loss or gain associated with water condensing or evaporating [J/mole]
ΔH_{abs}	Enthalpy of absorption [J/mole]
Cp^E	excess molar heat capacity [J/mole K]
W	Water content in gas mixture [kg/10^6 m^3]
E_{MV}	Murphree stage efficiency

Greek Symbols

Symbol	Meaning
α_t	Gas loading [mole/mole MDEA]
γ_i	Symmetrical activity coefficient of component
γ_i^*	Unsymmetrical activity coefficient of component
γ_i^∞	Symmetric activity coefficient of at infinite dilution
μ_i^V	Activity of component in gas phase
μ_i^L	Activity of component in liquid phase
ϕ_i^V	Fugacity coefficient of component in gas phase
ϕ_i^L	Fugacity coefficient of component in liquid phase
ϕ_i^{sat}	Fugacity coefficient at saturation component
α	Attractive forces between molecules in Peng-Robinson EoS
ω	Acentric factor
Ψ	UNIFAC interation parameter

$\Gamma^{\dot{}}_{k}$	Residual activity coefficient of group (UNIFAC)
θ_i	Area fraction (UNIFAC)
Φ_i	Volume fraction (UNIFAC)
ρ_i	number density of ion [m^{-3}]
σ_i	diameter of ion [m]
ε_i	dielectric constant of solution
Γ	shielding length in MSA
η	packing factor
λ	Heat of evaporation [kJ/mole]

Abbreviations

Abbrev.	Meaning
CPA	Cubic-Plus-Association
DEA	Diethanolamine
DGA	Diglycol-amine
DIPA	Diisopropanolamine
ElecGC	Electrolyte Group Contribution
EoS	Equation of State
EQ	Equilibrium
HS	Hard Sphere
MDEA	Methyldiethanolamine
MEA	Monoethanolamine
MESH	Mass, Equilibrium relationship, Summation, and Heat balance
MSA	Mean Spherical Approximation
NEQ	Non-Equilibrium
NRTL	Nonrandom Two-Liquid
PR	Peng Robinson
RKS	Redlich-Kwong-Soave
SAFT	Statistical Association Fluid Theory
TEA	Triethanolamine
UNIFAC	Universal Quasi-Chemical Functional Activity Coefficient
UNIQUAC	Universal Quasi-Chemical
VLE	Vapor-Liquid Equilibrium

CHAPTER 1

INTRODUCTION

1.1 Background

Absorption refers to the transfer of one or more components of a gas phase into a liquid phase in which they are soluble. It is one of the basic operations in many industrial processes, such as fertilizer industry, natural gas processing, and crude oil processing (Zarzycki and Chacuk, 1993). In the natural gas processing, absorption process is applied for removal of gas impurities like acid gases (CO_2 and H_2S) as absorbate by removing them to certain solvents functioning as the absorbent. Acid gases must be eliminated from the gas stream to avoid poisoning of the catalysis, to increase the heating value of the natural gas, and to achieve the product specifications (Kohl and Nielsen, 1997).

The solvents used to absorb the acid gases in gas processing can be a physical solvents or chemical solvents. The difference in the two solvents is that chemical reactions take place when acid gases dissolve in the chemical solvents, but not for the physical solvents. Propylene carbonate (Flour solvent), dimethyl ether of polyethylene glycol (Selexol solvent) and methanol are classified as physical solvents, while alkanolamines and alkali salt solvents (eg: potassium carbonate and sodium carbonate) are classified as chemical solvents.

The aqueous alkanolamine solvents have proven to have commercial interest. Monoethanolamine (MEA), diethanolamine (DEA) and Diisopropanol-amine (DIPA) have been the most widely used alkanolamine in gas processing. Later, methyldiethanolamine (MDEA) has found increased used (Kohl and Nielsen, 1997) due to its several properties which make it attractive for acid gases removal, which are:

1. High solution concentration (up to 50-55 wt-%)
2. High acid gas loading
3. Low corrosion even at high solution loadings
4. Lower heats of reaction
5. Low vapor pressure and solution losses.

1

The primary disadvantages of MDEA are:

1. Slow reaction rate with CO_2
2. Tendency to foam at high concentration
3. Higher cost

The slow reaction rate of MDEA with CO_2 can be amplified with small addition of primary such as MEA or secondary amine such as DEA (Dawodu and Meisen, 1994). Activator, such as Piperazine, can also be used to improve CO_2 solubility in MDEA solution (Chakma and Meisen, 1987).

Figure 1.1 shows a basic flow scheme for alkanolamine acid gases removal. The sour natural gas that contains acid gases enters the bottom of the absorption column. The alkanolamine solvent (lean amine) is introduced at the top of the absorption column and come into contact in a counter-current fashion with the sour feed gas. The rich alkanolamine solvent that contains the dissolved acid gases exits the bottom of the column and is sent to a stripping column. In the stripping section, the acid gases are released from the solvent, while the solvent is recycled back to the absorption column.

Inside the absorption column, the acid gases and the small amount of hydrocarbon are dissolved into the alkanolamine solution. Chemical reactions take place between the acid gases and the solvent components in the liquid phase. At the steady state condition, a vapor-liquid equilibrium exists between the vapor and the liquid phases for each of the components, while the chemical equilibrium exists in the liquid phase. Figure 1.2 illustrates the chemical equilibrium, the vapor liquid equilibrium and the components exist in the acid gases-aqueous MDEA system. The methane component represents the hydrocarbon existence.

Studies of acid gases absorption into aqueous MDEA solution and the process design are required to improve the industrial scale process. The solubility of the gases in the MDEA solutions is the main consideration of the absorption process. Several investigators (Addicks and Owren, 2002; Chakma and Meisen, 1987; Dawodu and Meisen, 1994; Jou et al, 1982; Jou et al, 1993; Jou et al, 1994; Li and Mather, 1994) have measured carbon dioxide and hydrogen sulfide solubility in aqueous methyldiethanolamine solutions.
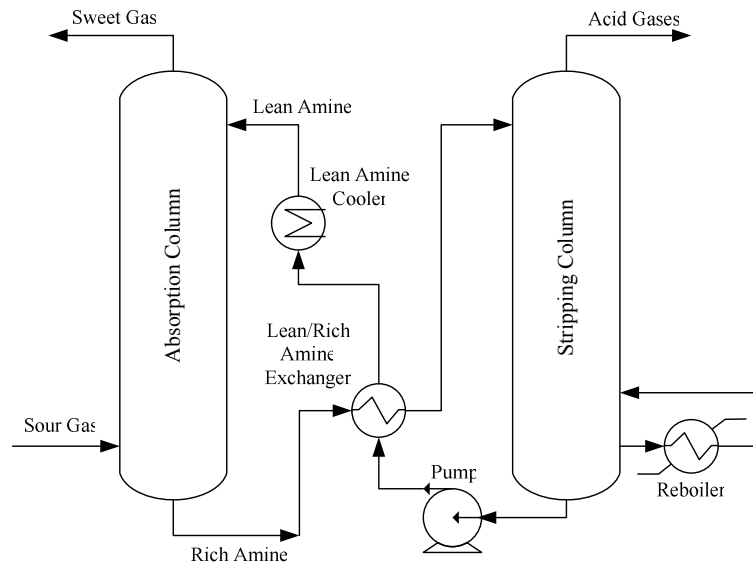
Figure 1.1 Basic flow scheme for alkanolamine acid gases removal
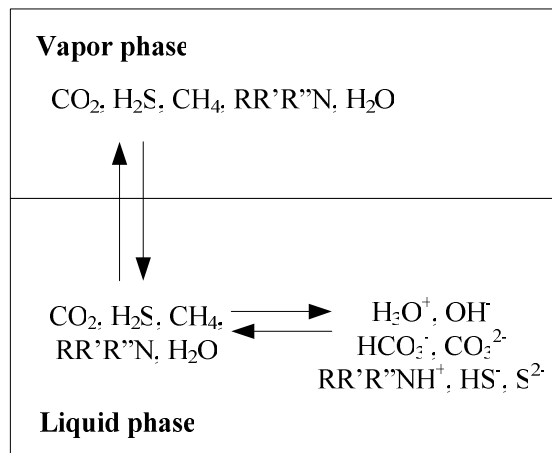
Figure 1.2 Illustration of the chemical equilibrium, the vapor liquid equilibrium and the components exist in the acid gases-aqueous MDEA system.

Improving equipment design for natural gas treatment requires better knowledge on the phase equilibrium and the chemical equilibrium between the acid gases and methyldiethanolamine solution. Several studies have been conducted in modeling the vapor-liquid equilibrium of the acid gases-alkanolamine systems [Autsgen, 1989; Deshmukh and Mather, 1981; Haji Sulaiman, 1998; Kaewsichan, 2001; Lee, 1996; Posey, 1996; Rangsunvigit, 1998; Solbraa, 2002). One of the published vapor-liquid equilibrium models is ElecGC model which is used in this study. A brief explanation on the model is given in Chapter 2.

1.2   Problem Statement

Simulation program on the absorption column is very useful to evaluate the design and operation systematically. There are two main considerations in designing absorption process. First, the acid gas fraction in sweet gas or the percent acid gas recovery is specified. For a given solvent rate, the number of stages has to be calculated. Second, the number of stages is specified, and then the acid gas fraction in sweet gas or the percent acid gas recovery has to be calculated. The former consideration is related with designing of new absorption column configuration. While the later is related to evaluating existing absorption column configuration for a different gas specification.

There are several calculation procedures available for acid gases absorption using alkanolamine system (Vaz, 1980; Loh, 1987; Kohl, 1997) that focuses on the first design consideration. But, the procedures have some limitation. Vaz (1980) performed a calculation procedure for amine contactor and estimated of equilibrium stage requirement. The study has limitation due to the lack of attention given on the solubility of hydrocarbon in the system. The hydrocarbon solubility in the solvent is necessary to get a better design of the gas sweetening process. Vaz's calculation procedure is unreliable to have a converged solution. Loh (1987) performed stage-by-stage calculation procedure with reliability to meet a converged solution. The procedure also does not give attention to the hydrocarbon solubility. Kohl (1997) designed an absorption calculation procedure that has capability to determine the lean amine circulation rate. But, it has inability of determining equilibrium composition at each stage, number of stage required, and temperature profile along the column.

A more rigorous stage-by-stage calculation procedure has to be constructed to simulate the acid gases absorption from methane using methyldiethanolamine solution. The limitations of the previous procedure have to be solved. The procedure must be able to calculate the hidrocarbon solubility, have a reliable converged solution, and have the ability to predict the temperature and liquid and gas phase composition at each stage.

The mathematical formulation of acid gases absorption using alkanolamine is very complex. In the stage-by-stage calculation procedure, the mass and energy balance relate

4

each stage with the others. The energy balance itself is relatively not simple due to the existence of the heat of absorption and heat of water condensation or evaporation. At every stage, the liquid and vapor phase are related by phase equilibrium. The acid gas-alkanolamine-water system is a highly non-ideal system. The terms of activity coefficient and fugacity coefficient have to be combined to the phase equilibrium equation.

In the liquid phase, the component composition is described by the chemical reaction equilibrium, the component mole balance and the charge balance. The equations that follow these three terms are non-linear equations. Solving on these non-linear equations produces the equilibrium composition of the components. The common way to solve the non-linear equations is a numerical method such as Newton method. However, the equations involves is very different in the order of the magnitude of the unknowns, leading to problems of a convergence and numerical instability. Initial guesses that are very close to unity have to be provided. For this problem, the iterative procedure will lead to high computation times.

Hoff (2003) applied the Astarita representation to calculate the equilibrium composition of the component in the liquid phase for the system of CO_2-MDEA-H_2O system. The Astarita representation method is a simple and quick procedure to solve the non-linear equation in acid gases-alkanolamine system. The computation time required in the method is very short compare to the Newton method and it does not require an initial guesses. This method has not been applied to the H_2S-MDEA-H_2O and CO_2-H_2S - MDEA-H_2O systems.

1.3   Objectives of Research

The objectives on this research are as follows:
1. To examine the ElecGC model for CO_2 and H_2S absorption using MDEA solvent.
2. To apply the Astarita representation method in calculating the liquid phase composition for systems of CO_2-MDEA-H_2O, H_2S-MDEA-H_2O, and CO_2-H_2S-MDEA-H_2O.
3. To construct a calculation procedure for CO_2 and H_2S absorption process from methane using MDEA solvent. The solubility of methane is taken into account in the

simulation. The procedure used to simulate the steady state absorption process is based on the equilibrium model.

4. To do the sensitivity analysis and analyze the influence of changing solvent concentration and solvent flow rate on the purity of the gas product.

1.4   Scope of Research

The scope of research focuses on developing a reliable combination of mathematical models that capable of describing the acid gases absorption process using aqueous MDEA solvent. In this work, compatible algorithms are proposed to solve the mathematical models. The first algorithm would be the algorithm to calculate the liquid phase compositions involving the Astarita representation. The simulation results are compared with the literature data. The liquid phase composition algorithm becomes a part of the vapor liquid equilibrium algorithm that can be used to calculate the solubility of the acid gases in the MDEA solvent. The simulation results are compared to the established solubility data available in literature. Finally, the algorithm that solves the mathematical models will be served to simulate the absorption process. The parametric analysis is performed on the absorption system. This involves evaluating the changing of the solvent flow rate and the solvent concentration to the acid gas composition in the sweet gas. The simulations are performed in the MATLAB program.

The first part of the study is to evaluate the single acid gas (CO_2 and H_2S) solubility in the MDEA solvent. The methane solubility is also evaluated as this component becomes the main constituent in the methane. The absorption column simulation is performed on the single acid gas absorption from methane using MDEA solvent. The second part of the study is evaluating the mixture acid gases solubility in the MDEA solvent. Then, the simulation of CO_2 and H_2S mixture separation from the methane stream is executed.

1.5   Outline of Thesis

The structure of the thesis is as follows. In Chapter 2, the review of the literatures on the acid gases absorption using methyldiethanolamine solvent is given. These include the

experimental data on acid gases solubility and heat of absorption and the phase equilibrium models. In Chapter 3, the mathematical models for the acid gas absorption system are derived. Several additional relations are constructed to improve the mathematical model of the system. In Chapter 4, the algorithms for the computer simulation of the acid gases removal system are presented. In Chapter 5, the simulation results on the acid gases absorption system with the literature data validation are displayed. Some conclusions and recommendations based on this research are given in Chapter 6.

CHAPTER 2

LITERATURE REVIEW

2.1   Introduction

Acid gases (CO_2 and H_2S) are the main impurities in natural gas. Acid gases are corrosive to the pipeline and have a very low heating value. These impurities have to be eliminated from the natural gas to increase the heating value and fulfill the product demand specification. One common method to remove the acid gases from natural gas is absorption process using alkanolamine solvents.

The acid gases sweetening process using alkanolamines have been studied for decades. Kohl and Nielsen (1997) stated that triethanoamine (TEA) was the first commercially applied solvent used for the gas sweetening process. But, its low reactivity and low capacity due to high molecular weight has caused it to be replaced. The amines that have proven to be of commercial interest for gas purification are monoethanolamine (MEA), diethanolamine (DEA), and methyldiethanolamine (MDEA). Figure 2.1 shows the molecular structure of the alkanolamines.
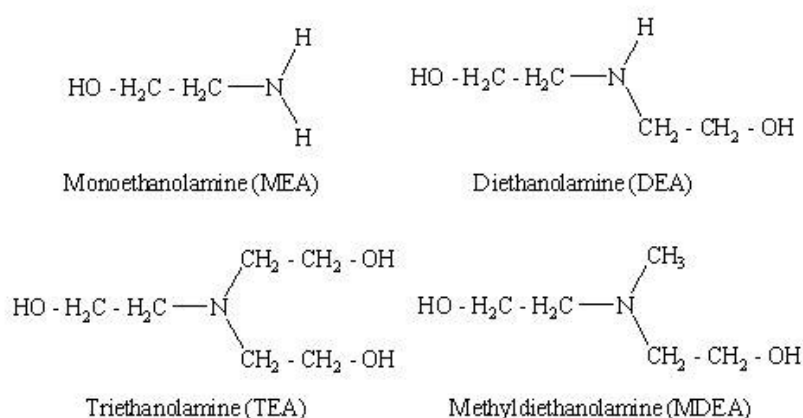
Figure 2.1 Molecular structure of some alkanolamine

MDEA was introduced by Frazier and Kohl (1950) at Flour Daniel for the acid gases removal process from natural gas. Since then, studies about the application of the aqueous MDEA solvent as the acid gases absorbent has been intensively growing until nowadays.

Selection on the absorption column height, solvent circulation rate and solvent strength are required to get an optimum acid gases removal (Jou et al, 1982). Design and analysis of this absorption configuration require information about the equilibrium solubility of the gases in the solvents, the heat of absorption, and the equilibrium model. In the next section, the review of the studies will be highlighted.

2.2 Solubility of Acid Gases in Aqueous MDEA Solution

Several experiments have been conducted to study the solubility of the gases in the aqueous MDEA solution. Table 2.1 gives the literature review of the study. Data on acid gases solubility on aqueous MDEA solutions are in the form of partial pressure on the variation of gas loading (moles acid gas per moles of amine). The hydrocarbon solubility and mixture of hydrocarbon and acid gas solubility were also explored in the recent studies (Jou and Mather, 2006; Addicks and Owren, 2002). Figure 2.2 show the collection of experimental data on CO_2 solubility in MDEA solvent available on the literatures at various concentrations of solvent and temperatures. Figure 2.3 show the literature data on H_2S solubility in MDEA solvent while Figure 2.4 shows the CH_4 solubility data. The graphs were reploted based on data

Jou and Mather (1982) published the first equilibrium solubility data of CO_2 and H_2S in the aqueous MDEA solution. Approximately 285 solubility data were given by the authors. In general, the solubility of the CO_2 and H_2S decreases with increasing temperature and increasing solvent strength. Chakma and Meisen (1987) published solubility data of CO_2 at higher temperature compared to the prior data. The solubility data of CO_2 at 4.28 M MDEA was slightly lower than that of the previous data. The experimental data produced by Autsgen and Rochelle (1989) for CO_2 solubility at 2 M MDEA was in good agreement with measurement made by Jou and Mather (1982). Whilst at the 4.28 M, slightly higher results were obtained by Autsgen and Rochelle (1989).

The experimental results obtained by Shen and Li (1992), Li and Shen (1993) and Dawodu and Meisen (1993) becomes additional data for the prior data. Relatively small data for CO_2 solubility were produced by Dawodu and Meisen (1994) and these data were

compared with the first two studies. Large deviations were observed at low loading compare to the high loading. The relatively similar conditions were applied by Jou et al (1994) and Xu et al (2002) to obtain the CO_2 solubility. The data were compared with the Shen and Li (1992) data. The lack of data agreement was obtained by Jou et al (1994), meanwhile a good agreement data was obtained by Xu et al (2002).

Table 2.1 Data of gases solubility in aqueous MDEA solutions

References	MDEA concentration mole/L (wt%)	Temperature ^oC	Gas
Jou et al (1982)	1.0, 2.0, 4.28	25 – 120	CO_2, H_2S
Chakma and Meisen (1987)	1.69, 4.28	100 – 200	CO_2
Autsgen and Rochelle (1989)	2.0, 4.28	40	CO_2
Shen and Li (1992)	(30)	40 – 100	CO_2
Li and Shen (1993)	2.57	40 – 100	H_2S
Jou et al (1993)	(35)	40, 100	Mixtures
Dawodu and Meisen (1994)	4.28	100, 120	CO_2
Jou et al (1994)	(30)	40 – 100	CO_2
Kuranov et al (1996)	2 molal, 4 molal	40 – 140	CO_2, H_2S
Jou et al (1998)	3.0	25-130	CH_4
Haji-Sulaiman et al (1998)	2, 4	30 – 50	CO_2
Kamps et al (2001)	4 molal, 8 molal	40 – 120	CO_2, H_2S
Xu et al (2002)	(30)	40, 60	CO_2, H_2S
Addicks and Owren (2002)	2.633 molal, (30), (50)	25, 40, 80	CO_2 CO_2+CH_4
Jenab et al (2005)	2	25 – 70	CO_2
Mamun et al (2005)	(50)	55 – 85	CO_2
Jou and Mather (2006)	8.6	25-130	CH_4

Additional data were reported by Kuranov et al (1996), Jou et al (1998), Haji-Sulaiman (1998), and Mamun et al (2005). They applied different solution strength to get the data. The next set of data was published by Kamps et al (2001) for the CO_2 and H_2S solubility. The data have small deviation with those one reported by Kuranov et al (1996). Jenab et al (2005) produced few data on CO_2 solubility and compare with that by Jou et al (1982). A good agreement data were produced with relatively small deviation.
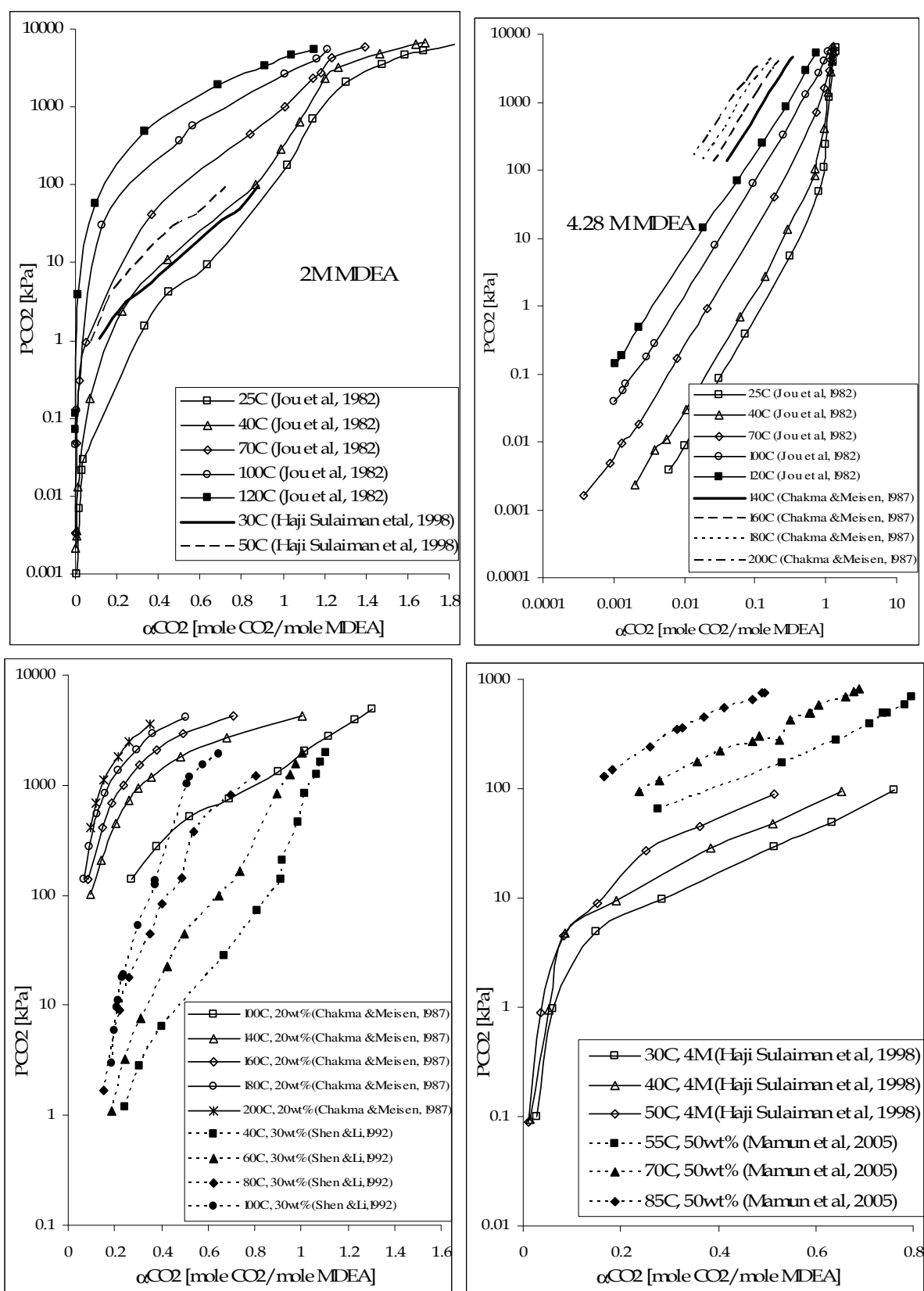
Figure 2.2 Literature data on CO_2 partial pressure for system CO_2-MDEA-H_2O
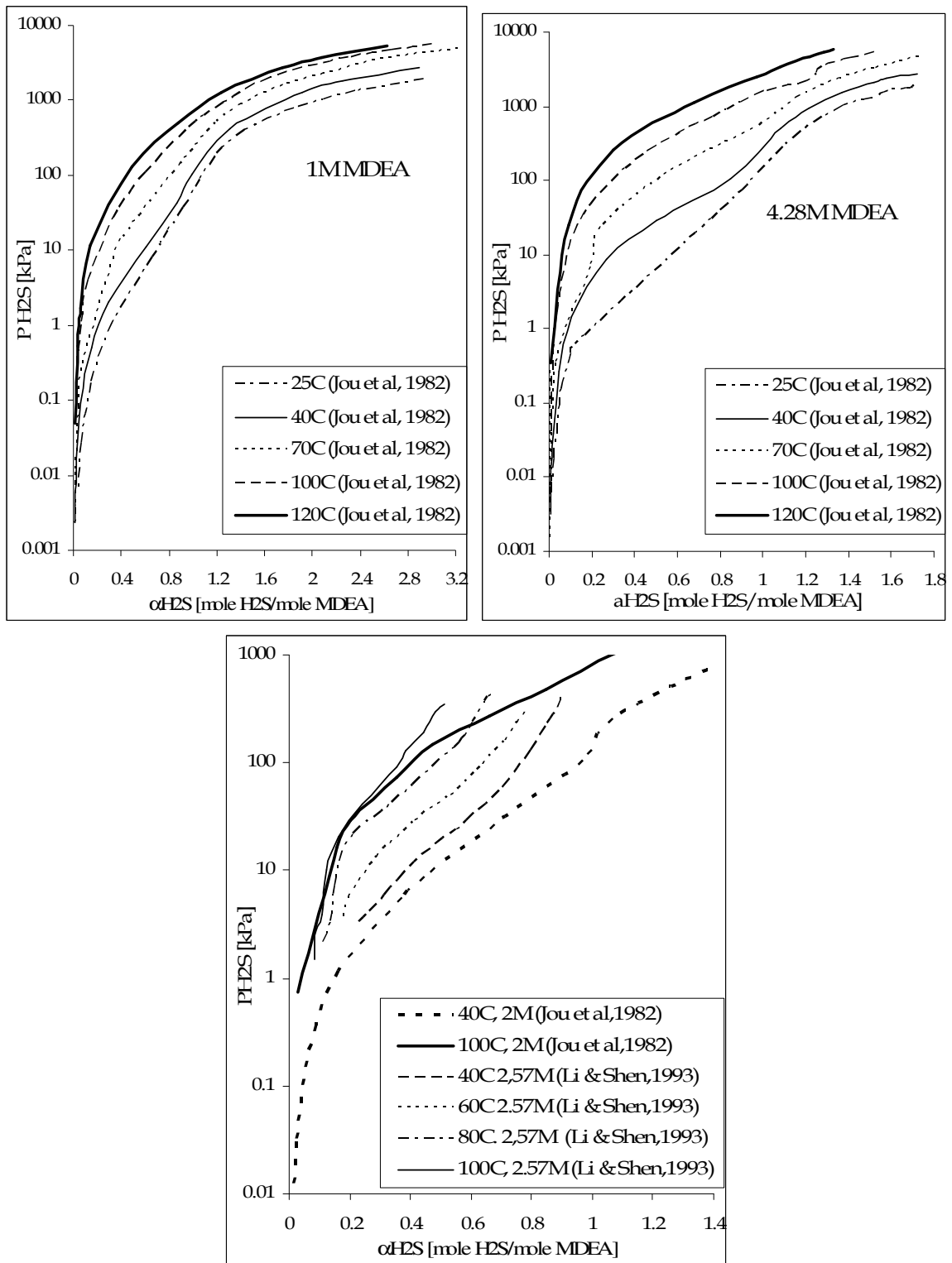
Figure 2.3 Literature data on H$_2$S partial pressure for system H$_2$S-MDEA-H$_2$O
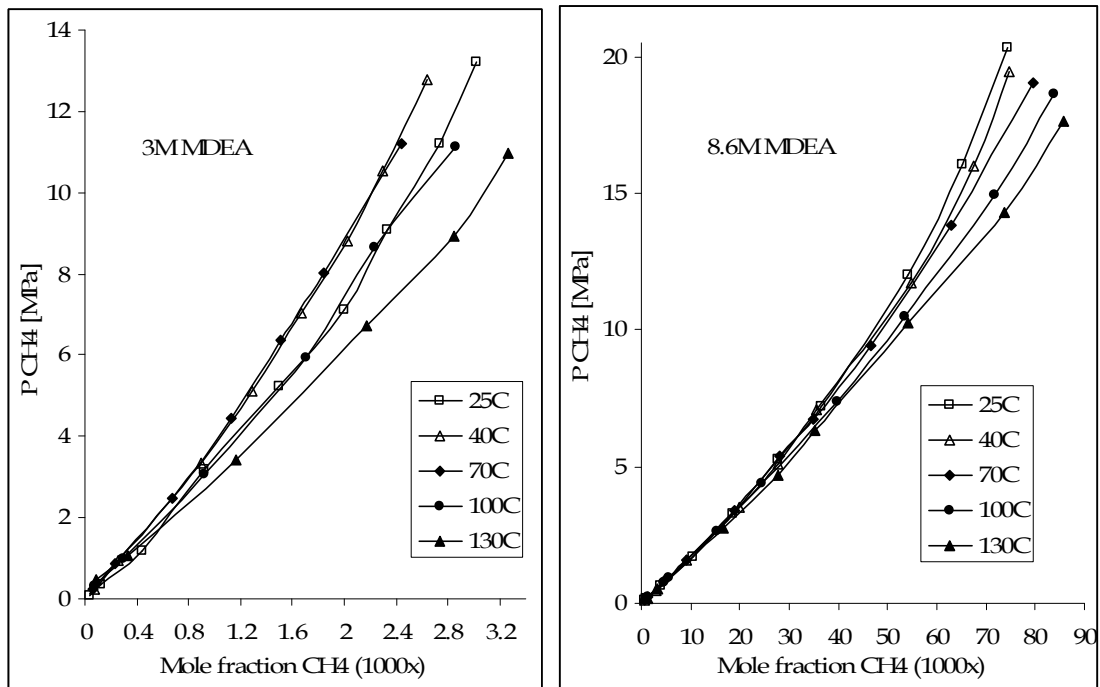
Figure 2.4 Literature data on CH_4 partial pressure for system CH_4-MDEA-H_2O

[Data taken from Jou etal (1998)]

From all the experiments conducted by previous researchers, most of them measured the solubility of the gases at relatively high partial pressure. Only small data are available for CO_2 and H_2S solubilities at very low partial pressure (lower than 0.01 kPa) which were pervormed by Jou et al (1982). The solubility measurements at very low loading or very low partial pressure are important to be done since the real acid gases absorption process desire a very low acid gases partial pressure in the gas product. The overall solvent strength used in the experiments have been represent the ussuall values utilized in the real acid gases absorption process using MDEA solvent.

2.3   Heat of Absorption of Acid Gases in MDEA Solvent

The absorption of acid gases into the aqueous MDEA solvent produce some heat that is called heat of absorption. Several studies on the heat of absorption of the acid gases in the aqueous MDEA solution have been conducted. Table 2.2 gives the literature review of the study. The published heat of absorption data are divided into the experimental data and the calculated data.

The heat of absorption values depend strongly on the acid gas loading at the solution. The values are only less affected by the solution strength, while the gas pressure has virtually no effect on the values (Oscarson et al, 1990). Jou et al (1982) reported that their average value on the calculated heat of absorption for CO_2 is 60.0 kJ/mole CO_2, while for H_2S is 41.2 kJ/mole H_2S. The calculated heat of absorption of CO_2 obtained by Jou et al (1994) has an average value of approximately 62 kJ/mole CO_2. Kim et al (2009) did not show distinctly the calculated heat of absorption values. But, from the figures, their results show a good agreement with the published experimental data.

Oscarson et al (1990) determined that within their experimental condition the heat of absorption of H_2S values ranged from 28 kJ/mole H_2S to 56 kJ/mole H_2S. The next three experiments were performed to produce the heat of absorption of CO_2 [Mathonat et al (1997), Carson et al (2000), and Arcis et al (2008)]. Mathonat et al (1997) published the values ranged from 49 kJ/mole CO_2 to 58 kJ/mole CO_2 for the heat of absorption at infinite dilution of CO_2. Carson et al (2000) have the experimental data values ranged from 48.4 kJ/mole CO_2 to 50.6 kJ/mole CO_2 for the heat of absorption of CO_2 at room temperature. Arcis et al (2008) experimental data on heat of absorption of CO_2 have a good agreement with Mathonat et al (1997) data. Their heat of absorption at infinite dilution values range from 49.6 kJ/mole CO_2 to 59.2 kJ/mole CO_2.

Table 2.2 Data of heat of absorption of acid gases in aqueous MDEA solutions

References	MDEA concentration mole/L (wt%)	Temperature ^{o}C	Gas
Jou et al (1982) [b]	1.0, 2.0, 4.28	25 – 120	CO_2, H_2S
Oscarson et al (1990) [a]	1.7, 3, 4.3	299.8 – 399.8 K	H_2S
Jou et al (1994) [b]	2.56	40 – 100	CO_2
Mathonat et al (1997) [a]	2.56	40 – 120	CO_2
Carson et al (2000) [a]	(10 – 30)	25	CO_2
Arcis et al (2008) [a]	15 and 30	322.5 K	CO_2
Kim et al (2009) [b]	30	40 – 120	CO_2

[a] Experiment

[b] Calculation
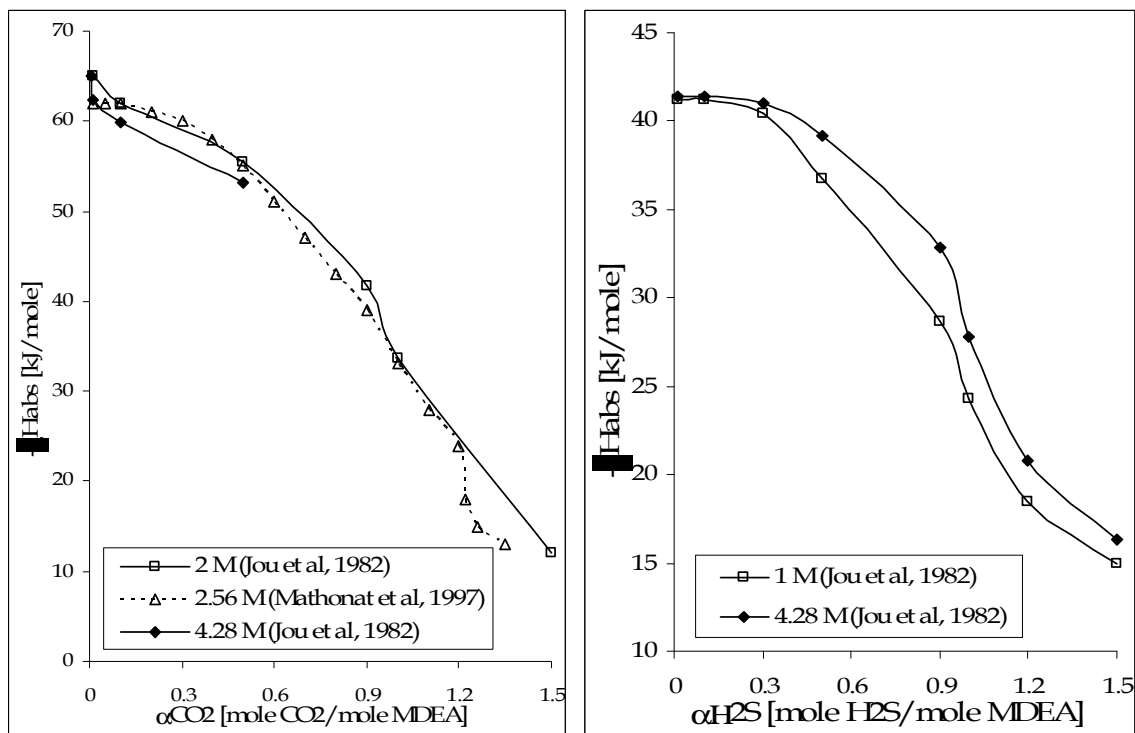
Figure 2.5 Literature data on heat of absorption of CO_2 and H_2S in MDEA solvent

From the Table 2.2, it can be seen that quite a few number of experiments have been done on measuring the heat of absorption for CO_2 absorption in MDEA solvent. Only small data have been given for H_2S absorption in MDEA solvent. The amine concentration and temperature range used in the experiment are wide. Figure 2.5 shows distinctly that heat of absorption of CO_2 is higher than that of H_2S.

2.4   Reviews on Equilibrium Models

Studies on the acid gases absorption using alkanolamine solvents were not only performed on the experimental investigation, bur also on the mathematical modeling that can represent the real process. The modeling study comprises of the vapor liquid model and the absorption column model. Studies on the vapor-liquid equilibrium model for acid gases-alkanolamine system have been done for decades. These include the model to account for the non-idealities of the liquid and the vapor phase. The non-ideality of the gas phase was accounted through the use of fugacity coefficient, while the liquid phase was accounted for using activity coefficient.

2.4.1 Kent Eisenberg Model

The first widely used model for simulating acid gases-alkanolamine treatment is the Kent and Eisenberg (1976) model. A simple model used to describe CO_2-H_2S-H_2O-alkanolamine system consists of a set of reactions and their respective equilibrium constants. The values of the activity coefficients and fugacity coefficients are assumed to be unity. Henry's law relationship is used to calculate the equilibrium partial pressure. The component balances are incorporated to compute the liquid phase composition. The following reactions take place when the CO_2 and H_2S dissolve into alkanolamine solution:

$$RR'NH_2^+ \leftrightarrow H^+ + RR'NH \tag{2.1}$$

$$RR'NCOO^- + H_2O \leftrightarrow RR'NH + HCO_3^- \tag{2.2}$$

$$H_2O + CO_2 \leftrightarrow H^+ + HCO_3^- \tag{2.3}$$

$$H_2O \leftrightarrow H^+ + OH^- \tag{2.4}$$

$$HCO_3^- \leftrightarrow H^+ + CO_3^{2-} \tag{2.5}$$

$$H_2S \leftrightarrow H^+ + HS^- \tag{2.6}$$

$$HS^- \leftrightarrow H^+ + S^{2-} \tag{2.7}$$
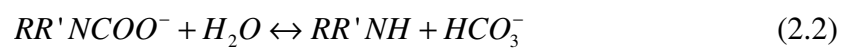
The pseudo-equilibrium constant for the reactions are described below:

$$K_1 = [H^+][RR'NH] \big/ [RR'NH_2^+] \tag{2.8}$$

$$K_2 = [HCO_3^-][RR'NH] \big/ [RR'NCOO^-] \tag{2.9}$$

$$K_3 = [H^+][HCO_3^-] \big/ [CO_2] \tag{2.10}$$

$$K_4 = [H^+][OH^-] \tag{2.11}$$

$$K_5 = [H^+][CO_3^{2-}] \big/ [HCO_3^-] \tag{2.12}$$

$$K_6 = [H^+][HS^-] \big/ [H_2S] \tag{2.13}$$

$$K_7 = [H^+] + [S^{2-}] \big/ [HS^-] \tag{2.14}$$

The equilibrium partial pressures are defined by:

$$P_{CO_2} = H_{CO_2}[CO_2] \tag{2.15}$$

$$P_{H_2S} = H_{H_2S}[H_2S] \tag{2.16}$$

The charge balance and components balances equations are stated as:

$$\left[RR'NH_2^+\right]+\left[H^+\right]=\left[OH^-\right]+\left[RR'NCOO^-\right]+\left[HCO_3^-\right]+2\left[CO_3^{2-}\right]+\left[HS^-\right]+\left[S^{2-}\right] \quad (2.17)$$

$$M=\left[RR'NH\right]+\left[RR'NH_2^+\right]+\left[RR'NCOO^-\right] \quad (2.18)$$

$$\alpha_{H_2S}M=\left[H_2S\right]+\left[HS^-\right]+\left[S^{2-}\right] \quad (2.19)$$

$$\alpha_{CO_2}M=\left[CO_2\right]+\left[HCO_3^-\right]+\left[CO_3^{2-}\right] \quad (2.20)$$

where M is amine concentration and α is the acid gas loading. Kent and Eisenberg (1976) simplify and manipulate the eq. (2.08) to (2.20) to calculate the partial pressure of acid gases of the system. The simplification results in;

$$P_{CO_2}=\frac{H_{CO_2}B\left[H^+\right]^2\big/K_3K_5}{1+\left[H^+\right]\big/K_7+M\left[H^+\right]\big/CK_2K_5} \quad (2.21)$$

$$P_{H_2S}=\frac{H_{H_2S}A\left[H^+\right]^2\big/K_6K_7}{1+\left[H^+\right]\big/K_7} \quad (2.22)$$

$$\left[H^+\right]=\frac{A\left(1+K_7\big/\left(K_7+\left[H^+\right]\right)\right)}{\left(1+M\big/CK_1\right)}+\frac{K_4}{\left[H^+\right]\left(1+M\big/CK_1\right)}$$

$$+\frac{B\left(1+K_2K_5\big/\left(K_2K_5+K_2\left[H^+\right]+M\left[H^+\right]\big/C\right)\right)}{\left(1+M\big/CK_1\right)} \quad (2.23)$$

where

$$A=M\alpha_{H_2S}-P_{H_2S}\big/H_{H_2S} \quad (2.24)$$

$$B=M\alpha_{CO_2}-P_{CO_2}\big/H_{CO_2} \quad (2.25)$$

$$C=1+\left[H^+\right]\big/K_1+P_{CO_2}K_3\big/\left(K_2H_{CO_2}\left[H^+\right]\right) \quad (2.26)$$

The equilibrium reaction constants are the function of temperature where the first two constants were forced fit to the experimental data of CO_2/H_2S -H_2O-MEA/DEA. The fitted parameters were tested to mixed system and the results were found to be satisfactory. This model succeeds in predicting the correct partial pressure, but failed to predict the concentration of the ionic species The model also failed to predict the partial pressure when the acid gas loading were either very low or very high (Posey, 1996).

2.4.2   Deshmukh-Mather Model

Deshmukh and Mather (1979) used the same set of reactions as Kent and Eisenberg did. The component balances were also applied. They calculate the values of fugacity coefficient and activity coefficient of the model. The Peng-Robinson equation of state was used to calculate the fugacity coefficients value. The activity coefficients were determined using Guggenheim's equation which extends the Debye-Huckel expression.

$$\ln \gamma_k = \frac{-A(z_k)^2 \mu^{0.5}}{(1 + b_k \mu^{0.5})} + 2 \sum \beta_{kj} m_j \tag{2.27}$$

The first term expresses the Debye-Huckel law and represents the electrostatic forces. The second term takes into account the short range of van der Waals forces. Water activity coefficient was assumed to be unity. However, the real value can be very different. The interaction parameter β_{kj} were determined by fitting the model to the experimental data of H_2S/CO_2-MEA-H_2O systems. The fitted interaction parameters were only been served for single gas-amine system and not for the mixed gas. Nevertheless, the values were used to predict the mixed acid gases equilibrium.

The equilibrium reactions constants and components balances were solved to calculate the liquid phase composition. Brown's method which is similar to Gaussian elimination was used to solve the problem. The model is valid up to an ionic strength of 5 molal. Deshmukh and Mather (1979) model was very popular and widely used in industrial application.

2.4.3   Electrolyte NRTL Model

Autsgen (1989) used the electrolyte-NRTL (Nonrandom Two-Liquid) equation to account for the liquid phase activity coefficients and Soave-Redlich-Kwong equation of state to account for the vapor phase fugacity coefficients. These two equations were incorporated to the Kent-Eisenberg set of reaction equilibrium and component balances to account for the non-ideality of the gas phase and electrolyte liquid phase. In the absence of acid gases from the system, the Electrolyte NRTL reduces to the NRTL.

18

Autsgen (1989), calculated and fitted the parameters from the available data on acid gases VLE in MDEA, MEA, DEA, and DGA. He applied the model and parameter to his experimental data for CO_2 and H_2S in 2 M MDEA solvent and also mixture of MDEA-DEA and MDEA-MEA each at 2 molar at 40°C and 80°C. The binary parameter was fitted to the binary system (amine-water) and ternary parameter to the ternary and quaternary systems (CO_2-amine-water, H_2S-amine-water, and CO_2-H_2S-amine-water).

Because of the lack of confidence in the MDEA-H_2O binary parameters, Autsgen (1989) set them to zero. This means his MDEA-acid gas model asymptote to ideal solution as the gas concentrations approach zero. The model is also insensitive at acid gas loadings below approximately 0.01.

Posey (1996) used the same model as Autsgen (1989) did, electrolyte-NRTL and RKS equation of state to study the system of acid gases in MDEA, DEA, and mixed amine. The main difference between the two works is that Posey (1996) utilized the freezing point data, heat of mixing data, pH data, conductivity data and VLE data as Autsgen (1989) used the VLE data only. The values of the interaction parameters are different. Posey (1996) improved the parameter that was set to zero by Autsgen (1989). The improvements also exist at low acid gas loadings. Posey (1996) found that accurate low loading prediction cannot be based upon VLE data alone. The additional pH and conductivity data are also required for the low loading prediction.

2.4.4   ElecGC Model

Lee (1996) combined the Mean Spherical Approximation (MSA), Hard Sphere (HS) and Born models to calculate the ionic activity coefficient while the neutral polar charge components were treated using UNIFAC group contribution (GC) of Wu-Sandler (1991). The Gibbs-Duhem integration for the activity coefficient was applied to account for the presence of the charged species to the neutral components. The MSA and HS take into account of the long range and the short range interaction effect, while the Born model converts the water solvent to aqueous alkanolamine solvent condition. The combination of this ionic and neutral charge activity coefficient models are called ElecGC model. The activity for the neutral and ion components are defined by:

19

$$\ln \gamma_i = \ln \gamma_i^{UNIFAC} + \ln \gamma_i^{GD}$$
$$\ln \gamma_j = \ln \gamma_j^{MSA} + \ln \gamma_j^{Born}$$

<div align="right">(2.28)</div>

The non-ideality in the gas phase was accounted using Peng-Robinson equation of state. Lee (1996) successfully calculates the solubility of H_2S and CO_2 in the MEA, DEA, MDEA, and their blends covering wide range of conditions.

2.4.5 Electrolyte-UNIQUAC Model

Kaewschian et al (2001) used a similar approach based upon the electrolyte-UNIQUAC model to predict the activity. This resulted in a simplification of the activity coefficient expressions compared to electrolyte-NRTL model, and required fewer interaction parameters. The fugacity coefficient was determined using Soave-Redlich-Kwong equation of state. Predicted H_2S and CO_2 vapor pressures were in a good agreement with the reported experimental data for aqueous solutions of a single acid gas as well as mixtures of H_2S and CO_2 in MEA and MDEA and their mixtures.

2.4.6 Electrolyte Equation of State Model

A few authors have modeled the VLE of acid gases-alkanolamine-water using an equation of state for the liquid phase. Button and Gubbins (1999) used the Statistical Association Fluid Theory (SAFT) equation of state to model the vapor-liquid equilibrium of CO_2 in aqueous MEA and DEA. The equation is expressed as the sum of repulsion/dispersion, chain formation, and association to the free energy. It does not require the knowledge of chemical reactions and the equilibrium constant. They obtained results that agree with experimental value of vapor liquid equilibrium for the binary system of CO_2 water or ternary system of CO_2 aqueous alkanolamines.

Chunxi and Fürst (2000) applied electrolyte equation of state to the vapor liquid equilibrium of CO_2 and H_2S in aqueous solution of MDEA. The model, the molar Helmholtz energy is expressed by four terms. The first two terms are based on Redlich-Kwong-Soave equation of state. The third term takes into account interaction between

ions and molecules or between cations and anions. This contribution is considered as solvation interaction. The last term express the long range electrostatic interaction contribution that is represented with a simplified MSA model. Chunxi and Fürst (2000) approach, succeeds in representing the various data over a large range of experimental conditions.

Solbraa (2002) evaluated the CO_2 solubility in aqueous MDEA solution. Solbraa developed two electrolyte equation of state to model the thermodynamic properties of the fluid systems. The first equation is electrolyte SRK equation of state with additional MSA and Born term. The model was able to correlate and predict equilibrium properties of CO_2-MDEA-water solution with good precision and also able to correlate the high pressure data system of methane-CO_2-MDEA-water. The second model was electrolyte CPA (cubic-plus-association) Equation of State which has the capability to treat higher pressures.

2.4.7   Other Models

Li and Mather (1994) applied the new Pitzer equation to predict the solubility of CO_2 in MDEA, MEA, and mixture of MDEA-MEA solution. Li-Mather used the same case condition as Autsgen (1989) did. The model is not reliable for the high loading acid gas because it does not consider the free CO_2 species. The model neglects the gas phase non-ideality and thus only suitable for the low pressure system.

Poplsteinova (2004) combined the group contribution UNIFAC approach by Lee (1996) and extended Debye-Huckel expression by Deshmukh and Mather (1979) to calculate the activity coefficients. The fugacity coefficients were treated by Peng-Robinson Equation of State. Polpsteinova (2004) applied the model to CO_2-MEA/MDEA-H_2O system. This model is applicable for a wide range of loadings and temperatures.

Table 2.3 Comparison on vapor liquid equilibrium model

Author	VLE model		Application	
	Activity coefficient	Fugacity coefficient	Advantages	Disadvantages
Kent & Eisenberg (1976)	-	-	• Accurate at loading greater than 0.1	• Can not calculate ionic speciation • Inaccurate for very low loading
Deshmukh & Mather 1979)	Guggenheim's equation	-	• Valid for ionic strength up to 5 molal • Widely used in industrial application	• Neglect mixed acid gas parameter
Autsgen (1989)	electrolyte-NRTL	SRK	• Binary and ternary parameter were fitted to binary and ternary data	• Inaccurate for loading under 0.01 • MDEA-H_2O parameter setted to 0
Posey (1996)	electrolyte-NRTL	SRK	• Improved parameter from previous • Accurate for low loading prediction	
Lee (1996)	ElecGc (UNIFAC+MSA)	PR	• Accurate calculate binary, ternary and quaternary system	
Kaewschian (2001)	Electrolyte UNIQUAC	SRK	• Good prediction of single and mixed gas	
Chunxi & Fürst (2000)	Electrolyte EoS		• Succeed presenting data on large range experimental condition	
Solbraa (2002)	Electrolyte EoS		• Good precision on CO_2-MDEA-H_2O	
Poplsteinova (2004)	UNIFAC+extended Debye Huckle	PR	• Applicable for wide range loading and temperature	

2.4.8   Model Selection

Table 2.3 summarized the comparison on the vapor-liquid equilibrium model. In this study, the ElecGC model by Lee (1996) is chosen. The parameter from the UNIFAC group contribution which has reliable results for predicting vapor-liquid equilibrium for a wide variety of components was used. The UNIFAC model has been successfully used worldwide for synthesis and design of separation processes (Gmehling, 1995).

The development of ElecGC model on equilibrium model has been extensive. The model can accurately calculate binary, ternary, and quaternary system's VLE by using parameters which are consistent. ElecGC can also predict the VLE of mixed gases (acid gases, hydrocarbon-acid gases) in amine system. Therefore, the ElecGC model is quite sufficient to be adopted for simulation of acid gases absorption from methane.

2.5   Modeling and Simulation of Acid Gases Absorption Using Alkanolamine

There are two approaches reported in the literature, used to model the absorption column. The first is equilibrium model (EQ) which was introduced by Vaz (1980) and Loh (1987). The second is non-equilibrium model (NEQ) which was introduced by Tontiwachmuthikul (1990), Rinker (1997), and Baghli (2001). The later is more rigorous than the former. Due to the complexity of the non-equilibrium model, many researchers preferred to use equilibrium model for their study. The differences between the two approaches will be explained in this section.

2.5.1   Equilibrium modeling

The equilibrium (EQ) stage model assumes that the vapor and liquid phases are in thermodynamic equilibrium. In every single equilibrium stage of absorption column, the gases and liquid phases entering and leaving are described using MESH equations (Mass balance, Equilibrium relation, Summation of mole fraction, and Heat balance). The reaction equations are integrated to the equilibrium relation, to describe the reaction

phenomenon taking place at liquid phase at each stage. The overall separation process consists of several equilibrium stages.

Figure 2.2 shows the schematic diagram of equilibrium model. The gas stream from the bottom stage is counter currently contact with the liquid stream from the above stage. The equilibrium exists between the gas and liquid phases leave the stage. The major process variables to be considered in the equilibrium stage calculation are amine circulation rate, column temperature, and number of trays (Vaz, 1980). The column hardware design such as column diameter and absorber height cannot be determined using this model.

$$T_{g,out}, V_{out}, y_{i,out} \qquad T_{l,in}, L_{in}, x_{i,in}$$

Stage n

$$T_{g,in}, V_{in}, y_{i,in} \qquad T_{l,out}, L_{out}, x_{i,out}$$
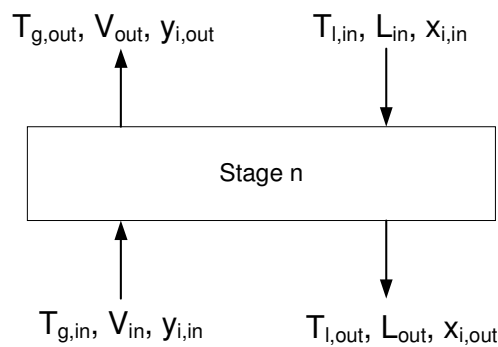
Figure 2.6 Schematic diagram of equilibrium model

2.5.2   Rate-Base Approach (Non-Equilibrium modeling)

The non-equilibrium set of equations (NEQ) are not as simple as equilibrium equations. The NEQ analyze the mass and heat transfer occurring on an actual tray by considering separate mass and energy balance for each phase. The rate equation across the interface that connects the balances, are calculated using film theory. Physical equilibrium is assumed to exist at the gas liquid interface and the chemical equilibrium is assumed to be at the bulk liquid solution (Al-Baghli et al, 2001). Figure 2.3 shows the schematic diagram of the film model as applied to a tray in an absorption column.

The column hardware design such as column diameter, tray configuration (sieve plates, valve plates, or bubble-cap plates), and size will have a significant influence on the interphase heat and mass transfer rates which are not taken into account in the EQ stage model. In addition, physical properties such as surface tension, diffusion coefficients,

viscosities, and others for calculation of mass and heat transfer coefficients and interfacial areas are required. These parameters are hardly available in open literature and restricted the approach from being used widely.
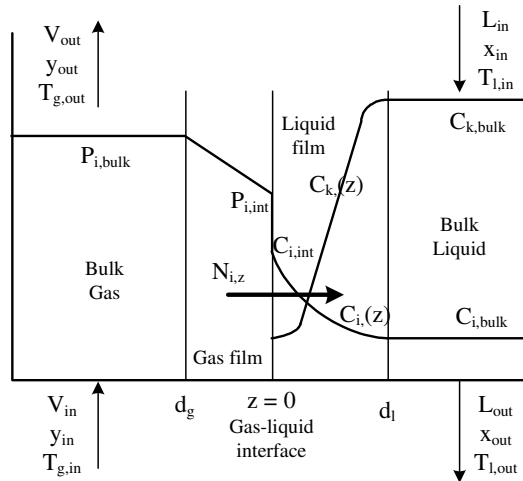
Figure 2.7 Schematic diagram of the film model as applied to a tray absorption column.

2.5.3 Simulation Model Adopted

In this study, the equilibrium model was adopted to the simulation of equilibrium stages of acid gas absorption column using aqueous MDEA solution. By using of the equilibrium model, the process design variables that can be observed are amine circulation rate, column temperature profile, and number of trays. The gas and the liquid composition can also be determined.

The equilibrium model is more simple compare to non-equilibrium model which requires much information that is hardly available. Altough numbers of study have been performed on the non-equilibrium model of an absorption column, but really few attempts concentrated on the acid gases absorption using MDEA solvent.

CHAPTER 3

MODELING OF THE ACID GASES ABSORPTION SYSTEM

In Chapter 1, it has been explained that vapor-liquid equilibrium exists on each stage of the absorption column. Meanwhile, the reactions take place between the dissolved acid gases and the solvent components. In this Chapter, the mathematical models on the vapor liquid equilibrium will be described together with the reaction equilibrium accompanied. Furthermore, the mathematical model on the equilibrium stage of acid gas absorption column will be explained.

3.1   Equilibrium Model of Acid Gases-MDEA Solvent

The ElecGC model as the selected model is applied in this study and the detail of the model will be explained briefly in this chapter. Previously, the explanation on the chemical reaction equilibrium and its connection with the vapor liquid equilibrium will be described in section.

3.1.1   Chemical Reaction Equilibrium

In every stage of absorption column, reactions take place in the liquid phase between the acid gas molecules, the MDEA molecules and the water molecules. At the steady state condition, the compositions of the components are related by the reaction equilibrium and the component balance. The reaction equilibrium constants are defined in the form of mole fractions of components. The non-ideality of the system is addressed using the activity coefficients.

The reactions involved in the acid gases absorption into aqueous MDEA solution are described below.

Dissociation of water:

$$2H_2O \leftrightarrow H_3O^+ + OH^- \qquad (3.1a)$$

$$K_{H_2O} = \frac{\gamma^*_{H_3O^+} \gamma^*_{OH^-}}{\gamma^2_{H_2O}} \frac{x_{H_3O^+} x_{OH^-}}{x^2_{H_2O}} \qquad (3.1b)$$

Protonation of MDEA

$$MDEAH^+ + H_2O \leftrightarrow MDEA + H_3O^+ \qquad (3.2a)$$
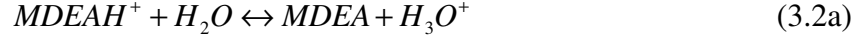
$$K_{MDEA} = \frac{\gamma_{MDEA} \gamma^*_{H_3O^+}}{\gamma^*_{MDEAH^+} \gamma_{H_2O}} \frac{x_{MDEA} x_{H_3O^+}}{x_{MDEAH^+} x_{H_2O}} \qquad (3.2b)$$

Dissociation of Carbon dioxide

$$CO_2 + 2H_2O \leftrightarrow HCO_3^- + H_3O^+ \qquad (3.3a)$$

$$K_{CO_2} = \frac{\gamma^*_{HCO_3^-} \gamma^*_{H_3O^+}}{\gamma^*_{CO_2} \gamma^2_{H_2O}} \frac{x_{HCO_3^-} x_{H_3O^+}}{x_{CO_2} x^2_{H_2O}} \qquad (3.3b)$$

$$HCO_3^- + H_2O \leftrightarrow CO_3^{2-} + H_3O^+ \qquad (3.4a)$$

$$K_{HCO_3^-} = \frac{\gamma^*_{CO_3^{2-}} \gamma^*_{H_3O^+}}{\gamma^*_{HCO_3^-} \gamma_{H_2O}} \frac{x_{CO_3^{2-}} x_{H_3O^+}}{x_{HCO_3^-} x_{H_2O}} \qquad (3.4b)$$

Dissociation of Hydrogen Sulfide

$$H_2S + H_2O \leftrightarrow H_3O^+ + HS^- \qquad (3.5a)$$

$$K_{H_2S} = \frac{\gamma^*_{HS^-} \gamma^*_{H_3O^+}}{\gamma^*_{H_2S} \gamma_{H_2O}} \frac{x_{HS^-} x_{H_3O^+}}{x_{H_2S} x_{H_2O}} \qquad (3.5b)$$

$$HS^- + H_2O \leftrightarrow S^{2-} + H_3O^+ \qquad (3.6a)$$
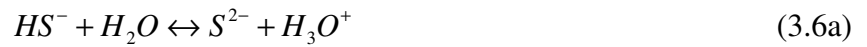
$$K_{HS^-} = \frac{\gamma^*_{S^{2-}} \gamma^*_{H_3O^+}}{\gamma^*_{HS^-} \gamma_{H_2O}} \frac{x_{S^{2-}} x_{H_3O^+}}{x_{HS^-} x_{H_2O}} \qquad (3.6b)$$

The reaction equilibrium constants are calculated using eq. (3.7). The parameters used for all components are given in Table 3.1.

$$\ln K_{reaction\ i} = A_i + B_i/T + C_i \ln T + D_i T \qquad (3.7)$$

The acid gases reactions with aqueous alkanolamine solution produce some ions. The amount of the ions produced is determined using reaction equilibrium, the liquid

27

component balance and the charge balance. The material balances of each component and the charge balance for the system can be presented as:

$$[MDEA]_{total} = [MDEA] + \left[MDEAH^+\right] \tag{3.8}$$

$$[H_2S]_{total} = \alpha_{H_2S}[MDEA]_{total} = [H_2S] + \left[HS^-\right] + \left[S^{2-}\right] \tag{3.9}$$

$$[CO_2]_{total} = \alpha_{CO_2}[MDEA]_{total} = [CO_2] + \left[HCO_3^-\right] + \left[CO_3^{2-}\right] \tag{3.10}$$

$$\left[MDEAH^+\right] + \left[H_3O^+\right] = \left[OH^-\right] + \left[HCO_3^-\right] + 2\left[CO_3^{2-}\right] + \left[HS^-\right] + \left[S^{2-}\right] \tag{3.11}$$

For a system that contains only one component of acid gas in the gas phase (CO_2 or H_2S), the other acid gas component attributes can be removed. For example if only CO_2 acted as the acid gas, the dissociation of hydrogen sulfide, the H_2S component balance and the HS^- and S^{2-} ions in the charge balance are neglected.

Furthermore, phase equilibrium occurs for the neutral components in the liquid and the gas phases. The determination of the phase equilibrium model is given in the section 3.1.3. The composition of the component in the liquid phase has to be solved in order to make the vapor liquid equilibrium determination complete.

Table 3.1 Equilibrium reaction constant parameters

Reaction	A	B	C	Sources
$\ln K_{H_2O}$	132.899	-13445.9	-22.4773	Austgen (1989)
$\ln K_{CO_2}$	231.465	-12092.1	-36.7816	Austgen (1989)
$\ln K_{HCO_3^-}$	216.049	-12431.7	-35.4829	Austgen (1989)
$\ln K_{H_2S}$	214.582	-12995.4	-33.5471	Edwards et al (1978)
$\ln K_{HS^-}$	-32	-3338	0	Austgen (1989)
$\ln K_{MDEA}$	-46.086	-4756.9	6.4268	Posey (1996)

3.1.2   Astarita Representation of Chemical Equilibrium

The reaction equilibrium constants, the component balance and charge balance have to be solved simultaneously in order to calculate the liquid phase composition. The set of eq.

(3.1) to (3.11) are highly non-linear and can be solved using Newton method. Such method needs very good initial guesses that are really close to the solution values in order to get the solution. Hoff (2003) used the Astarita representation to solve the non-linear equations in calculating the equilibrium composition for CO_2 absorption using MEA and MDEA solvent. In this study, the Astarita representation was not only applied to the CO_2-MDEA-water system, but also for H_2S-MDEA-water system, as well as CO_2-H_2S-MDEA-water system.

3.1.2.1 Astarita Representation for System of Acid Gas/MDEA/Water (for Only One Volatile Component CO_2 or H_2S)

If only one volatile component exist (eg: CO_2), combination of the reactions (3.2) and (3.3) produces:

$$CO_2 + MDEA + H_2O \leftrightarrow MDEAH^+ + HCO_3^- \tag{3.12}$$
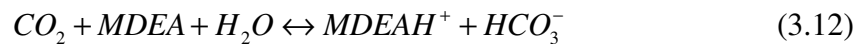
$$K_{abs1} = \frac{K_{CO_2}}{K_{MDEA}} = \frac{\left[MDEAH^+ \right]\left[HCO_3^- \right]}{[MDEA][CO_2][H_2O]} \tag{3.13}$$

One other equilibrium is required to describe how the chemically combined CO_2 distributed between two different forms of bicarbonate and carbonate. Combination of the eq. (3.2) and (3.4) yields the bicarbonate/carbonate equilibrium

$$MDEA + HCO_3^- \leftrightarrow MDEAH^+ + CO_3^{2-} \tag{3.14}$$
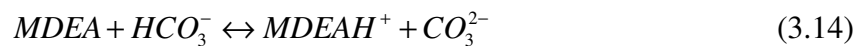
$$K_{C1} = \frac{K_{HCO_3^-}}{K_{MDEA}} = \frac{\left[MDEAH^+ \right]\left[CO_3^{2-} \right]}{[MDEA]\left[HCO_3^- \right]} \tag{3.15}$$

To simplify the derivation, the chemical species are now renamed as follows:

A = CO_2	B_4 = CO_3^{2-}
B_1 = MDEA	C_1 = H_2O
B_2 = $MDEAH^+$	C_2 = H_3O^+
B_3 = HCO_3^-	C_3 = OH^-

Two important concepts are introduced: the molarity (mol/l) of the chemical solvent and the degree of saturation (γ). The molarity m is the total equivalent concentration of the species in the liquid phase that may react equimolarly with A, or the concentration of the

amine. The degree of saturation Υ is defined as follow: $\bar{\Upsilon}m$ is the total concentration of chemically combined A in the liquid phase. Υm is not the total of A in the liquid phase because some of A will be physically absorbed, with concentration [A]. Value of Υ is varies from 0.57 for loading around 1.2 to value very near to 1 for loading 0.001. The total component of A or loading A is, therefore,

$$\bar{\Upsilon}m = [A] + \Upsilon m \tag{3.16}$$

The MDEA and CO_2 balance in the liquid can be formulated as:

$$m = [B_1] + [B_2] \tag{3.17}$$

$$\Upsilon m = \bar{\Upsilon}m - [A] = [B_3] + [B_4] \tag{3.18}$$

To choose the initial concentration, all chemically combined CO_2 is assuming the form of bicarbonate. Therefore, the values of $[B_j]^0$ are:

$$
\begin{aligned}
[B_1]^0 &= m(1-\Upsilon) \\
[B_2]^0 &= m\Upsilon \\
[B_3]^0 &= m\Upsilon \\
[B_4]^0 &= 0
\end{aligned}
\tag{3.19}
$$

Reaction (3.14) is preceded to the right until equilibrium is reached. This has the advantage that the equilibrium value for the extent of reaction ξ_1 will be positive. From eq. (3.14) components concentration at equilibrium are:

$$
\begin{aligned}
[B_1] &= m(1-\Upsilon) - \xi_1 \\
[B_2] &= m\Upsilon + \xi_1 \\
[B_3] &= m\Upsilon - \xi_1 \\
[B_4] &= \xi_1
\end{aligned}
\tag{3.20}
$$

Substituting the value of $[B_j]$ to the eq. (3.15) yields:

$$
\begin{aligned}
K_{C1} &= \frac{\left[MDEAH^+\right]\left[CO_3^{2-}\right]}{[MDEA]\left[HCO_3^-\right]} = \frac{[B_2][B_4]}{[B_1][B_3]} \\
&= \frac{(m\Upsilon + \xi_1)\xi_1}{\left[m(1-\Upsilon) - \xi_1\right](m\Upsilon - \xi_1)}
\end{aligned}
\tag{3.21}
$$

The solution of ξ_1 is given as roots of second order polynomial. The true solution must satisfy the following constrains in order for all the $[B_j]$ to be non-negative:

$$\xi_1 \geq 0$$
$$\xi_1 \leq m\Upsilon$$
$$\xi_1 \leq m(1-\Upsilon)$$
(3.22)

The solution for ξ_1 which follows the above constrains is

$$\xi_1 = \frac{K_{C1}m + \Upsilon m - m\sqrt{K_{C1}^2 + 6K_{C1}\Upsilon + \Upsilon^2 - 4K_{C1}^2\Upsilon + 4K_{C1}^2\Upsilon^2 - 4K_{C1}\Upsilon^2}}{2(K_{C1}-1)}$$
(3.23)

From the mole balance and charge balance, the concentration of A, C_1, C_2, and C_3 can be calculated as follow.

$$[C_1] = \frac{([H_2O]_{total} + [B_2] - [B_3] - 2[B_4])}{\left(1 + \frac{2K_{H_2O}[B_4]}{K_{HCO_3}[B_3]}\right)}$$
(3.24)

$$[C_2] = [H_2O]_{total} - \frac{K_{H_2O}}{K_{HCO_3}}\frac{[C_1][B_4]}{[B_3]} - [C_1]$$
(3.25)

$$[C_3] = \frac{K_{H_2O}}{K_{HCO_3}}\frac{[C_1][B_4]}{[B_3]}$$
(3.26)

$$[A] = \frac{[B_2][B_3]}{[B_1][C_1]K_{abs}}$$
(3.27)

For the case where only H_2S is absorbed, the following relations are taken:

$$H_2S + MDEA \leftrightarrow MDEAH^+ + HS^-$$
(3.28)

$$K_{abs2} = \frac{K_{H_2S}}{K_{MDEA}} = \frac{[MDEAH^+][HS^-]}{[MDEA][H_2S]}$$
(3.29)
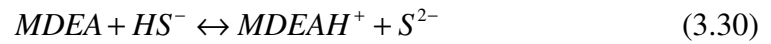
$$MDEA + HS^- \leftrightarrow MDEAH^+ + S^{2-}$$
(3.30)

$$K_{C2} = \frac{K_{HS^-}}{K_{MDEA}} = \frac{[MDEAH^+][S^{2-}]}{[MDEA][HS^-]}$$
(3.31)

The chemical species are now renamed as follows:

D = H_2S $E_4 = S^{2-}$

E_1 = MDEA $F_1 = H_2O$

$E_2 = DEAH^+$ $F_2 = H_3O^+$

$E_3 = HS^-$ $F_3 = OH$

Applying the similar procedure with the CO_2, the solution for extent of the reaction is given below

$$\xi_2 = \frac{K_{C2}m + \Upsilon'm - m\sqrt{K_{C2}^2 + 6K_{C2}\Upsilon' + \Upsilon'^2 - 4K_{C2}^2\Upsilon' + 4K_{C2}^2\Upsilon'^2 - 4K_{C2}\Upsilon'^2}}{2(K_{C2}-1)} \quad (3.32)$$

The concentration of D, F_1, F_2, and F_3 can be calculated as follow:

$$[F_1] = \frac{[H_2O]_{total} + [E_3] + [E_4] - [E_2]}{\left(1 + \dfrac{2K_{H_2O}[E_4]}{K_{HS^-}[E_3]}\right)} \quad (3.33)$$

$$[F_2] = [H_2O]_{total} - [F_1] - \frac{K_{H_2O}[F_1][E_4]}{K_{HS^-}[E_3]} \quad (3.34)$$

$$[F_3] = \frac{K_{H_2O}[F_1][E_4]}{K_{HS^-}[E_3]} \quad (3.35)$$

$$[D] = \frac{[E_2][E_3]}{[E_1]K_{abs2}} \quad (3.36)$$

3.1.2.2 Astarita Representation for System of Acid Gases/MDEA/Water (for Two Volatile Components CO_2 and H_2S)

For system of acid gases-MDEA solvent mixture, a similar procedure is applied. Since the second dissociation of H_2S is very slow, the component S^{2-} will not be added into the calculation and the eq. (3.6) is neglected. The chemical species are renamed as

$A_1 = CO_2$ $\qquad\qquad\qquad\qquad\qquad$ $B_4 = CO_3^{2-}$

$A_2 = H_2S$ $\qquad\qquad\qquad\qquad\qquad$ $B_5 = HS^-$

$B_1 = MDEA$ $\qquad\qquad\qquad\qquad\qquad$ $C_1 = H_2O$

$B_2 = MDEAH^+$ $\qquad\qquad\qquad\qquad\qquad$ $C_2 = H_3O^+$

$B_3 = HCO_3^-$ $\qquad\qquad\qquad\qquad\qquad$ $C_3 = OH^-$

The MDEA, CO_2, and H_2S balance in the liquid can be formulated as:

$$m = [B_1] + [B_2] \quad (3.37)$$

$$\Upsilon m = [B_3] + [B_4] \quad (3.38)$$

$$\Upsilon'm = [B_5] \quad (3.39)$$

The values of the initial concentrations are:

$$[B_1]^0 = m(1 - \Upsilon - \Upsilon')$$
$$[B_2]^0 = m(\Upsilon + \Upsilon')$$
$$[B_3]^0 = m\Upsilon'$$
$$[B_4]^0 = 0 \tag{3.40}$$
$$[B_5]^0 = m\Upsilon'$$

At equilibrium, the concentrations of the components are given below:

$$[B_1] = m(1 - \Upsilon - \Upsilon') - \xi_1$$
$$[B_2] = m(\Upsilon + \Upsilon') + \xi_1$$
$$[B_3] = m\Upsilon' - \xi_1 \tag{3.41}$$
$$[B_4] = \xi_1$$
$$[B_5] = m\Upsilon'$$

Substituting the value of $[B_j]$ to the eq. (3.15) yields:

$$
\begin{aligned}
K_{C1} &= \frac{\left[MDEAH^+ \right]\left[CO_3^{2-} \right]}{[MDEA]\left[HCO_3^- \right]} = \frac{[B_2][B_4]}{[B_1][B_3]} \\
&= \frac{\left(m\Upsilon + m\Upsilon' + \xi_1 \right)\xi_1}{\left[m - m\Upsilon - m\Upsilon' - \xi_1 \right]\left(m\Upsilon - \xi_1 \right)}
\end{aligned} \tag{3.42}
$$

The solution for ξ_1 is derived below

$$
\xi_1 = \frac{K_{C1}m - K_{C1}m\Upsilon' + \Upsilon m + \Upsilon' m - m\sqrt{\begin{array}{l} K_{C1}^2 + 6K_{C1}\Upsilon + \Upsilon^2 - 4K_{C1}^2\Upsilon + 4K_{C1}^2\Upsilon^2 \\ -4K_{C1}\Upsilon^2 - 2K_{C1}^2\Upsilon' + 2K_{C1}\Upsilon' - 6K_{C1}\Upsilon\Upsilon' \\ +K_{C1}^2\Upsilon'^2 - 2K_{C1}\Upsilon'^2 + 2\Upsilon\Upsilon' + \Upsilon'^2 + 4K_{C1}^2\Upsilon\Upsilon' \end{array}}}{2(K_{C1} - 1)} \tag{3.43}
$$

The concentration of A_1, A_2, C_1, C_2, and C_3 can be calculated as follows:

$$[C_1] = \frac{[H_2O]_{total} - [B_5] - 2[B_3] - 3[B_4] + [B_2]}{\left(1 + \dfrac{[B_2]K_{MDEA}}{[B_1]} \right)} \tag{3.44}$$

$$[C_2] = \frac{[B_2][C_1]K_{MDEA}}{[B_1]} \tag{3.45}$$

$$[C_3] = \frac{[C_1]^2 K_{H_2O}}{[C_2]} \tag{3.46}$$

33

$$[A_1] = \frac{[B_2][B_3]}{[B_1][C_1]K_{abs1}}$$ (3.47)

$$[A_2] = \frac{[B_2][B_5]}{[B_1]K_{abs2}}$$ (3.48)

3.1.2.3   Conversion of Equilibrium Constants

The equilibrium reaction constants in Section 3.1.1 are reported in mole fraction scale. Since the liquid speciation calculation is performed based on molar concentration, a conversion for the equilibrium constant is required especially for the first reaction of CO_2 dissociation. This reaction equilibrium constant is corrected by the molar density of water, $c_w{}^0$.

$$K_{CO_2} = \frac{K_{CO_2,origin}}{c_w^0} = \frac{1}{c_w^0}\exp\left(231.465 - 12092.1/T - 36.7816\ln T\right)$$ (3.49)

The other conversion that has to be adjusted is the reaction equilibrium constants. As shown by eq. (3.1) to eq. (3.6), the activity coefficients are put together with the value of mole fractions in the establishment of the reaction equilibrium constants. For example reaction (3.3)

$$K_{CO_2} = \frac{\gamma_{HCO_3^-}^* \gamma_{H_3O^+}^*}{\gamma_{CO_2}^* \gamma_{H_2O}^2} \frac{x_{HCO_3^-} x_{H_3O^+}}{x_{CO_2} x_{H_2O}^2}$$ (3.50)

$$K_i = K_{\gamma,i} K_{x,i}$$ (3.51)

Hoff (2003) called the $K_{x,i}$ as the *apparent* equilibrium constants. These apparent equilibrium constants are the ones that are used in Astarita representation to calculate the liquid phase composition. So that, the value $K_{x,i}$ have to be determined by the following equation. The activity coefficient values are calculated using the activity coefficient model which is described in the Section 3.1.5.

$$K_{x,i} = \frac{K_i}{K_{\gamma,i}}$$ (3.52)

3.1.3 Vapor Liquid Equilibrium

After the liquid composition has been solved, the vapor liquid equilibrium can be determined. In this part, the vapor liquid equilibrium model is given. The basis for the formulation of vapor-liquid equilibrium was described using chemical potentials which must be the same in both phases.

$$\mu_i^V = \mu_i^L \tag{3.53}$$

However, the chemical potential term cannot relate distinctly the temperature, pressure, liquid phase composition, and gas phase composition. Since the chemical potential has some practical and conceptual shortcomings, the term fugacity, f, was introduced.

$$f_i^V = f_i^L \tag{3.54}$$

The non-idealities of the liquid phase involve the two types of component, non-supercritical component and supercritical component. The components are non-supercritical if they are liquid at temperature and pressure system. The supercritical components are the components which is gas or solid at temperature and pressure system. In the case of acid gases treatment, the non-supercritical components are water and alkanolamine while the supercritical components are CO_2, H_2S, and CH_4. Different approach is used to treat the two types of component. Eq. (3.2) is applied to non-supercritical components while eq. (3.28) to the supercritical components.

$$y_i \phi_i^V P = \gamma_i x_i \phi_i^{sat} P_i^{sat} \exp\left(\frac{V_i^{sat}}{RT}\left(P - P_i^{sat}\right)\right) \tag{3.55}$$

$$y_i \phi_i^V P = \gamma_i^* x_i H_{i,S}^0 \exp\left(\frac{V_{i,S}^\infty}{RT}\left(P - P_i^{sat}\right)\right) \tag{3.56}$$

where ϕ_i^V is the fugacity coefficient, y_i is the fraction of the component in gas phase and P is total pressure of gas phase. ϕ_i^{sat} is the fugacity coefficient at saturation of each component, x_i is the mole fraction of the component in the liquid phase, γ_i is the activity coefficient of component i, while P_i^{sat} is saturated pressure at temperature system. $H_{i,s}$, V_i^{sat} and $V_{i,S}^\infty$ are Henry's law constant at system condition, saturation molar volume of component i, and molar volume of component i at infinite dilution, respectively. The saturated pressure of water is estimated using the Antoine's equation below.

$$\ln P_w^{sat}[kPa] = 16.5362 - \frac{3985.44}{T[K] - 38.9974} \tag{3.57}$$

The water molar volume (V_w^{sat}) is taken to be 18.0 cm^3/mole (Lee, 1996). The partial molar volume of gas at infinite dilution in water is calculated using the following equation

$$V_{i,S}^{\infty} = a_i + b_i T + c_i T^2 \tag{3.58}$$

with the coefficient a_i, b_i, and c_i are given in Table 3.2.

Table 3.2 Coefficients for partial molar volume at infinite dilution in water

Component	a	b	c
CO_2	74.31498	-0.309091	5.7 x 10^{-4}
H_2S	78.70247	-0.32458	6 x 10^{-4}
CH_4	80.1504	-0.32459	6.102 x 10^{-4}

Source : Brelvi and O'Connell (1972)

3.1.4 Fugacity Coefficient Model

The fugacity coefficient of components in the gas phase is required for calculating the deviation of gas fugacity from the ideal gas. This value is important for calculating the vapor-liquid equilibrium. In this study, Peng-Robinson equation of state is used to calculate the fugacity coefficient of the components in the gas phase. The equation is described as follow:

$$P = \frac{RT}{v-b} - \frac{a}{v(v+b) + b(v-b)} \tag{3.59}$$

where constants a and b for pure component are given by

$$a_i = 0.45724 \left(\frac{R^2 T_{c,i}^2}{P_{c,i}} \right) \alpha$$

$$b_i = 0.0778 \left(\frac{RT_{c,i}}{P_{c,i}} \right) \tag{3.60}$$

36

Subscript c denotes the critical point and α is the temperature-dependent function which takes into account the attractive forces between molecules. The values of α are calculated using eq. (3.61).

$$\alpha = \left(1 + \varpi_i \left(1 - T_r^{1/2}\right)\right)^2 \tag{3.61}$$

T_r is the reduced temperature T/T_C and ϖ is function of acentric factor ω, which can be derived from eq. (3.62).

$$\varpi_i = 0.37464 + 1.54226 \cdot \omega_i - 0.26992 \cdot \omega_i^2 \tag{3.62}$$

For mixture, the following mixing rules are used

$$\begin{aligned} a &= \sum_i \sum_j y_i y_j a_{ij} \\ b &= \sum_i y_i b_i \\ a_{ij} &= \left(1 - k_{ij}\right)\sqrt{a_i a_j} \end{aligned} \tag{3.63}$$

In the compressibility factor form, the Peng-Robinson equation of state is transform to

$$Z = \frac{v}{v-b} - \frac{av}{RT\left(v^2 + 2vb - b^2\right)} \tag{3.64}$$

Rearranging the eq. (3.64), a polynomial form of compressibility factor is obtained as

$$Z^3 - (1-B)Z^2 + \left(A - 3B^2 - 2B\right)Z - \left(AB - B^2 - B^3\right) = 0 \tag{3.65}$$

where A and B are defined below

$$\begin{aligned} A &= \sum_i \sum_j y_i y_j A_{ij} \\ B &= \sum_i y_i B_i \\ A_{ij} &= \left(A_i A_j\right)^{1/2}\left(1 - k_{ij}\right) \end{aligned} \tag{3.66}$$

k_{ij} are set to 0

$$\begin{aligned} A_i &= a_i \left(\frac{P}{R^2 T^2}\right) \\ B_i &= b_i \left(\frac{P}{RT}\right) \end{aligned} \tag{3.67}$$

To calculate the fugacity coefficient, the following relations is used:

$$\ln\left(\phi_i\right) = \frac{B_i}{B}(Z-1) - \ln\left(Z-B\right) - \frac{A}{B\sqrt{8}} \ln\left[\frac{Z+\left(1+\sqrt{2}\right)B}{Z+\left(1-\sqrt{2}\right)B}\right]\left[\frac{2\sum_i y_i A_i}{A} - \frac{B_i}{B}\right] \tag{3.68}$$

37

Critical properties are required to obtain the parameters above. The MDEA component is assumed to be non-volatile and only the acid gases, hydrocarbon and water exist in the gas phase. The critical properties of the components involved are given in Table 3.3.

Table 3.3 Critical properties of gas phase components

Component	MW	T_C [K]	P_C [bar]	ω
H_2O	18.015	647.13	220.55	0.345
CH_4	16.043	190.58	46.04	0.011
CO_2	44.01	304.19	73.82	0.228
H_2S	34.082	373.53	89.63	0.083
MDEA	119.164	678	38.8	1.304

Source: Yaws, Chemical Properties Handbook (1999)

3.1.5 Activity Coefficient Model

The prediction of the activity coefficient is important to calculate the vapor liquid equilibrium and reaction equilibrium constant. The applications of activity coefficient to the vapor liquid equilibrium are shown by eq. (3.55) and (3.56). Activity coefficient is required to calculate the composition of the liquid phase from the reaction equilibrium constant. In the vapor liquid equilibrium, the activity coefficient is assigned only to neutral components (H_2O, CO_2, H_2S, and CH_4). Since the reaction also involves the ions, the activity coefficient model for electrolyte has to be determined.

There were various models proposed, such as NRTL, UNIQUAC, and UNIFAC. ElecGC model by Lee (1996) use the combination of the UNIFAC model and derivation of Gibbs-Duhem equation applied to calculate the activity coefficient of the neutral components. The UNIFAC model is applied to a system where ions do not exist. Since the acid gas aqueous alkanolamine systems contain ions which interact with the neutral ones, the value of activity coefficient has to be corrected. Lee (1996) used Gibbs-Duhem equation to solve this problem. The ions are treated using the mean spherical approximation (MSA) theory and Born's equation to cope with the change of reference state from

infinite dilution in water to infinite dilution in aqueous alkanolamine solution. The ElecGC model is described as

$$\ln \gamma_i = \ln \gamma_i^{UNIFAC} + \ln \gamma_i^{GD}$$
$$\ln \gamma_j = \ln \gamma_j^{MSA} + \ln \gamma_j^{Born}$$

(3.69)

where i is for all neutral species and j is for all ions. Each of the term is explained further in section.

3.1.5.1 Activity Coefficient Normalization

Activity coefficient is used to measure deviation of the liquid phase from ideality. In this work, the solvent activity coefficient value approach 1 as the solvent mole fraction approaches 1. The solute and ions activity coefficient value approach 1 as its mole fraction approaches 0 in solvent.

$$\text{Solvents: } \gamma_i \to 1, \text{ as } x_i \to 1$$

(3.70)

$$\text{Solutes, ions: } \gamma_i^* \to 1, \text{ as } x_i \to 0 \text{ in water}$$

(3.71)

Since solutes and ions are normalized differently than water, their activity coefficients are termed as unsymmetrically normalized. The convention for the activity coefficients of solvents is known as symmetrically normalized. The superscript * is an unsymmetric convention of activity coefficient.

The unsymmetric activity coefficient is derived from the symmetric activity coefficient by division with the symmetric activity coefficient at infinite dilution (Thomsen, 2005):

$$\gamma_i^* = \frac{\gamma_i}{\gamma_i^\infty} \text{ where } \gamma_i^\infty = \lim_{\substack{x_i \to 0 \\ x_{j \neq i} = 0}} \gamma_i$$

(3.72)

where γ_i^∞ is the symmetric activity coefficient of i at infinite dilution in the solvent. The unsymmetric activity coefficients utilized in the vapor liquid equilibrium and reaction equilibrium are derived from the above equation.

3.1.5.2   The UNIFAC Model

The UNIFAC is the abbreviation of Universal quasichemical Functional Activity Coefficient. The model works based on functional groups that built in a molecule and it is called group-contribution method. The UNIFAC method provides a reasonable method for predicting the properties of mixtures in the absence of reliable experimental data. For a mixture, the intermolecular parameter of the functional groups can be found from the other mixtures that have the same functional groups. The UNIFAC model contains two sub terms which are expressed below:

$$\ln \gamma^{UNIFAC} = \ln \gamma^C + \ln \gamma^R \tag{3.73}$$

The subscript C and R stands for combinatorial and residual. The combinatorial part is given by the following equation:

$$\ln \gamma^C = \ln \frac{\Phi_i}{x_i} + \frac{z}{2} q_i \ln \frac{\theta_i}{\Phi_i} + l_i - \frac{\Phi_i}{x_i} \sum_j x_j l_j \tag{3.74}$$

$$l_i = \frac{z}{2}(r_i - q_i) - (r_i - 1); \quad z = 10; \tag{3.75}$$

$$\theta_i = \frac{q_i x_i}{\sum_j q_j x_j} \quad ; \qquad \Phi_i = \frac{r_i x_i}{\sum_j r_j x_j} \tag{3.76}$$

$$r_i = \sum_k v_k^{(i)} R_k \qquad q_i = \sum_k v_k^{(i)} Q_k \tag{3.77}$$

where x_i is the mole fraction of component i; θ_i and Φ_i are the area fraction and segment (similar to volume) fraction. Parameter R_i and Q_i are the measures of molecular van der Waals volumes and molecular surface areas of component i. $v_k^{(i)}$ is the number of k group in component i. The residual part of UNIFAC equation is given by:

$$\ln \gamma^R = \sum_k v_k^{(i)} \left[\ln \Gamma_k - \ln \Gamma_k^i \right] \tag{3.78}$$

where Γ_k is the group residual activity coefficient, and Γ_k^i is the residual activity coefficient of group k. Γ_k can be expressed as:

$$\ln \Gamma_k = q_k \left[1 - \ln\left(\sum_m \Theta_m \Psi_{mk} \right) - \sum_m \Theta_m \Psi_{km} / \sum_n \Theta_n \Psi_{nm} \right] \tag{3.79}$$

$$\Theta_m = \frac{Q_m X_m}{\sum_m Q_m X_m} \qquad \text{and} \quad X_m = \frac{\sum_j v_m^{(j)} x_j}{\sum_j \sum_n v_n^{(j)} x_j} \tag{3.80}$$

$$\Psi_{mn} = \exp\left[-\left(a_{mn} + \frac{b_{mn}}{T} + \frac{c_{mn}}{T^2}\right)/RT\right] \tag{3.81}$$

The required parameters for the use of UNIFAC are group volume, R_k, group surface area, Q_k, and interaction parameters, Ψ_{nm}. Lee (1996) applied eq. (3.81) to calculate the interaction parameters. The group division of MDEA based on Wu-Sandler's prescription (1991) was used and shown in Figure 3.1. Table 3.4 exhibits the value of group volume and group surface area parameter of the UNIFAC equation. The CH_4, CO_2, H_2S, and H_2O components are stand alone as single group.
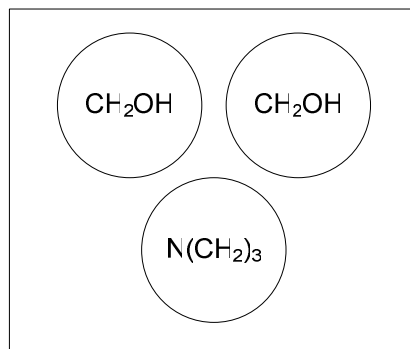
Figure 3.1 Group division for MDEA for UNIFAC model

Table 3.4 Group volume and group surface area parameters for UNIFAC model

Functional group	R_k	Q_k
CO_2	1.3000	1.12
H_2S	1.1723	1.070
CH_4	1.2390	1.152
H_2O	0.9200	1.400
$N(CH_2)_3$	2.5353	2.020
CH_2OH	1.2044	1.124

Sources: Fredenslund et al (1977), Bondi (1968)

3.1.5.3   The MSA Model

As explained in Section 3.1.5, the liquid phase in acid gases absorption using aqueous MDEA consists not only of the neutral components, but also ions. The ions that are

formed by the acid gases-solvent reactions comprise of $MDEAH^+$, HCO_3^-, CO_3^{2-}, HS^-, S^{2-}, H_3O^+, and OH^-. The ions are treated using the mean spherical approximation (MSA) theory. Born's equation is used to handle the change of reference state from infinite dilution in water to infinite dilution in aqueous alkanolamine solution.

The mean spherical approximation (MSA) is a simple analytical theory that is very powerful to calculate the thermodynamic properties of electrolytes (Nakhaei, 2004). The MSA includes the volume of the ions, the charge, the concentration of the ions, and the short range as well as the long range interaction effect, so that it can be used for a wide range concentration of the solutions. A hard sphere equation of state (HS-EoS) is put together to the model to represent the effect of ions volume. The MSA expression for the activity coefficient of electrolyte solution can be presented by the expression below:

$$\ln \gamma_j^{MSA} = \ln \gamma_j^{ele} + \ln \gamma_j^{HS} \tag{3.82}$$

where, $\quad \ln \gamma_j^{ele} = \dfrac{z_j e^2}{\varepsilon kT} \left(\dfrac{2\Gamma a_j}{\sigma_j \alpha^2} - \dfrac{z_j}{\sigma_j} \right) - \dfrac{P_n \sigma_j}{4\Delta} \left(\Gamma a_j + \dfrac{\pi}{12\Delta} \alpha^2 P_n \sigma_j^2 \right) \tag{3.83}$

$$\alpha^2 = \dfrac{4\pi e^2}{\varepsilon kT} \tag{3.84}$$

$$\Delta = 1 - \xi_3 \tag{3.85}$$

$$\xi_n = \dfrac{\pi}{6} \sum_{j=1}^{n} \rho_j \sigma_j^n \quad n = 0,1,2,3 \tag{3.86}$$

$$P_n = \dfrac{1}{\Omega} \sum_{j=1}^{N} \dfrac{\rho_j \sigma_j z_j}{1 + \Gamma \sigma_j} \tag{3.87}$$

$$\Omega = 1 + \dfrac{\pi}{2\Delta} \sum_{j=1}^{N} \dfrac{\rho_j \sigma_j^3}{1 + \Gamma \sigma_j} \tag{3.88}$$

$$a_j = \dfrac{\alpha^2 \left[z_j - \left(\dfrac{\pi}{2\Delta} \right) \sigma_j^2 P_n \right]}{2\Gamma \left(1 + \Gamma \sigma_j \right)} \tag{3.89}$$

where N = number of species in the solution

ρ_i = number density of ion j [m^{-3}]

σ_j = diameter of ion j [m]

z_j = charge of ion j

42

ε_j = dielectric constant of solution

Γ = shielding length

k = Boltzmann's constant = 1.38045 x 10^{-16} erg/K

T = temperature in Kelvin

e = electronic charge = 1.60206 x 10^{-19} coulomb

The shielding length can be obtained from the formula below

$$4\Gamma^2 = \alpha^2 \sum_{j=1}^{N} \rho_j \left[\frac{z_j - (\pi/2\Delta)\sigma_j^2 P_n}{1+\Gamma\sigma_j} \right]^2 \tag{3.90}$$

The term Γ represents the long-range electrostatic interaction while the term P_n represents the short-range interaction. An iterative calculation with an initial guess for $\Gamma = \kappa/2$, where κ is the Debye inverse length, the eq. (3.90) can be solved.

$$\kappa = \alpha \left(\sum_{j=1}^{N} \rho_j z_j^2 \right)^{1/2} \tag{3.91}$$

The hard sphere (HS) contribution to the activity coefficient of ionic species is expressed as

$$\ln \gamma_j^{HS} = -\ln \Delta + \frac{\sigma_j^3 \xi_0 + 3\sigma_j^2 \xi_1 + 3\sigma_j \xi_2}{\Delta} + \frac{3\sigma_j^3 \xi_1 \xi_2 + 9/2\,\sigma_j^2 \xi_2^2}{\Delta^2} + \frac{3\sigma_j^3 \xi_2^3}{\Delta^3} \tag{3.92}$$

$$\Delta = 1 - \frac{\pi}{6} \sum_j \rho_j \sigma_j^3 \tag{3.93}$$

$$\xi_n = \frac{\pi}{6} \sum_j \rho_j \sigma_j^n \quad ; n = 0,1,2,3 \tag{3.94}$$

Number density of ion (ρ_j) has unit of [m^{-3}] and is defined as

$$\rho_j = N_L C_j \tag{3.95}$$

N_L is the Avogadro number (6.02214178 x 10^{23} mole^{-1}) while C_j is ionic concentration in mole/m^3. The values of σ_j are given in Appendix A.

3.1.5.4 The Born Model

An expression is required to change the activity coefficient from the reference state of infinite dilution in water to the infinite dilution in aqueous alkanolamine solution. The Born contribution is applied to solve this problem and is expressed as

$$\ln \gamma_j^{Born} = \frac{-e^2}{2kT} \frac{z_j^2}{\sigma_j} \left(\frac{1}{\varepsilon_M} - \frac{1}{\varepsilon_W} \right) \tag{3.96}$$

where ε_M and ε_W are the dielectric constants of ion in the aqueous alkanolamine solution and in the pure water continued.

Dielectric constant is the value of compound's ability to stabilize ions. The higher the dielectric constants, the more likely the components exist in the form of ions. The dielectric constant of MDEA is taken from Austgen (1989) who fitted the equation to his experimental results. A mixing rule is required to calculate the value for mixture (ε_{mix}). Equations (3.97-3.99) show the formula to calculate the dielectric constant value which the parameters are listed in Table 3.5.

$$\varepsilon_{MDEA} = A + B\left(\frac{1}{T} - \frac{1}{273.15} \right) \tag{3.97}$$

$$\varepsilon_{H_2O} = A\left(1 - B \cdot \Delta T + C \cdot \Delta T^2 \right) \; ; \Delta T = Tc - 25 \tag{3.98}$$

$$\varepsilon_{mix} = \sum_i x_i^{sf} \varepsilon_i \tag{3.99}$$

where

T = temperature in K

Tc = temperature in ^{o}C

x_i^{sf} = the solute free mass fraction

ε_i = dielectric constant of component i.

Table 3.5 Parameters for dielectric constant

	A	B	C	Ref
MDEA	24.74	8989.3	-	Autsgen (1989)
H_2O	78.54	0.0046	8.8×10^{-6}	Lee (1996)

3.1.5.5 Gibbs-Duhem equation

Lee (1996) modified the Gibbs-Duhem equation to get the activity coefficient derivation. The following equation is applied for each neutral species that take place in the acid gases-MDEA-water system.

44

$$\ln \gamma_i^{GD} = \frac{1}{\displaystyle\sum_k^{\substack{neutral \\ species}} \rho_k} \left[\frac{\Gamma^3}{3\pi} + \frac{\alpha^2}{8} \left(\frac{P_n}{\Delta} \right)^2 - Z^{HS} \sum_i^{\substack{all \\ ion}} \rho_i \right] \tag{3.100}$$

The Z^{HS} is hard sphere compressibility factor that can be found from Carnahan-Starling equation (Carnahan-Starling, 1969) as follow

$$Z^{HS} = \frac{1 + \eta + \eta^2 - \eta^3}{(1-\eta)^3} \tag{3.101}$$

where η is packing factor which can be described as

$$\eta = \frac{\pi \rho \sigma^3}{6} \tag{3.102}$$

ρ is the number density of the component and σ is the hard sphere diameter that can be calculated using eq. (3.103). b is van der Waals volume parameter with unit m^3/mole. The values of critical properties for calculating the parameter b is shown in Table 3.3.

$$\sigma = \left(\frac{3b}{2N_L \pi} \right)^{1/3} \tag{3.103}$$

$$b = \frac{RT_c}{8P_c} \tag{3.104}$$

3.1.6   Henry's Law Constants Determination

The Henry's law constants are required to fulfill the vapor-liquid equilibrium determination. The Henry's law constant of CO_2 and H_2S are determined base on their value in pure water. The CH_4 is treated based on its solubility in both solvent i.e. water and amine.

The Henry's law constant correlation is a function of temperature. Since the determination of this correlation is based on experimental data, several equations are formed differently. Here, the different determination for the three components is used.

$$\ln H_{i,w} [Pa] = A_i + \frac{B_i}{T} + C_i \ln T + D_i T \qquad i = CO_2, H_2S \tag{3.105}$$

45

$$\ln H_{CH_4,j}\left[bar\right] = A_i + \frac{B_i}{T} + \frac{C_i}{T^2} \qquad (3.106)$$

$$\ln H_{CH4,mix} = x_1 \ln H_{CH4,w} + x_2 \ln H_{CH4,MDEA} - \alpha_{12} x_1 x_2$$
$$\alpha_{12} = 0.0715 \cdot T - 19.531 \qquad (3.107)$$

where x is the mole fraction of the component in the mixture. The subscripts *1* and *2* defined the water and MDEA respectively.

In this study, Henry's constant parameter for CH_4 in MDEA was fitted to Jou-Mather (2006) data with the same correlation used for CH_4 in H_2O. Jou-Mather (2006) used a mixing rule and a parameter related to the deviation of the two solvents from an ideal mixture (α_{12}) to calculate the Henry's law constant of CH_4 in mixture of H_2O/MDEA. Eq. (3.105) shows the applied equation. All the parameter used in Henry's law constants are displayed in Table 3.6.

Table 3.6 Henry's law constants parameters

i/j	A	B	C	D	Ref
CO_2	110.034525	-6789.04	-11.4519	-0.010454	Posey (1996)
H_2S	18.1937	-2808.5	2.5629	-0.01868	Posey (1996)
CH_4 in H_2O	0.1305	7.8879×10^3	-1.4196×10^6		Ferrando, et al (2006)
CH_4 in MDEA	5.6776	1.5357×10^3	-2.6776×10^5		This work

3.2 Equilibrium model of Acid Gases Absorption Process

In this section the equilibrium model for absorption column is provided. Inside the absorption column, the gas from the bottom is counter currently contacted with the liquid solvent from the top. At steady state condition, the absorption column consists of several numbers of stages. In each stage, the vapor phase from the stage below come into contact with the liquid phase descendants from the upper stage. Some amount of acid gases is transferred to the liquid phase during the contact. As the vapor phase move up along the column, the acid gases composition decreases. Figure 3.2 shows the equilibrium stage of absorption column.

The temperature of a stage and also the composition of the gas and liquid phase leaving and entering the stage can be calculated from the column material and energy balance. Equilibrium of the vapor and liquid phase takes place in each stage. The MESH (Mass balance, Equilibrium relationship, Summation equation, and Energy (Heat) balance) are used to solve the composition of individual components an temperature at each stage. The equilibrium relationship has been explained in the previous section.
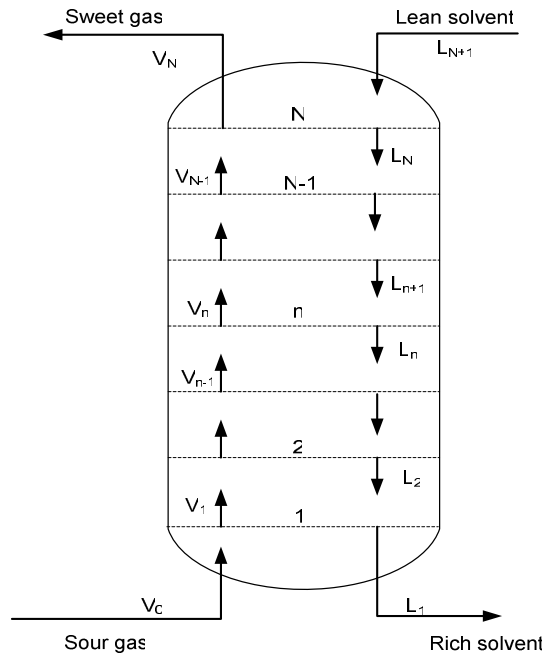
Figure 3.2 Equilibrium tray of absorption column

3.2.1 Material Balance

The material balance calculation of each equilibrium stage involves the gas and the liquid streams entering and leaving the stage. In the absorption column, the calculation of steady state composition and temperature along the column are determined by solving the material and energy balance simultaneously. Figure 3.3 shows the heat and material balance model of one equilibrium stage of absorption. In the gas phase, T is temperature, V is flowrate in mole/hr, W_G is mass flowrate in kg/hr, P_{tot} is total pressure of gas stream, y_i is mole fraction of components, H_G is enthalpy of the gas stream, $P_{par,i}$ is partial pressure of components in gas stream, and V_{H2O} is amount of water in gas. Meanwhile, the specification for the liquid phase consists of; L is flowrate in mole/hr, W_L is mass flowrate in kg/hr, x_j is mole fraction of components in liquid phase, and Cp_L is heat

capacity of the stream. The components i in the gas phase comprise of CO_2, H_2S, CH_4 and H_2O. The existence of the MDEA component can be ignored due to its extremely low volatility. The j components in the liquid phase are CO_2, H_2S, CH_4, H_2O, MDEA and the ions are $MDEAH^+$, HCO_3^-, CO_3^{2-}, HS^-, S^{2-}, H_3O^+, and OH^-.
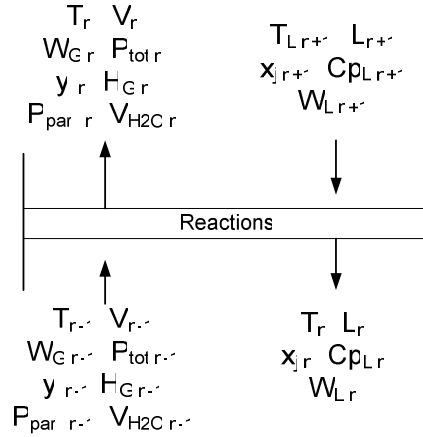
Figure 3.3 Heat and material balance model of one equilibrium stage of absorption

The material balance equation comprises of two general terms namely total material balance and components balances. Both are in the unit of mole flow rate. The equations for both terms are shown below.

Total material balance:

$$V_{n-1} + L_{n+1} = V_n + L_n \qquad (3.108)$$

Components balance:

$$V_{n-1}y_{CH_4,n-1} + L_{n+1}x_{CH_4,n+1} = V_n y_{CH_4,n} + L_n x_{CH_4,n}$$

$$V_{n-1}y_{CO_2,n-1} + L_{n+1}x_{CO_2,total,n+1} = V_n y_{CO_2,n} + L_n x_{CO_2,total,n}$$

$$V_{n-1}y_{H_2S,n-1} + L_{n+1}x_{H_2S,total,n+1} = V_n y_{H_2S,n} + L_n x_{H_2S,total,n} \qquad (3.109)$$

$$V_{n-1}y_{H_2O,n-1} + L_{n+1}x_{H_2O,total,n+1} = V_n y_{H_2O,n} + L_n x_{H_2O,total,n}$$

$$L_{n+1}x_{MDEA,total,n+1} = L_n x_{MDEA,total,n}$$

The x_j in the liquid phase does not only represent the mole fraction of the neutral component but also the ions that are formed from the reactions. The x_j for the components in the liquid phase consists of:

48

$$x_{CO_2,total} = x_{CO_2} + x_{HCO_3^-} + x_{CO_3^{2-}}$$

$$x_{H_2S,total} = x_{H_2S} + x_{HS^-} + x_{S^{2-}}$$

$$x_{MDEA,total} = x_{MDEA} + x_{MDEAH^+}$$

$$x_{H_2O,total} = x_{H_2O} + x_{H_3O^+} + x_{OH^-}$$

(3.110)

3.2.2 Energy Balance

Derivation of the energy balance equations are shown in this section. From figure 3.3, the energy balance of stage n is written as:

$$V_{n-1}H_{G,n-1} + L_{n+1}Cp_{L,n+1}\left(T_{n+1} - T_{ref}\right) + Q_{abs} + Q_{H_2O} =$$
$$V_n H_{G,n} + L_n Cp_{L,n}\left(T_n - T_{ref}\right)$$

(3.111)

Given that the stage number is counted from bottom up, the subscript $n-1$ represents for the gas entering the stage and $n+1$ represents the liquid entering the stage n. The subscript n is for gas or liquid leaving the stage. The Q_{abs} is the heat of absorption for the acid gases absorption into alkanolamine solution while Q_{H2O} is the heat loss or gain associated with water condensing or evaporating.

Enthalpies of gas entering and leaving the stage n are calculated using eq. (3.112). Vaz (1980) and Loh (1987) set the reference temperature to be the same as the temperature of gas inlet to simplify the energy balance equation.

$$H_G = \int_{T_{ref}}^{T} y_i Cp_{i,G}\ dT$$

(3.112)

$$T_{ref} = T_{n-1}$$

The gas heat capacity formula is taken from Yaws (1999) and given in the following formula with the parameters values are specified in Table 3.7.

$$Cp_{G,i} = a_i + b_i T + c_i T^2 + d_i T^3 + e_i T^4$$

(3.113)

The enthalpy loss or gain is calculated using the following equation:

$$Q_{H_2O} = \lambda_{H_2O,T_n}\left(V_{H_2O,n-1} - V_{H_2O,n}\right)$$

(3.114)

49

$$\lambda_{H_2O,T} = 52.053\left(1 - T/647.13\right)^{0.321} \tag{3.115}$$

where λ is heat of vaporization in kJ/mole and T in Kelvin

Table 3.7 Parameter for heat capacity of gas

Component	a	b	c	d	e
CO_2	27.437	4.2315e-2	-1.9555e-5	3.9968e-9	-2.9872e-13
H_2S	33.878	-1.1216e-2	5.2578e-5	-3.8397e-8	9.0281e-12
CH_4	34.942	-3.9957e-2	1.9184e-4	-1.5303e-7	3.9321e-11
H_2O	33.933	-8.4186e-3	2.9906e-5	-1.7825e-8	3.6934e-12

Source: Yaws, Chemical Properties Handbook (1999)

The heat of absorption is the heat produced when a quantity of acid gas is absorbed to change the loading from the initial loading to the final loading. In this matter, the initial loading is the loading of the stage *n-1* and the final loading is the loading of the stage *n*. The quantity of acid gas that is absorbed by stage *n* can also be found from the difference of the mole acid gas in the gas entering the stage and leaving the stage. Furthermore, the heat of absorption derivation is given below

$$Q_{abs} = \Delta H_{abs}\left(V_{acid\ gas,n-1} - V_{acid\ gas,n}\right) \tag{3.116}$$

Bullin (2006) stated that the heat of absorption either for CO_2 or H_2S can be expressed in simplified terms as follows:

$$\text{Heat of absorption} = \begin{bmatrix} \text{Fraction} \\ \text{physically} \\ \text{absorbed} \end{bmatrix}\begin{bmatrix} \text{Heat of} \\ \text{physical} \\ \text{absorption} \end{bmatrix} + \begin{bmatrix} \text{Fraction} \\ \text{ionized} \end{bmatrix}\begin{bmatrix} \text{Heat of} & \text{Heat} \\ \text{physical} & + & \text{of} \\ \text{absorption} & & \text{dissociation} \end{bmatrix} \tag{3.117}$$

Enthalpy of absorption that covers both heat of physical absorption and heat of dissociation can be calculated using the following Gibbs-Helmholtz equation:

$$\left(\frac{\partial \ln P_i}{\partial 1/T}\right)_{x_i} = \frac{-\Delta H_{abs}}{R} \tag{3.118}$$

where P is the partial pressure of the acid gas component i and x is the mole fraction of the acid gas component in the liquid.

The other term that has to be determined is liquid heat capacity, Cp_L. Chiu and Li (1999) reported the heat capacity of aqueous MDEA solution for different amine mass fraction and temperature. The Redlich-Kister equation for excess molar heat capacity expression was applied to count the heat capacity of alkanolamine aqueous solutions. The liquid heat capacity for binary mixture is defined in the following equation.

$$Cp_L = Cp^E + \sum \chi_i Cp_i \qquad (3.119)$$

$$Cp^E = \chi_{H2O} \chi_{MDEA} \sum_{i=1}^{n} A_i \left(\chi_{MDEA} - \chi_{H2O} \right)^{i-1} \qquad (3.120)$$

$$A_i = a_i + b_i T \qquad (3.121)$$

$$Cp_i = c_1 + c_2 T + c_3 T^2 + c_4 T^3 \qquad (3.122)$$

where Cp_L = liquid heat capacity [J/mole K]

Cp^E = excess molar heat capacity [J/mole K]

T = temperature in [Kelvin]

χ_i = mole fraction of components

Subscript: i = MDEA, H_2O

The parameters used in excess molar heat capacity calculation are served in Table 3.8, while the heat capacity of each substance listed in Table 3.9.

Table 3.8 Excess molar heat capacity parameters

Parameters	Values
a_1	-105.74
b_1	0.45871
a_2	11.466
b_2	-0.07449

Source: Chiu and Li (1999)

Table 3.9 Heat capacity parameters for single component

i	A	b	c	d
MDEA	105.151	1.3564	-3.3459×10^{-3}	3.4589×10^{-6}
H_2O	92.053	-3.9953×10^{-2}	-2.1103×10^{-4}	5.3469×10^{-7}

Source: Yaws (1999)

3.2.3 Summation of Phases

For each gas and liquid phase at every stage, the total component mole fraction must be unity. These summation constraints are defined by eq. (3.124). The x_j is for the liquid phase composition while the y_i is for the gas phase.

$$\sum_j x_j = 1$$
$$\sum_i y_i = 1 \tag{3.123}$$

3.3 Other Relations

Several other relations involve in the mathematical models of the absorption column. These relations are the equation to calculate the water content in sour methane and the density of aqueous MDEA solvent.

3.3.1 Water Content in Sour Methane

In natural gas processing, the feed gas that enters the absorption column usually contains water. The calculation of this water content is required in the material and energy balance calculation. Method for calculating the water content in methane was adapted from Maddox (1998). The water content is contributed by CH_4, CO_2, and H_2S. The McKetta-Wehe charts are used to find the value for each gas. The elemental contributor gases to the total water content are calculated by the mol fraction of the gases in the mixture. The equation for the water content approximation is

$$W = yW_{hc} + y_1W_1 + y_2W_2 \tag{3.124}$$

where W = water content in gas mixture [kg/10^6 std m^3]

$\quad W_{hc}$ = water content in sweet gas

$\quad W_1$ = effective water content contribution of H_2S to the gas mixture

$\quad W_2$ = effective water content contribution of CO_2 to the gas mixture

$\quad y$ = mole fraction of sweet gas in mixture

$\quad y_1$ = mole fraction of H_2S in gas mixture

$\quad y_2$ = mole fraction of CO_2 in gas mixture

A mathematical expression needs to be constructed from the charts to facilitate the computer calculation. The pressure function correlation was defined as shown in eq. (3.125). To convert the unit into mole fraction, water content is divided by the value of 751320 (Maddox, 1998). The linear interpolation is applied to calculate the effect of temperature. The values of constants A_1, A_2, and A_3 for carbon dioxide, hydrogen sulfide and methane are given in Appendix A.

$$\log W = A_1 \left(\log P \right)^2 + A_2 \log P + A_3 \tag{3.125}$$

where P in Mpa and Win kg/10^6 std m^3

3.3.2 Density of Aqueous MDEA Solution

In the design of absorption column, the composition of solvent entering the column is usually specified in the unit of either mass fraction or molarity. The density of aqueous MDEA solution must be determined for conversion between the two units. Density of aqueous MDEA solvent used was taken from Al-Ghawas (1989) which is described in the equation below.

$$\rho = K_1 + K_2 T + K_3 T^2$$
$$K_i = k_{i,1} + k_{i,2} w_M + k_{i,3} w_M{}^2 + k_{i,4} w_M{}^3 \tag{3.126}$$

where ρ = density of aqueous MDEA in g/mL

T   = temperature in Kelvin

w_M = MDEA mass fraction in the solvent

The variables $k_{i,j}$ are given in Table 3.10.

Table 3.10 Variable for density of water-MDEA solvent

i\j	$k_{i,j}$			
	1	2	3	4
1	0.715929	0.395951	0.927974	-0.794931
2	2.13799×10^{-3}	-1.98173×10^{-3}	-3.87553×10^{-3}	3.04228×10^{-3}
3	-4.00972×10^{-6}	3.07038×10^{-6}	3.58483×10^{-6}	-2.70947×10^{-6}

Source: Al-Ghawas, H.A. et.al. (1989)

3.4 Stage Efficiency

A stage is said to be theoretical stage when the concentration of components in the gas and liquid streams leaving the stage are in equilibrium. On a real stage it is impossible to reach physicochemical equilibrium since this would require an infinitely long contact time. The different in the behavior of the real and theoretical stages is defined by Murphree stage efficiency. The efficiency of Murphree stages for the *j*-th stage for component *i* is determined from the formula:

$$E_{MV,i,j} = \frac{y_{i,j-1} - y_{i,j}}{y_{i,j-1} - y_{i,j}^*}$$

(3.127)

If the Murphree stage efficiency for component *j* is assumed to be the same for each stage, the Murphree vapor stage efficiency of component *j* on top stage is the same as that on the bottom stage.

$$E_{MV,j,1} = E_{MV,j,N}$$

(3.128)

where $E_{MV,j,1}$ and $E_{MV,j,N}$ are the Murphree stage efficiency of component *j* on the bottom and top stage, respectively. This term also can be expressed with the partial pressure of component i in the contactor

$$\frac{P_{i,j-1} - P_{i,j}}{P_{i,j-1} - P_{i,j}^*} = \frac{P_{i,N-1} - P_{i,N}}{P_{i,N-1} - P_{i,N}^*}$$

(3.129)

where superscript * is the equilibrium value. Murphree stage efficiency is useful to scale-up the design from the equilibrium stage column to the actual stage column.

3.5 Summary

The equilibrium model expressed in this chapter generally is similar with the previous model applied by other researcher (Vaz, 1980; Loh, 1987). The differences exist on the phase equilibrium model and the Astarita representation used to calculate the liquid phase composition. The Astarita representation gives a faster solution in the simulation compare to the Newton method. White this improvement, the time consumed in the simulation part will be less. In the next section, the calculation procedure of an absorption column applied in this study will be explained further.

CHAPTER 4

COMPUTER SIMULATION OF THE ACID GASES ABSORPTION SYSTEM

In Chapter 3, the mathematical model of the acid gases absorption using aqueous MDEA solvent has been discussed. A simulation procedure was developed in this work to perform the rigorous stage-by-stage calculation of the gas absorption column based on the models discussed in Chapter 3. There were several assumptions made in line with the developed models. These assumptions were:

1. The system is an adiabatic system and there is no heat loss to the surrounding.
2. The alkanolamine substance has extremely low volatility and therefore only exists in the liquid phase. At temperature range 130-170°C, the range of vapor pressure of MDEA is 0.01-0.065 bar. At the operating temperature of amine absorption process (<100°C), the vapor pressure of MDEA is very low.
3. Heat of mixing at every stage is negligible.

Figure 4.1 shows the schematic representation of acid gases absorption column from methane using MDEA solvent. The gas phase contains the acid gases, methane and water. The acid gases dissolved in the solvent and so does the methane. The column contains N equilibrium stages where in each of the stage, vapor liquid equilibrium and chemical reaction equilibrium exist.

In designing the absorption column, the general input are the sour gas condition (composition, pressure, temperature and flow rate), and the lean solvent condition (concentration of the amine, temperature, and gas content). For a fixed number of stage required, the major process variables to be calculated were amine circulating rate, outlet gas purity (sweet gas), column temperature profile, and gas and liquid composition profile. The absorption simulation procedure is explained in the Section 4.1.
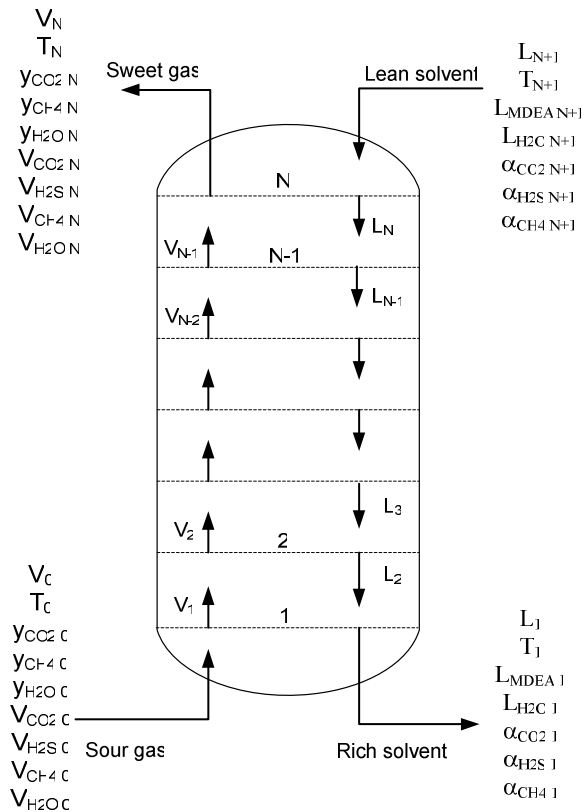
Figure 4.1 Schematic representation of the equilibrium tray of absorption column

4.1 Equilibrium Stage Absorption Column Calculation

The combination of material conservation, energy conservation, equilibrium relationship, and the summation constraint (MESH equations) are required to determine the temperatures and the gas composition at each stage of the contactor. The stage-by-stage calculations are executed to simulate the column at steady state operation. The calculation of the whole contactor starts from the bottom stage of the column. Figure 4.2 shows the algorithm for the equilibrium stage absorption column calculation and the calculation procedure is described below:

1. Input feed gas specification, lean solvent specification, and number of stages (N), and pressure drop per stage (ΔP). The feed gas specification consists of flow rate of feed gas stream (V_0), temperature (T_0), pressure (P_0), and dry gas composition ($y_{CO2,bulk}$, $y_{H2S,bulk}$ and $y_{CH4,bulk}$). The water content in the feed gas is calculated using the eq. (3.124). The feed gas composition is corrected with the additional composition of H_2O.

$$y_{CO_2,0} = y_{CO_2,bulk}\left(1 - y_{H2O}\right)$$

$$y_{H_2S,0} = y_{H_2S,bulk}\left(1 - y_{H2O}\right)$$

$$y_{CH_4,0} = y_{CH_4,bulk}\left(1 - y_{H2O}\right)$$

$$y_{H_2O,0} = y_{H_2O}$$

(4.1)

The lean solvent specification consists of temperature T_{N+1}, wt%-MDEA, flow rate (L_{N+1}), mole MDEA and H_2O in lean solvent ($L_{MDEA,N+1}$ and $L_{H2O, N+1}$) and loading CO_2, H_2S and CH_4 in lean solvent ($\alpha_{CO2,N+1}$, $\alpha_{H2S,N+1}$ and $\alpha_{CH4,N+1}$).

2. Guess the CO_2 and H_2S mole fraction in the sweet gas outlet ($y_{CO2,N,guess}$ and $y_{H2S,N,guess}$) within range 0.05 to 0.00005

3. Guess temperature of the sweet gas ($T_{N,guess}$). The value used is equal to T_{N+1}.

4. Guess temperature of rich solvent, $T_{1,guess}$. The value used is equal to T_0+20^oC.

5. Guess the percent amount of CO_2 and H_2S absorbed during the absorption process (%CO_2 and %H_2S recovery). A simple calculation can be used to calculate the initial value of %CO_2 recovery.

$$\%CO_2\ recovery = \frac{\left(y_{CO_2,sour}\times V_0 - \dfrac{y_{CH_4,sour}\times V_0 \times y_{CO_2,sw}}{\left(1 - y_{CO_2,sw} - y_{H_2S,sw}\right)}\right)}{y_{CO_2,sour}\times V_0}$$

(4.2)

$$\%H_2S\ recovery = \frac{\left(y_{H_2S,sour}\times V_0 - \dfrac{y_{CH_4,sour}\times V_0 \times y_{H_2S,sw}}{\left(1 - y_{CO_2,sw} - y_{H_2S,sw}\right)}\right)}{y_{H_2S,sour}\times V_0}$$

(4.3)

6. Calculate the total loading of CO_2 and H_2S in rich solvent using the following formula:

$$\alpha_{CO_2,1} = \frac{y_{CO_2,sour}\times V_0 \times \%CO_2\ recovery}{L_{MDEA,1}}$$

$$\alpha_{H_2S,1} = \frac{y_{H_2S,sour}\times V_0 \times \%H_2S\ recovery}{L_{MDEA,1}}$$

(4.4)

The MDEA was assumed to be non-volatile, so that the mole MDEA in rich solvent is equal to the amount of MDEA in lean solvent ($L_{MDEA,1} = L_{MDEA,N+1}$).

7. Guess the CH_4 loading in $\alpha_{CH4,1}$. The value of $\alpha_{CH4,1}$ is between 0.015-0.035 mole CH_4/mole MDEA.

Start

Input sour gas specification (T, y_i, $P_{par,i}$, flowrate),
and solvent specification (T, MDEA wt-%, x_{CO2}, x_{CH4}, flow rate)
number of stages (N), column Pressure P_{column}, pressure drop (ΔP)

Guess sweet gas composition ($y_{i,N,guess}$)

Guess T sweet gas ($T_{N,guess}$)

Guess T rich solvent ($T_{1,guess}$)

Guess % CO_2 & % H_2S recovery

Calculate α_{CO2} & α_{H2S} in rich solvent

Guess α_{CH4} in rich solvent

Calculate VLE of stage 1

$\Delta = |P_{tot,1}-P_1|$
$\Delta \leq 0.01$?   No

Yes

Calculate $y_{CO2,N}$ & $y_{H2S,N}$
from overall material balance

$\Delta = |y_{CO2,N,guess} - y_{CO2,N}|/y_{CO2,N,guess}$
$\Delta = |y_{H2S,N,guess} - y_{H2S,N}|/y_{H2S,N,guess}$
$\Delta \leq 0.01$?   No

Yes

Calculate T_1

No $\Delta = |T_1-T_{1,guess}|$
$\Delta \leq 0.1$?

Yes

Perform MESH calculation at stage n to get the
V_n, L_{n+1}, $x_{i,n+1}$, T_{n+1}, and $y_{i,n+1}$

Stage number (n+1) = N   No

Continue
to the next
equilibrium
stage

Yes

No $\Delta = |T_N-T_{N,guess}|$
$\Delta \leq 0.1$?

$\Delta = |y_{CO2,N,guess} - y_{CO2,N}|/y_{CO2,N}$
$\Delta = |y_{H2S,N,guess} - y_{H2S,N}|/y_{H2S,N}$
$\Delta \leq 0.01$?   No

Finish

Figure 4.2 Calculation algorithm for equilibrium stage absorption column

58

8. Perform a vapor liquid equilibrium (VLE) calculation for stage 1, with the input of T_1, $\alpha_{CH4,1}$, $\alpha_{CO2,1}$, $\alpha_{H2S,1}$, and wt% MDEA in rich solvent. The procedure for the VLE calculation is shown in Section 4.2. The wt% MDEA in rich solvent in the rich solvent is assume to be the same as the wt% of MDEA in lean solvent. From the VLE calculation, compare the total pressure ($P_{tot,1}$) with the stage pressure ($P_1=P_0-\Delta P$) with the formula $Diff = P_{tot,1} - P_1$. If the abs($Diff$) is smaller than tolerance, go to the next step, if not return to step 7 and renew the CH_4 loading. The tolerance value is 0.01. If the difference is negative, increase the value of $\alpha_{CH4,1}$. If difference is positive, decrease the value of $\alpha_{CH4,1}$.

9. Calculate the mole fraction of gases in the sweet gas ($y_{i,N}$). A simple mass balance can be applied to correlate the sour gas, lean solvent, rich solvent and sweet gas.

$$V_N = V_0 + L_{N+1} - L_1 \tag{4.5}$$

$$\begin{aligned} V_N y_{CH_4,N} &= V_0 y_{CH_4,0} + L_{N+1} x_{CH_4,N+1} - L_1 x_{CH_4,1} \\ V_N y_{CO_2,N} &= V_0 y_{CO_2,0} + L_{N+1} x_{CO_2,N+1} - L_1 x_{CO_2,1} \\ V_N y_{H_2S,N} &= V_0 y_{H_2S,0} + L_{N+1} x_{H_2S,N+1} - L_1 x_{H_2S,1} \\ V_N y_{H_2O,N} &= V_0 y_{H_2O,0} + L_{N+1} x_{H_2O,N+1} - L_1 x_{H_2O,1} \end{aligned} \tag{4.6}$$

Compare the value of calculated y_{CO2} and y_{H2S} with the specified $y_{CO2,N}$ and $y_{H2S,N}$ ($diff = (y_{CO2,N} - y_{CO2})/ y_{CO2,N}$). If the abs($diff$) is lower than tolerance, go to the next step. If not, renew the value of %CO_2 recovery and %H_2S recovery and return to step 6. The value of tolerance is 0.01. If the difference is positive, decrease values of %CO_2 recovery and %H_2S recovery, vice versa.

10. Perform an overall energy balance between the sour gas, sweet gas, lean solvent and rich solvent to calculate the rich solvent temperature (T_1)

$$T_1 = \frac{L_{N+1}Cp_{L,N+1}\left(T_{N+1}-T_{ref}\right)+Q_{abs}+Q_{H_2O}-V_N Cp_{V,N}\left(T_N-T_{ref}\right)}{L_1 Cp_{L,1}}+T_{ref} \tag{4.7}$$

$$\begin{aligned} Q_{abs} &= \Delta H_{abs,CO_2}\left(\alpha_{CO_2,1}L_{MDEA,1}\right)+\Delta H_{abs,H_2S}\left(\alpha_{H_2S,1}L_{MDEA,1}\right) \\ Q_{H_2O} &= \lambda_{H_2O,T_1}\left(V_{H_2O,0}-V_{H_2O,N}\right) \end{aligned} \tag{4.8}$$

T_{ref} is temperature of the sour gas (T_0).

Compare the calculated value of T_1 with the $T_{1,guess}$ in step 4. If abs($T_1 - T_{1,guess}$) is smaller than 0.1, go to the next step. If not, return to step 4. The next $T_{1,guess}$ is equal to T_1.

11. The next step is the stage by stage calculation until N stage to get the composition of the sweet gas. From Figure 3.2, the MESH equations at stage n have to be performed to get the temperature and the loading of the liquid entering the stage. Figure 3.2 is recall in this procedure to ease the calculation investigation.
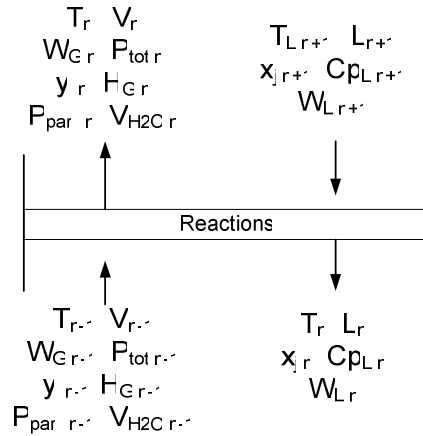
The MESH calculation is quite difficult to be solved simultaneously.

Therefore, the following procedure is used to assist in solving the equations.

a. Guess the mole fraction of the methane in the liquid entering the stage ($\alpha_{CH4,n+1}$). From the previous stage calculation, the gas V_{n-1}, $y_{i,n-1}$, L_n, $x_{i,n}$, and $y_{i,n}$ are specified

b. Solve the total material balance and component material balance to calculate the unknown flow rate and composition using the eq. (3.108) and (3.109).

c. Guess the temperature of liquid entering the stage ($T_{n+1,guess}$) and calculate the $Cp_{L,n+1}$.

d. Perform an energy balance to calculate the temperature of the stage n+1. The eq. (3.111) is rearranged to obtain the T_{n+1}

$$T_{n+1} = \frac{\left(V_n H_{G,n} - V_{n-1} H_{G,n-1} + L_n Cp_{L,n}\left(T_n - T_{ref}\right) - Q_{abs} - Q_{H_2O}\right)}{L_{n+1} Cp_{L,n+1}} + T_{ref} \qquad (4.9)$$

To simplify the equation, the value of T_{ref} is taken as the temperature of the gas inlet to the stage. So the second term inside the bracket is zero, and the equation become

60

$$T_{n+1} = \frac{\left(V_n H_{G,n} + L_n Cp_{L,n}\left(T_n - T_{ref}\right) - Q_{abs} - Q_{H_2O}\right)}{L_{n+1} Cp_{L,n+1}} + T_{ref} \qquad (4.10)$$

e. Compare the value of T_{n+1} with the guess $T_{n+1,guess}$ in step (c). If the difference is smaller than 0.1, go to the next step. If not, return to step c until the value converged. The next $T_{N+1,guess}$ is equal to T_{N+1}.

f. Perform VLE calculation for the stage n+1. The procedure to for VLE calculation is demonstrated in Section 4.2. Compare the total pressure ($P_{tot,n+1}$) with the stage pressure ($P_{n+1} = P_n - \Delta P$) using formula ($Diff = P_{tot,n+1,,1} - P_{n+1}$). If the abs($Diff$) is lower than tolerance, go to the next step. If not, return to stage (a) until the value converged. The tolerance value is 0.01. If the difference is negative, increase the value of $\alpha_{CH4,n+1}$. If difference is positive, decrease the value of $\alpha_{CH4,n+1}$.

12. Perform the material and energy balances and VLE calculation for the next stage followed by all the remaining stage.

After the equilibrium stage is obtained (N), compare the temperature of the gas outlet (T_N) the stage with the $T_{N,guess}$. If the difference (abs($T_N - T_{N,guess}$)) is lower than the tolerance, continue to the next stage. If not, return to step 3. The next $T_{N,guess}$ is equal to T_N. The value of tolerance is 0.1.

13. Compare the $y_{CO2,N}$ and $y_{H2S,N}$ with the guess values in step 2 using formula ($diff_1 = (y_{CO2,N} - y_{CO2,N,guess})/y_{CO2,N}$ & $diff_2 = (y_{H2S,N} - y_{H2S,N,guess})/y_{H2S,N}$). If the abs($diff_1$) and abs($diff_2$) are smaller than 0.01, continue to the next stage. If not, return to step 2. The next guess values are equal to $y_{CO2,N}$ and $y_{H2S,N}$. The calculation is finished.

The vapor liquid equilibrium calculation is treated as part of the absorption column calculation and the procedure is given in the following section.

4.2 Vapor Liquid Equilibrium Calculation

The vapor liquid equilibrium calculation procedure for the CO_2-H_2S-CH_4-aqueous MDEA system which connects with the absorption column is given in this section. The Murphree stage efficiency is applied to the partial pressure calculation for the acid gases. The calculation of the vapor liquid equilibrium requires the component composition in the

liquid phase at the system temperature and solvent composition. This liquid phase composition is discussed in Section 4.3. The block algorithm of the VLE calculation is shown in Figure 4.3 with the steps shown below:

1. Specify loading of the gases (α_{CO2}, α_{H2S} and α_{CH4}) in liquid phase, temperature (T), and solvent composition (wt% MDEA).

2. Calculate liquid phase composition for a given gases loading, temperature, and solvent composition.

3. From the liquid phase composition, the mole fraction of the CO_2, H_2S and CH_4 physically absorb, and H_2O (x_{CO2}, x_{H2S}, x_{CH4}, and x_{H2O}) will be identified.

4. Set the Poynting corrections, and fugacity coefficients of the components to unity.

5. Calculate the Henry's law constant pressure for CO_2, H_2S and CH_4 in the amine solvent by applying eq. (3.105) for CO_2 and H_2S eq. (3.107) for CH_4.

6. Calculate the partial pressure of each component by using eq. (3.55) for H_2O and eq. (3.56) for CO_2, H_2S and CH_4. The partial pressure of CO_2 and H_2S are corrected using the Murphree vapor efficiency as in the eq. (4.11).

$$P_{i,j} = P_{i,j-1} - E_{MV,i,j}\left(P_{i,j-1} - P_{i,j}^*\right) \tag{4.11}$$

7. Calculate total pressure for all four components by using the following equation

$$P_{tot} = \sum \frac{P_i^{par}}{\phi_i} \tag{4.12}$$

8. Calculate the mole fraction of gas phase (y_i) using the following equation

$$y_i = \frac{P_i^{par}}{P_{tot}\phi_i} \tag{4.13}$$

9. Update the value of the Poynting corrections, and the fugacity coefficient of the components.

10. Recalculate the partial pressure, total pressure, and mole fractions as done in step 6, 7, and 8.

11. Redo the calculation of the Poynting corrections, and the fugacity coefficient of the components.

12. Compare the calculated total pressure (P_{tot}) with the previous value ($P_{tot,old}$) using formula ($diff = P_{tot,old} - P_{tot}$). If abs($diff$) is lower than tolerance, vapor liquid equilibrium calculation is finish. If not, return to step 6 until the value converged. The tolerance value is 1×10^{-5}.

The above calculation steps are applied to calculate the vapor liquid equilibrium for each equilibrium stage in the absorption process where the presence of methane was taken into account. A simplified VLE calculation is required to calculate the single gas or mixture gases solubility in the aqueous MDEA solvent. The aim of the gases solubility calculation is to validate the model adopted. The folowing calculation steps are utilized to calculate the gas solubility for single gas (eg. CO_2) in MDEA solvent.

1. Specify loading of the gases (α_{CO2}) in liquid phase, temperature (T), and solvent composition (wt% MDEA).

2. Calculate liquid phase composition for a given gases loading, temperature, and solvent composition.

3. From the liquid phase composition, the mole fraction of the physically absorb, and H_2O (x_{CO2}, x_{H2O}) will be identified.

4. Set the Poynting corrections, and fugacity coefficients of the components to unity.

5. Calculate the Henry's law constant pressure for CO_2 using eq. (3.105.

6. Calculate the partial pressure of each component by using eq. (3.55) for H_2O and eq. (3.56) for CO_2.

7. Calculate total pressure for all four components using the following equation

$$P_{tot} = \sum \frac{P_i^{par}}{\phi_i} \tag{4.12}$$

8. Calculate the mole fraction of gas phase (y_i) using the following equation

$$y_i = \frac{P_i^{par}}{P_{tot}\phi_i} \tag{4.13}$$

9. Update the value of the Poynting corrections, and the fugacity coefficient of the components.

10. Recalculate the partial pressure, total pressure, and mole fractions as done in step 6, 7, and 8.

11. Redo the calculation of the Poynting corrections, and the fugacity coefficient of the components.

12. Compare the calculated total pressure (P_{tot}) with the previous value ($P_{tot,old}$) using formula ($diff = P_{tot,old} - P_{tot}$). If abs($diff$) is lower than tolerance, vapor liquid equilibrium calculation is finish. If not, return to step 6 until the value converged. The tolerance value is $1\text{x}10^{-5}$.

Figure 4.3 Vapor liquid Equilibrium Calculation Algorithm

4.3 Liquid Composition Calculation

The computation scheme to calculate the composition of the liquid for a given input of aqueous alkanolamine solution temperature is listed below. The block algorithm of the liquid phase composition calculation is shown in Figure (4.4).

1. Specify the solution temperature, the solvent composition (wt% of MDEA), acid gases loading ($\alpha_{CO2,input}$, $\alpha_{H2S,input}$) and methane loading ($\alpha_{H2S,input}$).
2. Calculate the chemical reaction equilibrium constants using eq. (3.7)
3. Set the activity coefficients of all components (neutral and ionic) to be 1.
4. Guess the fraction of acid gases loading reacted with amine (Ym). The best guess values for Ym are:

   If loading > 0.9 the value of Ym = 0.8 loading

   If 0.7 < loading ≤ 0.9 the value of Ym = 0.9 loading

   If 0.5 < loading ≤ 0.7 the value of Ym = 0.95 loading

   If loading ≤ 0.5 the value of Ym = 0.98 loading

5. Start the Astarita representation to calculate the mole fraction of components :

   a. Calculate the equilibrium extent reaction value, ξ. If the acid gas is CO_2 then eq. (3.23) is used. If the acid gas is H_2S then eq. (3.32) is applied. For the mixture of CO_2 and H_2S, the value for the extent of reaction is calculated using eq. (3.43).

   b. Calculate mole fraction of elemental components, x. The concentration of the components must be calculated previously using the following equation:

   - for CO_2, the eq. (3.20) and eq. (3.24) to (3.27) are used
   - for H_2S, the eq. (3.33) to (3.36) are used
   - for mixture CO_2 and H_2S, eq. (3.41) and eq. (3.44) to (3.48)are used.

   The concentration of methane is calculated using the multiplication of methane loading with amine concentration m.

6. Calculate the activity coefficient γ_i for the neutral and the ion components using mole fraction calculated in previous step.
7. Calculate *apparent* reaction equilibrium constant, $K_{x,i}$, using eq. (3.52) and the values of γ from step 6.
8. Recalculate the mole fraction using Astarita representation as described in step 5.
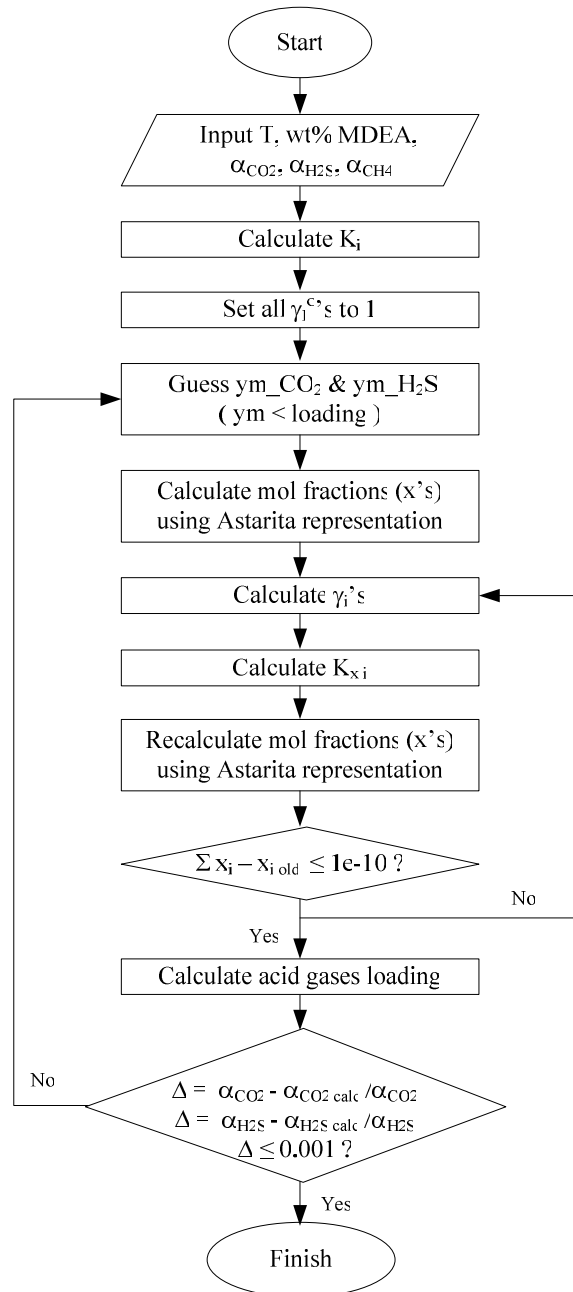
Figure 4.4 Liquid Phase Calculation Algorithm

9. Compare the mole fractions with the previous calculation in step 5. If the deviation ($\Sigma|x_i - x_{i,old}|$) within tolerance (1×10^{-10}), go to step 10. If not, return to step 6.

10. Calculate the total loading. Compare the calculated total loading with the specified loading ($\alpha_{CO2,input}$, $\alpha_{H2S,input}$) using formula ($diff_1 = (\alpha_{CO2,input} - \alpha_{CO2,calc})/\alpha_{CO2,input}$ & $diff = (\alpha_{H2S,input} - \alpha_{H2S,calc})/\alpha_{H2S,input}$). If abs($diff$) are lower than 0.001, the calculation has converged. If not, return to step 4 until the loading calculation converges.

4.4   Summary

In this chapter, a rigorous stage-by-stage calculation procedure for acid gases absorption from methane using aqueous MDEA solvent has been described. A detail explanation on the each step on the procedure has been given. A technique to get the converged solution with the value of the tolerance has also been explained. The Murphree vapor efficiency is applied to the simulation procedure to scale-up the design from the equilibrium stage column to the actual stage column. In Chapter 5, this procedure will be utilized for system of single and mixtureacid gases absorption from methane using MDEA solvent.

CHAPTER 5

RESULTS AND DISCUSSION

The ElecGC model for determining vapor liquid equilibrium of acid gases alkanolamine system was proposed by Lee (1996). In this study, the model was adopted to the system of acid gases in aqueous MDEA system. Lee (1996) applied the Newton method to calculate the liquid phase composition. The Astarita representation employed in this study provides the alternative way to calculate the liquid phase composition. The description of the ElecGC model, Astarita representation and the equilibrium model of acid gases absorption process were given in Chapter 3. Based on the models adopted, the calculation procedure was described in Chapter 4.

The mathematical model and calculation procedure of the absorption column was simulated in the MATLAB program. MATLAB is a high-performance language for technical computing in an easy-to-use environment. The simulations were performed using the iteration procedure of the main routines and sub-routines until the value converged and fulfill the tolerance values given.

The study consists of two parts. The first part is model validation which is performed on the gases solubility and heat of absorption in MDEA solvent at various conditions against published literature data. The second part is model extention for an absorption column calculation for acid gases separation from methane. The sequence of the results is as follow. First, the partial pressures of gas in the system of CO2-MDEA-H2O, H2S-MDEA-H2O, and CH4-MDEA-H2O in various MDEA strengths are described. The heat of absorption of single acid gas in explained further. Second, the simulation results on CO_2 or H_2S absorption from methane is described. Third, the model validation is given for mixture acid gases absorption in MDEA solvent (CO_2-H_2S-MDEA-H_2O system). At last, the simulation results on mixture of acid gases absorption column is provided.

5.1   CO$_2$ Solubility in Aqueous MDEA Solvent

The solubility of CO$_2$ in aqueous MDEA solvent was examined in this study. The CO$_2$ solubility study was in the form of partial pressure calculation on the specified CO$_2$ loading in the solvent. Before the partial pressure prediction is given, the liquid phase composition prediction of the system CO$_2$-MDEA-H$_2$O was conducted to prove the Astarita representation method. Figures 5.1 and 5.2 illustrate the mole fraction of species in the liquid phase for CO$_2$-MDEA-H$_2$O system. The simulation results were compared with the results from Jakobsen et al (2005) which were obtained experimentally at 23 wt% of MDEA and temperature 20°C and 40°C. Generally, the simulation results were found satisfy.

At the two temperatures, the simulation results on the components mole fraction show the same trend. The mole fractions of H$_3$O$^+$ and OH$^-$ were very low and thus, were not shown in the figures. The mole fractions of H$_2$O appear as horizontal lines with value near to unity. Reaction (5.1) shows that when CO$_2$ dissolved in the solvent, the MDEA dissociation is promoted and the MDEAH$^+$ and HCO$_3$$^{2-}$ ions are produced. The higher the loading, the amount (in term of mole) of CO$_2$ reacted with solvent is higher. But, the mole fraction of CO$_2$ reacted with the solvent is less. This is shown by the increasing of mole fraction of physically dissolved CO$_2$. As more amount of CO$_2$ reacted with solvent, MDEA will be consumed more. With the increasing of CO$_2$ loading, the mole fraction of MDEA decreases, while the MDEAH$^+$ and HCO$_3$$^{2-}$ ions increase.

$$CO_2 + MDEA + H_2O \leftrightarrow MDEAH^+ + HCO_3^- \qquad\qquad (5.1)$$
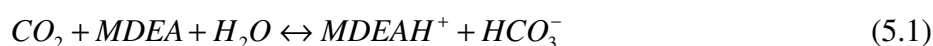
Reaction between CO$_2$ and MDEA solvent is an equilibrium reaction. When CO$_2$ dissolved in the solvent, not all of CO$_2$ will transform into HCO$_3$$^-$, but some will still remains as CO$_2$. The reacted CO$_2$ is chemically absorbed by the solvent, while the remaining CO$_2$ is physically absorbed by the solvent. At the observation temperature, it can be seen that when the loading exceed 0.8 mole CO$_2$/mole MDEA, the CO$_2$ mole fraction starts to increase rapidly, and the MDEAH$^+$ and HCO$_3$$^{2-}$ ions approach constant values. At this critical loading, the physical absorption starts to dominate the chemical absorption. The CO$_3$$^{2-}$ mole fraction curve also falls at loading 0.8 mole CO$_2$/mole MDEA. Due to the equilibrium reaction (5.1), one mole of MDEA will not consume one

mole of CO_2. In the other words, the critical loading will not be at the value of 1 mole CO_2/mole MDEA. It will be lower. Lee (1996) found that the critical loading of the CO_2-MDEA-H_2O system is 0.8 mole CO_2/mole MDEA

The Jakobsen et al data on the mole fraction of CO_2 for both temperatures were only given at the loading 0.8 mole CO_2/mole MDEA. Meanwhile, the simulation can predict the mole fraction of CO_2 for a wider range of CO_2 loading. Jakobsen et al (2005) explained that due to the limitation of the equipments, the effect of temperature on the CO_2 mole fraction can not be observed. At temperature of 20^oC and 40^oC, the mole fractions of CO_2 have the same value which is 0.0001 (Jakobsen et al, 2005). Meanwhile, for the same CO_2 loading, the simulation results in this study show that the CO_2 mole fraction at 40^oC is higher than that at 20^oC. This result indicates that at temperature 40^oC, less fraction of CO_2 reacts with the solvent compared at temperature of 20^oC. Reaction between CO_2 and MDEA solvent is an exotermic reaction. The behaviour of an exotermic reaction is that when the temperature lower, the reaction (5.1) is shifted to the forward direction and more reactants CO_2 and MDEA will react.

Figure 5.1 Mole fractions of species in liquid phase for CO_2-MDEA-H_2O system at 23 wt-% MDEA and 20^oC [Lines are generated from the model and symbols are experimental data of Jakobsen et al (2005)]

Figure 5.2 Mole fractions of species in liquid phase for CO2-MDEA-H2O system at 23 wt-% MDEA and 40°C [Lines are generated from the model and symbols are experimental data of Jakobsen et al (2005)]

From Figures 5.1 and 5.2, the Astrarita representation and ElecGC model can predict the liquid phase composition of CO_2-MDEA-H_2O system. The accuracy of the predicted mole fraction of all the components is acceptable.

The CO_2 partial pressure prediction for variation loading was examined. The simulation results were compared to the experimental data published by Jou et al (1982). Figure 5.3 shows the comparison on partial pressure between the model and the data at high CO_2 loading. Meanwhile Figure 5.4 shows the comparison at low loading. Jou et al (1982) served a numbers of data of CO_2 partial pressure varying from 0.001 to more than 1000 kPa. Generally, for the same CO_2 loading, the CO_2 partial pressure increases as the temperature increases. Shown in Figure 5.3, the model gives a good agreement at low temperature. As the temperature increases, larger deviation from experimental data was noticed. Figures 5.3 and 5.4 show that partial pressure increase with increasing loading.

Figure 5.3 Partial pressure of CO_2 in 2 M MDEA solution at high loading [Lines are generated using the model and symbols are experimental data of Jou et al (1982)]

Figure 5.4 Partial pressure of CO_2 in 2 M MDEA solution at low loading [Lines are generated using the model and symbols are experimental data of Jou et al (1982)]

Figure 5.3 demonstrates that the model can predict the CO_2 partial pressure with good agreement for loading higher than 0.1. While Figure 5.4 shows that the model gives significant disagreement at loading lower than 0.1. These are probably due to the

inconsistent of the data. Jou and coworkers (1982) utilized two different equipments for different range of loading. For the high loading, the closed system equipment was used. The acid gases was circulated and bubbled through an amine solution contained in a windowed equilibrium cell. For the low loading, the flow apparatus was used where the gas bubbles through series of amine solution container. The second equipment was more difficult to operate, particularly at the higher temperature. At temperature $40^{\circ}C$, the relative error of the result for loading higher than 0.1 is 26%. Meanwhile, for the loading lower than 0.1, the relative error is 84.7%. The relative error for the high loading at temperature of 70 $^{\circ}C$ is 44% while for low loading is 72.4%. The relative error for temperature $100^{\circ}C$ is 98%. Overall, the model is only fit for low temperature and high loading.

The relatively low agreement on the low loading may be affected by the equilibrium reaction constants for MDEA protonation reaction, K_{MDEA}. There are several K_{MDEA} correlations available in literature. Each of them gives different results on the solubility of CO_2 in MDEA solvent. Lee (1996) applied the K_{MDEA} relation from Schwabe (1959). This K_{MDEA} could give good results for the CO_2 solubility at low loading. But, on high loading case, the K_{MDEA} gives a large deviation. If the K_{MDEA} relation from Schwabe (1959) were applied to the system of H_2S-MDEA-H_2O and CO_2-H_2S-MDEA-H_2O, the large deviations were also observed.

5.2 H_2S Solubility in Aqueous MDEA Solvent

The speciation of H_2S-MDEA-water ternary system is provided. During this study, the experimental data on this system were unavailable. Figure 5.5 illustrates the mole fraction of components in the liquid phase for the H_2S absorption in the 50 wt% of MDEA solution. Due to the very low mole fractions of the S^{2-} and OH^- ions, the values were not shown. The main ionic species are $MDEAH^+$ and HS^-. The concentrations of the two ions balance each other due to the charge neutrality. The mole fraction of H_2O also appears as a horizontal line with a value close to unity. The following reaction described distinctly how H_2S react with MDEA.

$$H_2S + MDEA \leftrightarrow MDEAH^+ + HS^-$$
(5.2)

As the loading increase, the fraction of the H_2S react with MDEA is lower. This is shown by the increase in mole fraction of physically dissolved H_2S. These are because at high loading, the amount of H_2S reacted with the solvent decreases as the physical absorption dominates of the absorption process. From reaction (5.2), the ions $MDEAH^+$ and HS^- are formed when H_2S react with MDEA. At certain value of loading, the mole fraction of bort ions will appear constant as the physical absorption dominates of the absorption process. The value of this loading is a critical loading. The critical loading for H_2S-MDEA-H_2O is around 0.8 mole H_2S/mole MDEA. Lee (1996) reported the critical loading of the H_2S-MDEA-H_2O system is 0.8 mole H_2S/mole MDEA.
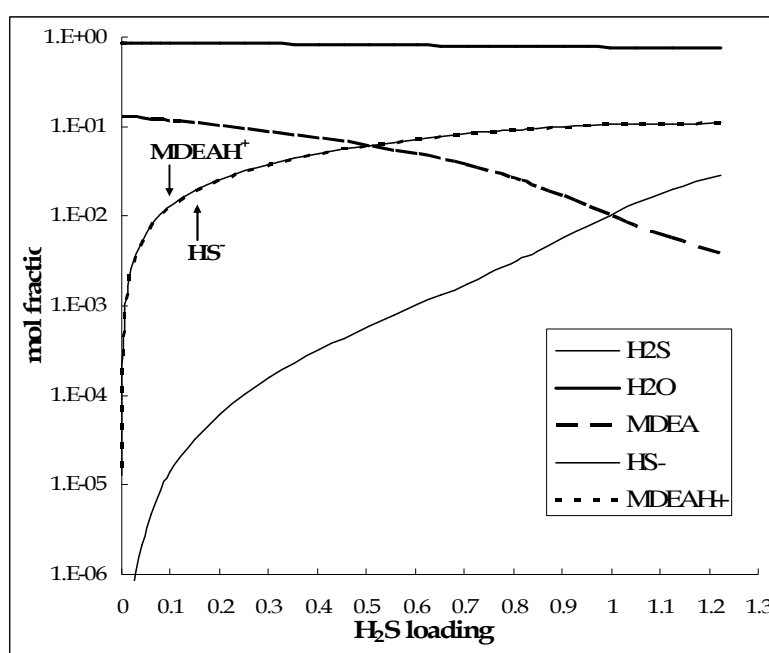
Figure 5.5 Mole fractions of species in liquid phase for H2S-MDEA-H2O
at 50 wt-% MDEA and 40 ^{o}C

Figure 5.6 shows the partial pressure of H_2S in the 1 M of aqueous MDEA solution. Figure 5.7 depicts the same system as Figure 5.6 focusing on the low loading region. The simulation results were compared with the experimental data from Jou, et.al (1982). The solubility of H_2S prediction was executed at temperature of 40^oC, 70^oC, and 100^oC. At the range of the temperature observed, the VLE model with the Astarita representation was able to predict the partial pressure of H_2S satisfactorily although the deviation seems to be higher at temperature 100^oC. The relative error for all the data shown in the Figure 5.6 and 5.7 is 32%.
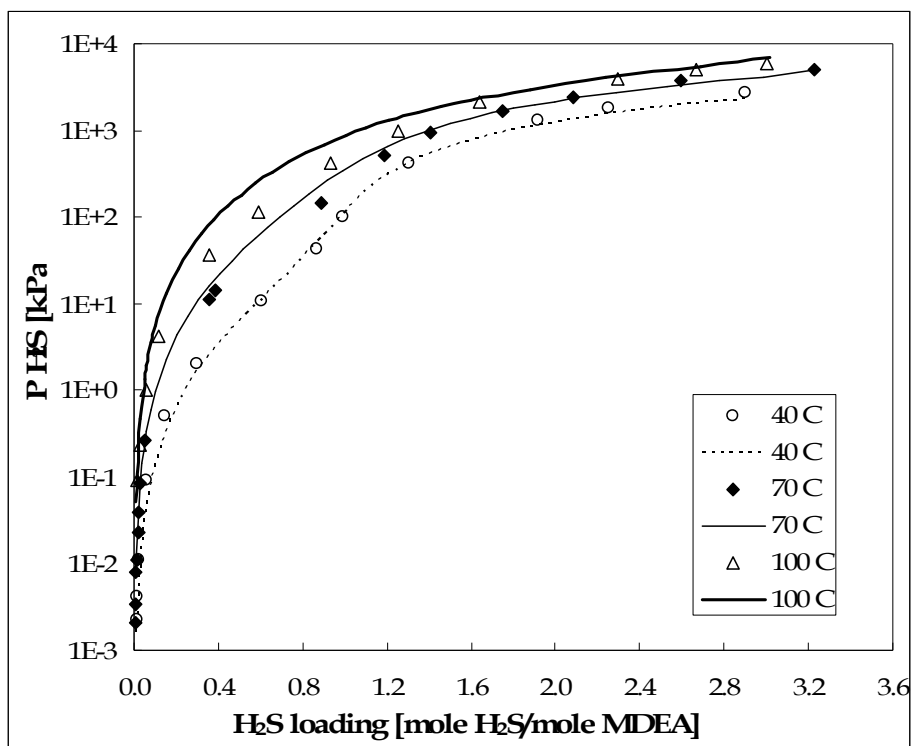
Figure 5.6 Partial pressure of H_2S in 1 M MDEA solution at high loading. [Lines are generated using the model and symbols are experimental data of Jou et al (1982)]
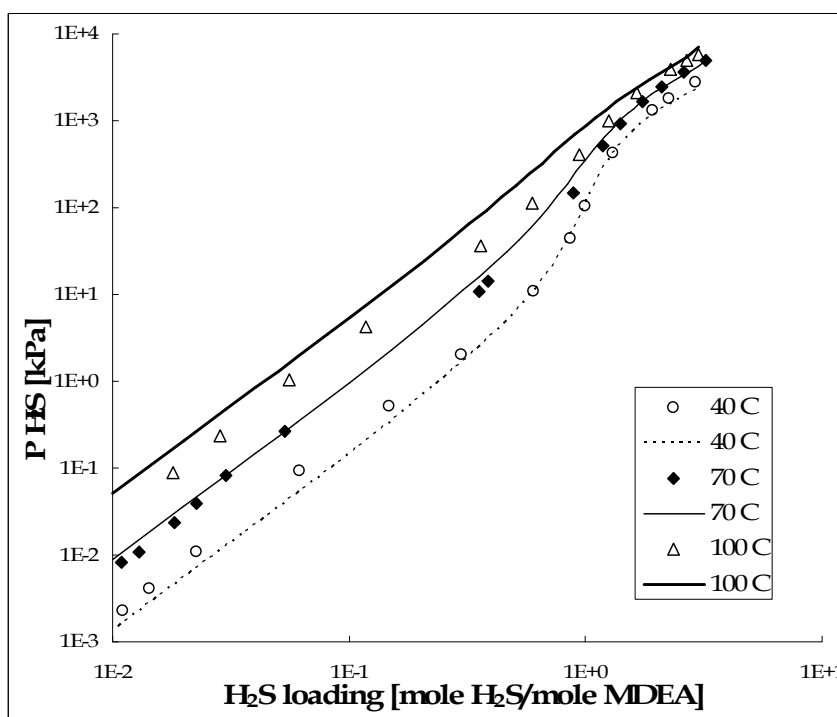
Figure 5.7 Partial pressure of H_2S in 1 M MDEA solution at low loading [Lines are generated using the model and symbols are experimental data of Jou et al (1982)]

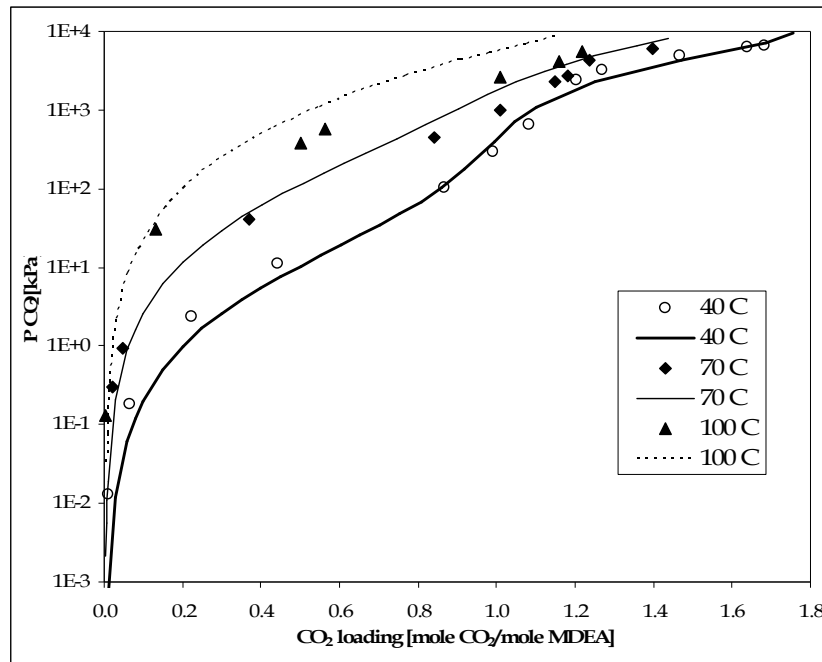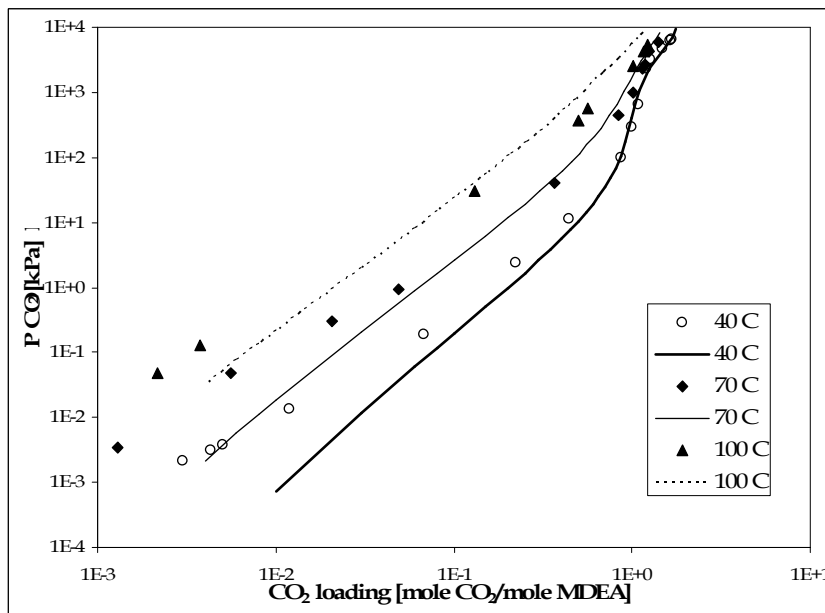The same phenomenon as for CO_2 system was observed for this system. As the temperature increases, partial pressure of H_2S increases. Reaction between H_2S and MDEA solvent is an exoterm reaction. From the reaction (5.2), as the temperature increase, the reaction is shifted to the reverse direction and more reactants are formed. As the temperature increases, higher pressure is required to achieve the same loading of H_2S.

5.3 CH_4 Solubility in Aqueous MDEA Solvent

The methane solubility prediction is provided in Figure 5.8. Jou et al (1998) experimental data were used as comparison. The calculation on the methane solubility was done for 3 M of MDEA solvent at temperature of $40^{o}C$ and $70^{o}C$. The experimental data shows that by changing the temperature from $40^{o}C$ to $70^{o}C$, the methane solubility only vary slightly, and so does the predicted values from the model. Over the range of temperature shown in Figure 5.8, the solubility of the methane in MDEA solvent is quite insensitive. This is due to methane remaining gaseous throughout this range of temperature (Carroll et al, 1998). Generally, the comparison on the literature data and the predicted value from the model has a very good agreement. The relative error produced is 16.9%
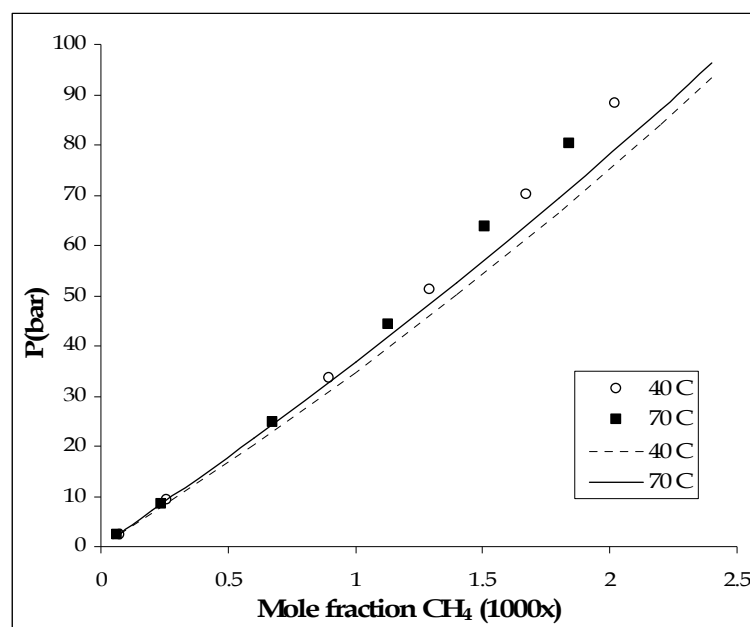
Figure 5.8 Partial pressure of CH4 in 3 M MDEA solution [Lines are generated from the model and symbols are experimental data of Jou et al (1998)]

76

5.4 Heat of Absorption of CO_2 and H_2S in Aqueous MDEA Solvent

The heat of absorption is an important variable in acid gases treatment. The heat is produced when the acid gases dissolve and react with the solvent. This heat raises the temperature of the solution. In Section 3.2.2, the formula to calculate the enthalpy change due to acid gas absorption was described. The heat of absorption was reported as a function of gas loading and concentration of solution. The enthalpy of absorption of CO_2 in aqueous MDEA solution is shown in Figure 5.9 where they are compared with the experimental data from Arcis et al (2008).

The predicted heat of absorption of CO_2 calculated using eq. (3.118) matches with the experimental data up to a loading of 0.8 mole CO_2/mole MDEA. A gradual decrease in the value of the heat of absorption was observed for the range of loading up to 0.8 mole CO_2/mole MDEA. When the loading exceeds 0.8 mole CO_2/mole MDEA the heat of absorption value decreases significantly until it reaches the enthalpy of physical absorption of CO_2 in MDEA solvent. At this high loading, the solution starts to get saturated with CO_2 and only physical absorption occurs.

Figure 5.9 demonstrates that the calculated heat of absorption of CO_2 shows different trend with the experimental heat of absorption of CO_2. In the calculated heat of absorption shown by the line, a sudden decrease presents at the loading near to 0.8. Meanwhile, a gradual decrease presents in the experimental heat of absorption shown by the symbol. The different trend of heat of absorption column is due to the different of loading interval used in the two terms. The calculated heat of absorption was obtained at a very small loading interval. Meanwhile, the experimental heat of absorption was obtained at interval zero loading to the final loading.

When acid gases dissolved in the MDEA solvent, a part of the gases remains physically absorbed while the other part is chemically absorbed. The heat of physical absorption is much lower than heat of chemical absorption. At low loading, the chemical absorption dominates the physical absorption. That is why the heat of absorption at the low loading is high. At loading higher than 0.8 mole CO_2/mole MDEA, the calculated heat of absorption which is integrated at very small loading interval will be the value of heat of

physical absorption. Meanwhile, the experimental heat of absorption which is obtained from zero loading and the final loading will be combination of physical absorption and chemical absorption, with the physical absorption dominates the chemical absorption. Therefore, the higher the loading the total heat of absorption is lower. The calculated heat of absorption is called differential heat of absorption while the experimental heat of absorption is an integral heat of absorption (Kim et al, 2009).

Figure 5.10 shows the heat of absorption for H_2S absorption into 1 M MDEA solution. These calculated results were compared with the literature data by Jou et.al (1982). In this study, the predicted heat of absorption of H_2S was calculated using eq. (3.118). The partial pressure of H_2S was taken from the calculated value obtained from the model. Jou et al (1993) also performed the calculation of heat of absorption using eq. (3.118). Jou et al (1993) used the partial pressure values obtained in their experiment study. The heat of absorption obtained in this study and Jou et al (1993) show similar trend. Relatively large deviation was found from the two studies. The deviation is probably obtained due to different sources of partial pressure data. Jou el al used the experimental data of partial pressure of their study. In this study, the simulation results give loading of H_2S 0.8 mole H_2S/mole MDEA as the critical loading point.
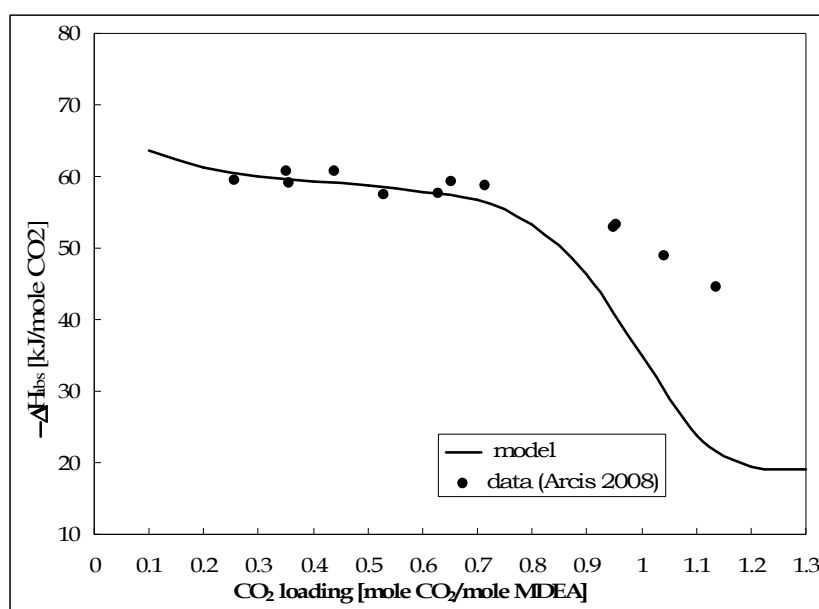
Figure 5.9 Enthalpy of absorption of CO_2 in 30-wt% MDEA solution
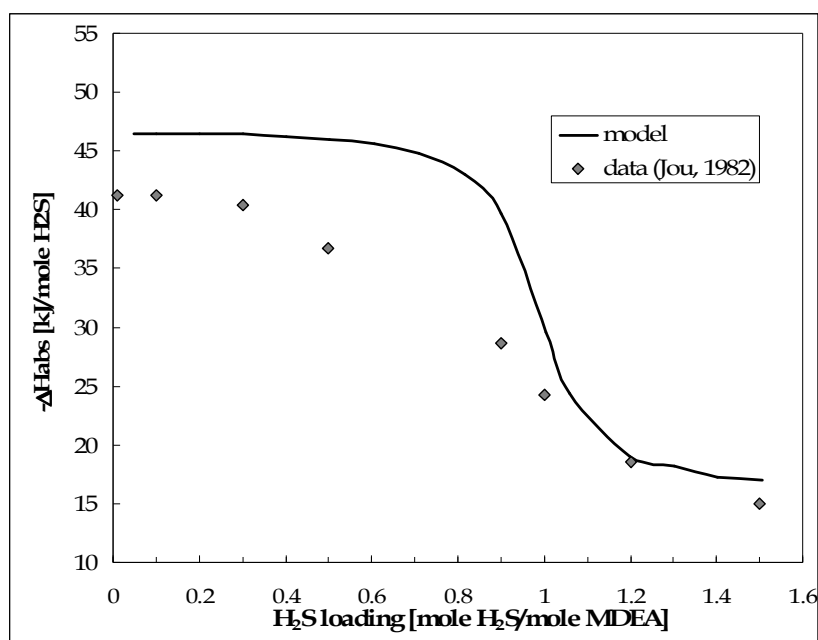
Figure 5.10 Enthalpy of absorption of H_2S in 1 M MDEA solution

The heat of absorption values depend strongly on the acid gas loading in the solvent. The values are only less affected by the solution strength, while the gas pressure has virtually no effect on the values (Oscarson et al, 1990). These phenomena can be seen in Figure 2.5. Due to the less effect of solution strength, the heat of absorption prediction result can be compared between CO_2 and H_2S. The comparison made at the loading below the critical loading. Jou et al (1982) made comparison between CO_2 and H_2S at loading range loading 0-0.3 mole gas/mole MDEA. Applying the same range of loading in this study, the average heat of absorption for CO_2 is 61.6 kJ/mole CO_2 and for H_2S is 46.5 kJ/mole H_2S. In conclusion, heat of H_2S absorption in MDEA is lower than heat of CO_2 absorption.

5.5   Sour Methane Treatment Containing either CO_2 or H_2S

In this work, the acid gases treatment from the methane was studied. The methane contains either one acid gas, CO_2 or H_2S. There are two approaches in designing the absorption process. The first approach is designing a new absorption column. In this case, the acid gas fraction in sweet gas or in the other words, the % acid gas recovery is specified. Then, the number of stages is calculated. The second approach is evaluating the existed absorption column. Here, the number of stages is specified, and the % acid gas

recovery is calculated. In this work the second approach was used for the system of CO_2 or H_2S absorption from methane. The algorithm described in Section 4.1 was applied.

To make a comparison between the case for CO_2 and H_2S, the feed gas and the lean solvent composition and condition were made equal. The strength of MDEA solvent is 45 wt% of MDEA and its flowrate is 3 MMSCFD. The circulation rates of amine solvent used were also made equal which was 2.73 mole solvent/mole sour gas. The total pressure drop along the column is assumed to be 1 bar. The mole fraction of acid gas in the amine is 10 mole%.

Loh (1987) performed a simulation of CO_2 from natural gas using MDEA solvent. He calculated the Murphree vapor efficiency of the separation from the overall vapor efficiency. The calculated Murphree vapor efficiency is 7.4% and 8.7%. Another study conducted by Mofarahi et al (2008) uses 35% value for Murphree vapor efficiency. From those two works, it can be concluded that the value of Murphree vapor efficiency is not fixed. In industrial absorption process, the Murphree vapor efficiency usually ranged between 65-85%. In this work the Murphree vapor efficiency of 65% is used for both gases.

Table 5.1 shows the comparison result for the CO_2 and H_2S systems. The number of stages was set to be 5 stages. This number was selected based on trial and error on the simulation to get the purity of desired gas product which is lower than 0.16 % mole acid gases. For the CO_2 absorption system, the outlet CO_2 fraction in sweet gas is 0.085%. The % CO_2 recovery is 99.33%. The same number of stages is applied to the H_2S absorption system. The outcomes are 0.059% for the H_2S mole fraction in sweet gas and 99.51 for % H_2S recovery. The detail stage to stage simulation results are provided in Appendix B.2.

In Section 5.1 and 5.2, it has been described the partial pressure prediction of acid gas based on equilibrium model given in Chapter 3. In general, the model can predict the partial pressure with an acceptable deviation. The VLE model which can predict the gas solubility becomes a part of the absorption column simulation. The result on the absorption column simulation can show explicitly the similar behaviour with the solubility prediction. In the solubility prediction, the H_2S partial pressure required is

lower than that of CO_2 to achieve the same loading. In the other word, the solubility of H_2S is higher than that of CO_2. The similar outcome happens to the absorption simulation where the H_2S mole fraction in gas product is lower than that of CO2.

Table 5.1 Simulation results for CO_2 and H_2S absorption from methane using MDEA solution

System	CO_2-CH_4-MDEA-H_2O	H_2S-CH_4-MDEA-H_2O
Solution, wt-% MDEA	45*	45*
Feed gas:		
Flow rate, MMSCFD	3.0*	3.0*
Temperature, ^oC	37*	37*
Acid gas, % mole	10*	10*
Methane, % mole	90*	90*
No. of Stages	5*	5*
Pressure, bar		
Top	59*	59*
Bottom	60*	60*
Stage Efficiency, %	65*	65*
Lean Solution analysis		
Temperature, ^oC	38*	38*
Loading, mole/mole amine	0.0001*	0.0001*
Circulation rate		
Mole solvent/mole sour gas	2.73*	2.73*
Acid gas recovery, %	99.33	99.51
Rich Solution analysis		
Temperature, ^oC	61.83	55.35
Loading, mole/mole amine	0.3306	0.3312
CH_4, mole/mole amine	0.01843	0.01833
Outlet gas		
Acid gas, % mole	0.085	0.059

* *indicate the specified values*

Figure 5.11 to Figure 5.13 show the column profile of the two separation system. Figure 5.11 shows the temperature profile along the column. The stage 0 is the inlet of feed sour gas. When the lean convent comes into contact with the gas at the top of the column, the heat is generated in the liquid phase due to the acid gas absorbed to the solvent. This heat raises the temperature of the liquid and causes further heat transfer to the gas. The liquid phase absorbs more acid gases from the gas phase when it moving down and the liquid temperature is increase. It can be seen that as the stage moving from the top to bottom, the temperature is increases and at the lowest part of the column, the temperature will extremely decreases (Kohl & Nielsen, 1997). The temperature "bulge" is a result of the cool inlet gas absorbing heat from rich solutions at the bottom of the column, then losing this heat to the cooler solution near to the upper part of the column (Kohl & Nielsen, 1997). The stage temperature of the CO_2 system is higher than that of the H_2S. This is due to the higher heat of absorption of CO_2 in aqueous MDEA solution compare to heat of absorption of H_2S as been described in Section 5.4.

Figure 5.12 illustrates the profile of the acid gas mole fraction in the gas phase. At the top of the column, the mole fraction of H_2S is lower than that of CO_2. This is due to the fraction of amine absorbed by the solvent is higher than that of CO_2. H_2S is react rapidly compare to CO_2 in MDEA solvent. This is because H_2S react simultaneously with MDEA by proton transfer. The CO_2 reaction can only occur after the CO_2 dissolves in the water to form a bicarbonate ion because MDEA is a tertiary amine and does not have hydrogen attached to the nitrogen (Savage & Funk, 1981).
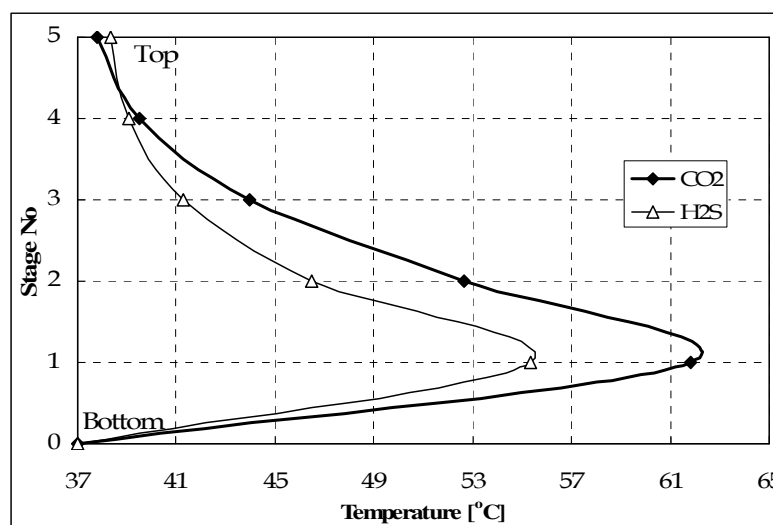
Figure 5.11 Column temperature profile of CO_2 and H_2S absorption in MDEA solution
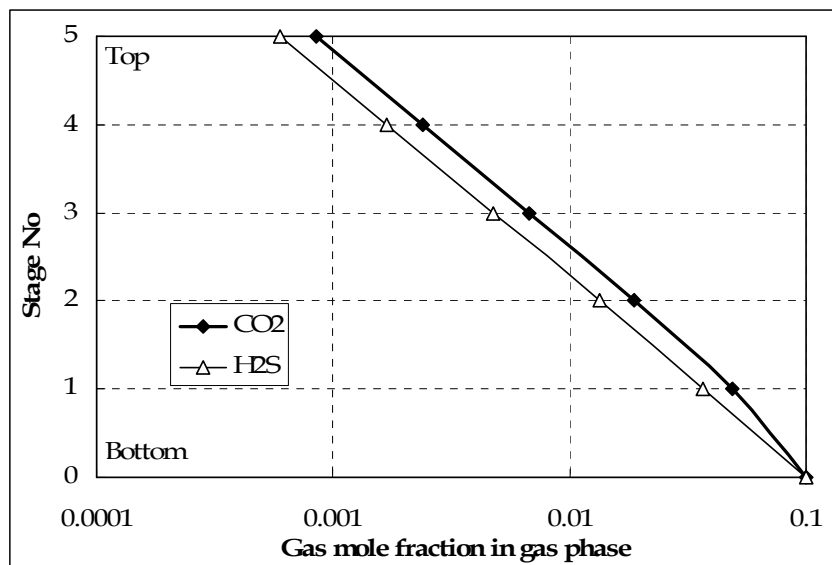
Figure 5.12 Profile of mole fraction of acid gas in gas phase for of CO_2 and H_2S absorption in MDEA solution

The effect of MDEA concentration and solvent flow rate were analyzed to determine their influence on acid gas recovery. Percent acid gas recovery is amount of gas transferred to solvent relative to the initial amount of the gas in the feed. In this study, the feed gas contains 20% of acid gas and the number of stages is fixed at 5 stages. For the effect of MDEA concentration study, the flow rate of the solvent is 3.638 mole solvent/mole feed gas. For the effect of the flow rate study, the concentration of solvent is fixed at 45 wt% MDEA. Figure 5.13 shows the effect of MDEA concentration to the % recovery of CO_2 absorption and H_2S absorption. The MDEA concentration was varied from 30 to 55 wt% MDEA. The concentration values were taken at the typical MDEA concentration used in industry. From Figure 5.13, it can be seen that recovery of the acid gas is increase by increasing the strength of solution. This is because more MDEA present in the liquid phase to react with the acid gas molecules. The higher H_2S recovery than CO_2 recovery is due to the H_2S react rapidly compare to CO_2. The results show that when the concentration increase from 30 to 55 wt% MDEA, the recovery of the CO_2 increases by 2.3%, while the recovery of H_2S increases by 1.7%.

For the effect of the flow rate study, the concentration of solvent is fixed at 45 wt% MDEA. The solvent flow rate was varied from 2.7 to 7.3 mole solvent/mole feed gas. Figure 5.14 shows that as the flow rate increases, the recovery of both gases increase. By increasing the flowrate of solvent, the more gases will transfer to the liquid phase. As the

83

flow rate increases from 2.7 to 7.3 mole solvent/mole feed gas, the CO_2 recovery was increased by 5.3%. While for H_2S, it was increased by 5 %.
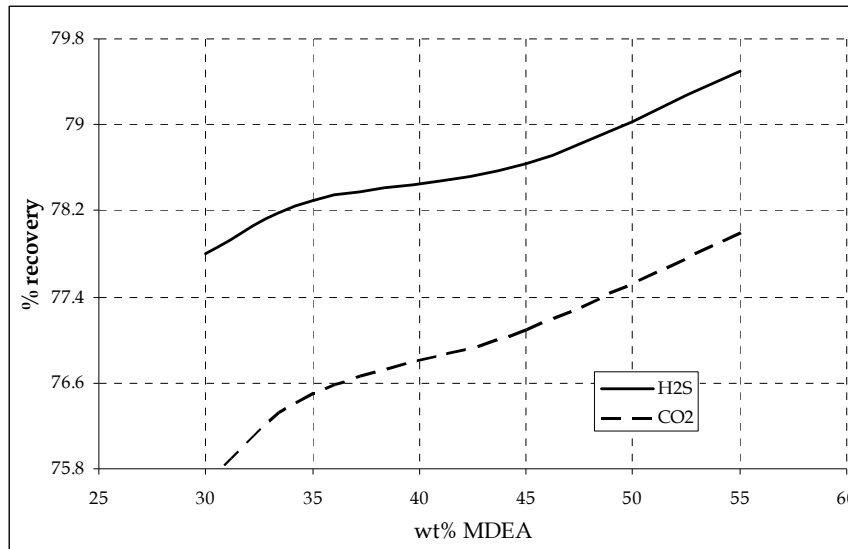
Figure 5.13 Effect of MDEA concentrations to the acid gas recovery
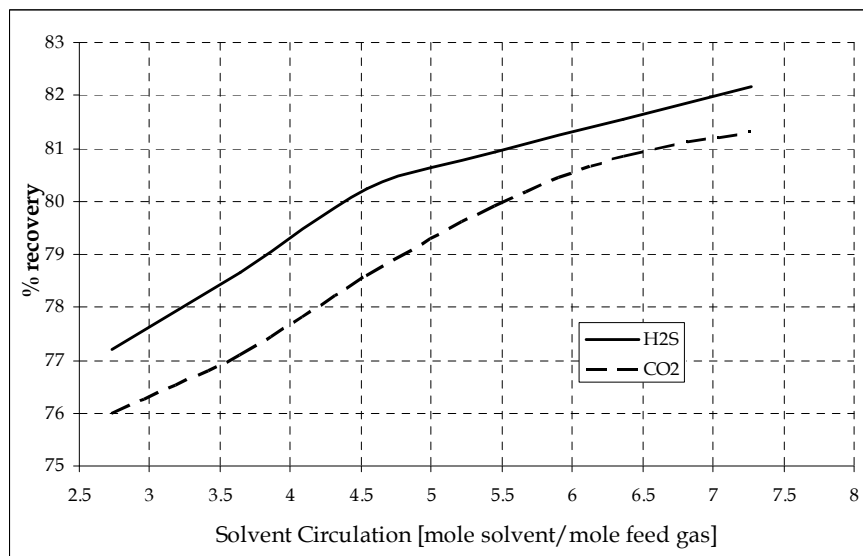
Figure 5.14 Effect of solvent flow rate to the acid gas recovery

From the results and explaination above, generally, the simulation absorption on acid gas either CO_2 or H_2S from methane using aqueus MDEA solution show a good prediction of the behaviour of the system. The absorption column simulation was extended to the mixture of CO_2 and H_2S absorption from methane. A result on the system is explained in Section 5.7.

5.6   Mixture of CO_2 and H_2S Solubility in Aqueous MDEA Solvent

In the real case of natural gas treatment, the gas feed usually contains not only CO_2 but also H_2S. The absorption process involves separating both gases. In this part, the solubility of mixture of the gases was analyzed. The experiment data on partial pressure of mixed acid gases in 35 wt-% MDEA solution system at 40^oC was taken from Jou et.al (1993). The comparison of the experimental partial pressure and calculated partial pressure of CO_2 and H_2S are shown in Figure 5.15 and 5.16, respectively. The complete data for this work is shown in Appendix B1.

The accuracy of the calculated partial pressure of CO_2 and H_2S are was found to be higher for partial pressure higher than 1 kPa compare to the partial pressure lower than 1 kPa. The relative errors for this range higher than 1 kPa are 38% for CO_2 and 25% for H_2S. Meanwhile, the relative errors for the low loading are 61.4% for CO_2 and 60% for H_2S. The total relative error for CO_2 partial pressure is 45.8%, while for H_2S is 30.7%. The low accuracy of the calculated partial pressure of CO_2 in CO_2-H_2S-MDEA-H_2O system is similar with the calculated partial pressure of CO_2 in CO_2-MDEA-H_2O system. The inconsictency of the experimental data and the application of the K_{MDEA} to the calculation of liquid phase composition are the main reasons of this low accuracy of the calculated partial pressure of CO_2. The same phenomena exist in the calculated partial pressure of H_2S in CO_2-H_2S-MDEA-H_2O system with the calculated partial pressure of H_2S in H_2S-MDEA-H_2O system. A better accuracy of H_2S partial pressure compare to CO_2 is found.

A study on the effect of the additional H_2S loading to the partial pressure of CO_2 for a variation of CO_2 loading at the same condition above was also made. The H_2S loading of 0.34 was selected randomly from the Jou et al (1993) data. The result from the study is shown in Figure 5.17. The additional of H_2S to the system increases the CO_2 partial pressure required to achieve the same loading as the system without H_2S, i.e, the solubility of CO_2 decreases. The existence of another acid gas component in the system affects the solubility of the other acid gas.
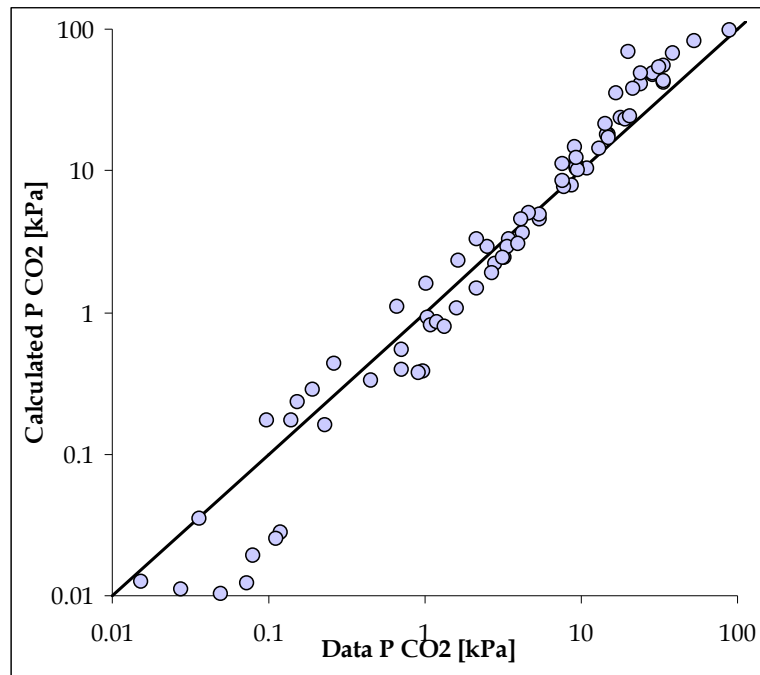
Figure 5.15 Comparison of the calculated partial pressure of CO_2 and experimental value for mixture of H_2S and CO_2 in aqueous MDEA solutions [Jou et al,1993]
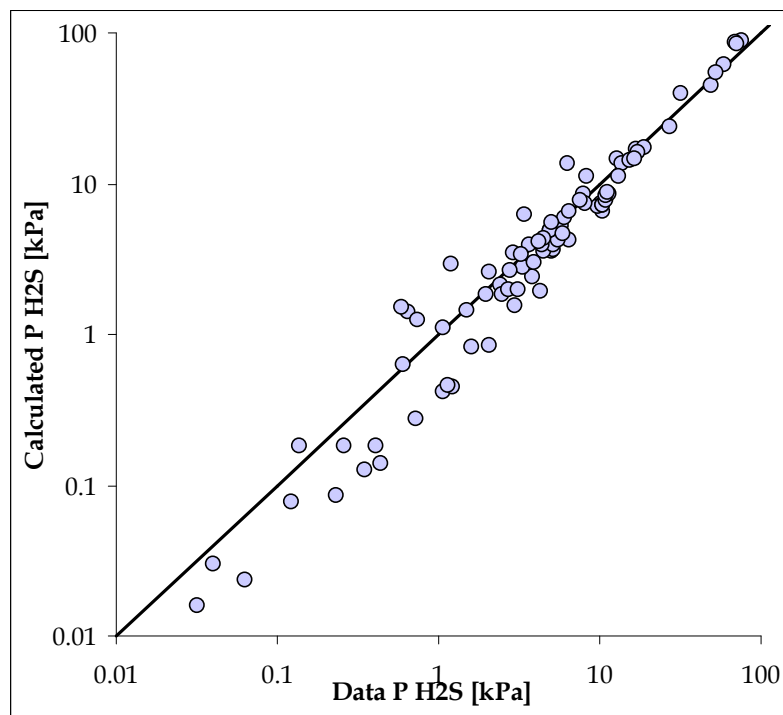
Figure 5.16 Comparison of the calculated partial pressure of H_2S and experimental value for mixture of H_2S and CO_2 in aqueous MDEA solutions [Jou et al,1993]
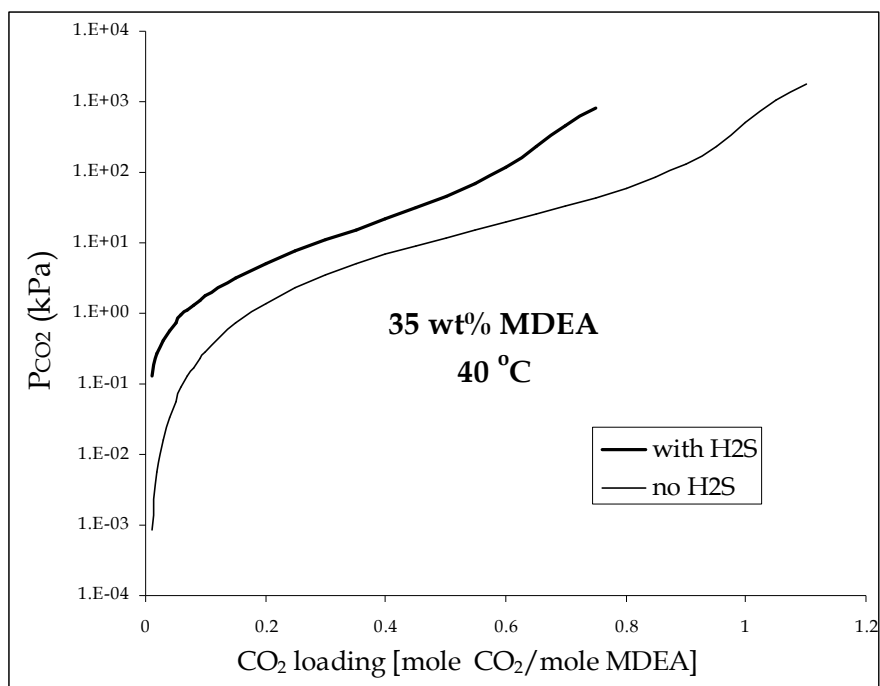
Figure 5.17 Effect of additional 0.34 H_2S loading to the partial pressure of CO_2 at the system of CO_2-H_2S-MDEA-H_2O at 40°C and 35 wt-% MDEA solvent

5.7   Sour Methane Treatment Containing Mixture CO_2 and H_2S

In the previous methane treatment, the feed gas contains either acid gas component (CO_2 or H_2S). In this section, the feed methane contains mixture of CO_2 and H_2S. Table 5.2 displays the summary of the absorption simulation of mixture acid gases absorption using aqueous MDEA solvent. The simulation parameter and specification was not based on the experimental or industrial absorption column data. Feed gas contains 8 mole% CO_2 and 8 mole% H_2S. The solvent concentration is 45 wt% MDEA. The number of stages was fixed to be 5 stages and the Murphree vapor efficiency for each of acid gas is 65%. The flow rate of the solvent is the same as previous single acid gas simulation, 2.73 mole solvent/mole feed gas.

For a given specification above, the outlet gas contains 0.23 mole% CO_2 and 0.085 mole% H_2S. These are equal to 97.37% CO_2 recovery and 99.05% H_2S recovery. For the same acid gas flow rate input, the outlet gas of H_2S is much lower than that of CO_2. Figures 5.19 shows profile of mole fraction of acid gas in gas phase for of CO_2 and H_2S absorption system using aqueous MDEA solution, while Figure 5.20 shows profile the

87

gases loading in the liquid phase in the absorption system. The figures show that the H_2S mole fraction in the gas phase and H_2S loading in liquid phase decreases faster than CO_2 from the bottom stage to the top. This is due to the H_2S reacts faster than that of CO_2. The fast H_2S reaction with MDEA is because H_2S react simultaneously with MDEA by proton transfer. The CO_2 reaction can only occur after the CO_2 dissolves in the water to form a bicarbonate ion (Savage & Funk, 1981).

In Section 5.5, simulation on single acid gas absorption from methane has been given. For the 10 mole% of acid gas in the feed gas and 5 equilibrium stages fixed to the system, the mole fraction of CO_2 in the gas product while 0.085 mole%, while H_2S was 0.059 mole%. In this system, the 8 mole% of CO_2 and 8 mole% of H_2S exist in the feed gas. The same number of stages was used. The gas product in this simulation has higher percentage of acid gases (0.23 mole% CO_2 and 0.085 mole% H_2S) compare to the single acid gas absorption, even for a lower acid gases composition in the feed gas. This is because the existence of another acid gas component in the system decreses the solubility of the acid gas. The same phenomenon has been shown in Section 5.6.
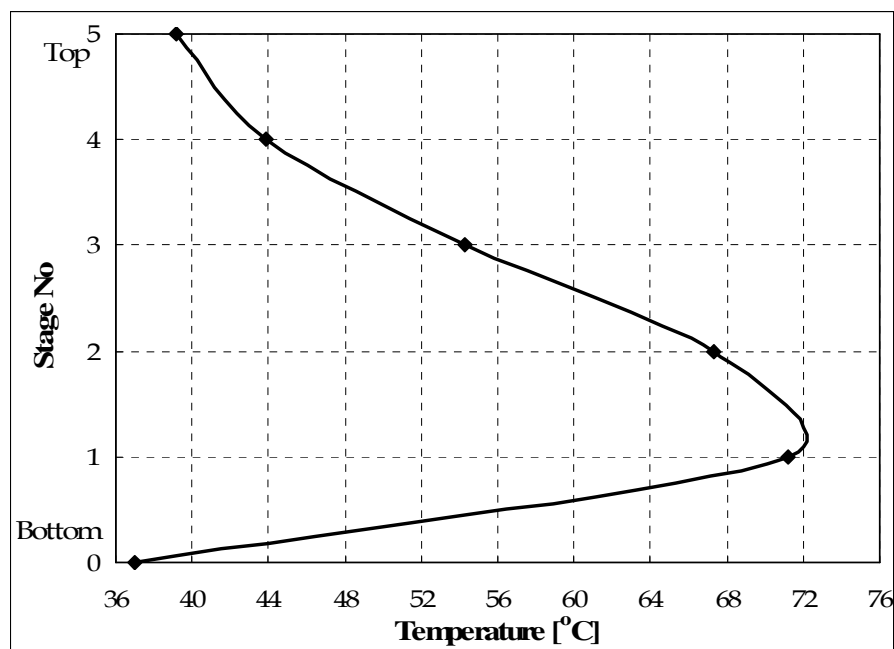
Figure 5.18 Column temperature profile of mixture CO_2 and H_2S absorption system in aqueous MDEA solution
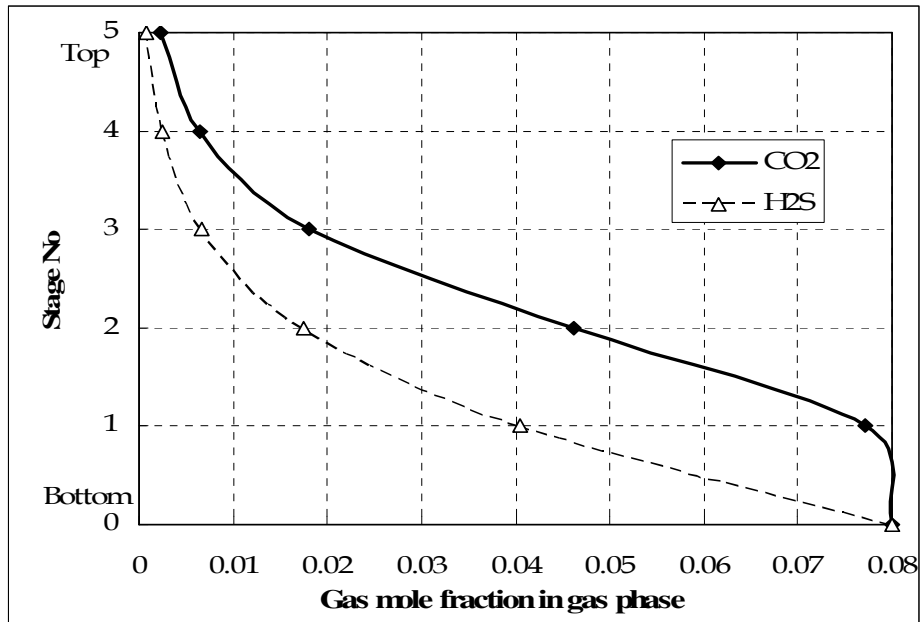
Figure 5.19 Profile of mole fraction of acid gas in gas phase for of CO_2 and H_2S absorption system in aqueous MDEA solution
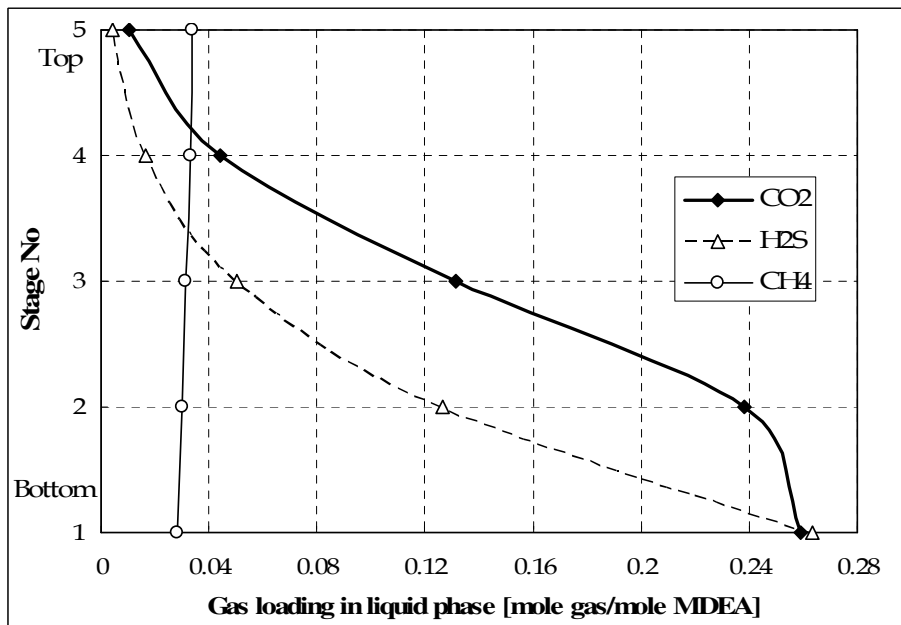
Figure 5.20 Gases loading profile in liquid phase for mixture CO_2 and H_2S absorption system in aqueous MDEA solution

Table 5.2 Simulation results for mixture CO_2 and H_2S absorption from methane using MDEA solution

Solution, wt-% MDEA	45
Feed gas:	
Flow rate, MMSCFD	3.0*
Temperature, ^{o}C	37*
CO_2, % mole	8*
H_2S, % mole	8*
CH_2, % mole	86*
No. of Stages	5*
Pressure, bar	
Top	59*
Bottom	60*
Stage Efficiency	
CO_2, %	65*
H_2S, %	65*
Lean Solution analysis	
Temperature, ^{o}C	38*
CO_2, mole/mole amine	0.0001*
H_2S, mole/mole amine	0.0001*
Circulation rate	
Mole solvent/mole sour gas	2.73*
CO_2 recovery, %	97.37
H_2S recovery, %	99.05
Rich Solution analysis	
Temperature, ^{o}C	71.1
CO_2, mole/mole amine	0.2592
H_2S, mole/mole amine	0.2637
CH_4, mole/mole amine	0.0281
Outlet gas	
CO_2, % mole	0.23
H_2S, % mole	0.085

* *specified values*

The partial pressure prediction of CO_2 and H_2S in the system of CO_2-H_2S-MDEA-H_2O have been shown in Section 5.5 Generally, a good prediction of the partial pressure was given by the VLE model. The VLE model was extent to the absorption column calculation. In conclusion, behaviour of the acid gases absorption from methane using MDEA solution can be predicted finely from the calculation procedure given in Chapter 4.

5.8   Summary

In this chapter, the results on modeling and simulation of acid gases absorption from methane using aqueous MDEA solution have been described. The solubility prediction of single gas (CO_2, H_2S, and CH_4) and mixture of gases (CO_2 and H_2S) in various strength of MDEA solvent have been given. Good results were obtained in the H_2S and CH_4 partial pressure prediction. CO_2 partial pressure prediction has relatively high error at the loading lower than 0.1 mole CO_2/mole MDEA. Meanwhile, the partial pressure prediction for the CO_2-H_2S-MDEA-H_2O has also a good agreement at high loading, but higher error was reported at low loading. The heat of absorption prediction of single acid gas in MDEA solvent were also has been given. The result was obtained satisfactory for CO_2-MDEA-H_2O system, but relatively high error was found for H_2S-MDEA-H_2O system. The simulations on the CO_2 or H_2S absorption and mixture acid gases absorption from methane using aqueous MDEA solution based on the calculation procedure in Chapter 4 have been given.

CHAPTER 6

CONCLUSIONS AND RECOMMENDATIONS

6.1 Conclusions

The following conclusions can be drawn based on results of this study:

1. The combination of the ElecGC model to describe the activity coefficient and Peng-Robinson equation of state to calculate the fugacity coefficient are capable to calculate the acid gases solubility in the aqueous methyldiethanol- amine solutions. For the system of CO_2-MDEA-H_2O, the model can predict finely the solubility at loading higher than 0.1 loading. Hence, for loading lower than 0.1 the predicted partial pressure has a relative error 84.7% with the published experimental data. In the other case, the model can predict precisely the H_2S solubility in aqueous MDEA solvent. The predicted solubilities of CO_2 and H_2S for the system of CO_2-H_2S-MDEA-H_2O have a good agreement with the published experimental data.

2. The Astarita representation that was used to solve the reaction equilibriums and component balance equations in the liquid can be applied to calculate the liquid phase composition of the acid gases-MDEA solvent systems. In this study, the Astarita representation was applied CO_2-MDEA-H_2O system, H_2S-MDEA-water system, and CO_2-H_2S-MDEA-H_2O system.

3. A rigorous stage by stage calculation procedure to predicting system of acid gases absorption from methane has been constructed. Moreover, the procedure was also capable to calculate the methane solubility in the solvent.

4. The procedure has capability of predicting the temperature profile along the column, gas composition of each stage, and gases loading in liquid at every stage, for a given feed gas and solvent specification and also the number of stages.

6.2 Recommendations

The following recommendations can be drawn based on results of this study:

1. The reaction equilibrium constant for protonation of MDEA, K_{MDEA} is an important value in calculating the acid gases solubility. There are various K_{MDEA} equations reported in literature. Investigation to the effect of the different K_{MDEA} is has to be done in order to get the better predicted value of acid gases in aqueous MDEA solution

2. An improvement has to be made to the Astarita representation to be applied to the CO_2 solubility at low loading. The solubility of acid gases at low loading is very important since the market demand on sweet gas product need the very low acid gases content.

3. The simulation of the single acid gas or mixture acid gases absorption from methane is important to be performed at the real plant gas specification and the sweet gas product specification in order to perify the model adopted and the calculation procedure. According to Flemming et al (2006), the sweet gas product must have below 0.16 mole% of acid gases befor entering the pipeline.

4. The application of another vapor-liquid equilibrium model is essential to be done. The model has to be able to predict the precisely the partial pressure of the single gas or mixture gases at low and high loading.

REFERENCES

1. Addicks, J. and Owren, G.A., 2002, Solubility od Carbondioxide and Methane in Aqueous Methyldiethanolamine Solutions, J. Chem. Eng. Data. 47, 855-860.

2. Al-Baghli, N.A., Pruess, S.A., Yesavage, V.F., Selim, M.S., 2001, A rate-based model for the design of gas absorber for removal of CO_2 and H_2S using aqueous solution of MEA and DEA, Fluid Phase Equilibria, 185, 31-34.

3. Al-Ghawas, H.A., Hagewiesche, D.P., Ruiz-Ibanez, G., Sandall, O.C., 1989, Phycochemical Properties Important for Carbon Dioxide Absorption in Aqueous Methyldiethanolamine, J.Chem. Eng. Data, 34, 385-391.

4. Arcis, H., Rodier, L., Ballerat-Busseroles, K., Coxam, J.Y., 2008, Enthalpy of solution of CO_2 in aqueous solutions of methyldiethanolamine at T = 322.5 K and pressure up to 5 MPa, J. Chem. Thermodynamics, 40, 1022-1029.

5. Aroonwilas, A., Chakma, A., Tontiwachwuthikul, P., Veawab, A., 2003, Mathematical modeling of mass-transfer and hydrodynamics in CO_2 absorber packed with structured packing, Chemical Engineering Science, 58, 4037-4053.

6. Aroua, M.K., Haji-Sulaiman, M.Z., Ramasamy, K., 2002, Modeling of carbon dioxide absorption in aqueous solutions of AMP and MDEA and their blends using Aspenplus, Separation and Purification Technology, 29, 153-162.

7. Astarita,G. Savage, D.W., Bisio, A., 1983, Gas treating with chemical solvents. John Wiley & Sons, New York.

8. Autsgen, D.M., 1989, A Model for Vapor-Liquid Equilibria for Acid gas-Alkanolamine-Water Systems, Ph.D Dissertation, Texas A&M University, Texas.

9. Benamor, A., and Aroua, M.K., 2005, Modeling of CO_2 solubility and carbamate concentration in DEA, MDEA, and their mixture using Deshmukh Mather model, 231,150-162.

10. Barreau, A., Bouhelec, E.B., Tounsi, K.N.H., Mougin, P., Lecomte, F., 2006, Absorption of H_2S and CO_2 in alkanolamine aqueous solution: Experimental data and modeling with the Electrolyte-NRTL model, Oil and Gas Science and Technology, 61(3), 345-361.

11. Barth, D., Tondre, C., Delpuech, J.J., 1981, Kinetic Study of Carbon Dioxide Reaction with Tertiary Amines in Aqueous Solution, J. Phys. Chem., 85, 3660-3667.

12. Brelvi, S.W. and O'connel, J.P., 1972, Corresponding States Correlation for Liquid Compressibility and Partial Molar Volumes of Gases at Infinite Dilution of Liquids, AIChE. J, 18, 1239.

13. Bullin, J.A., Polasek, J.C., Fitz, C.W., 2006, The impact of acid gases loading on heat of absorption, Bryan Research and Engineering Inc, Bryan, Texas.

14. Button, J.K., and Gubbins, K.E., 1999, SAFT prediction of vapor-liquid equilibria of mixture containing carbon dioxide and aqueous monoethanolamine or diathenolamine, Fluid Phase Equilibria, 158-160, 175-181.

15. Campbell, J.M., 1998, Gas conditioning and processing, Campbell Petroleum Series.

16. Carnahan, N.F., and Starling, K.E., 1969, Equation of state for Nonatracting Rigid Spheres, J. Chem. Phys., 51, 635.

17. Carroll, J.J., and Mather, A.E., 1997, A model for the solubility of light hydrocarbons in water and aqueous solutions of alkanolamines, Chem. Eng. Sci., 52, 4, 545-552.

18. Carroll, J.J., Maddox, J., and Mather, A.E., 1998, The solubility of hydrocarbons in amine solutions, Laurance Reid Gas Conditioning Conference, Norman, Oklahoma.

19. Carson, J.K., Marsh, K.N., Mather, A.E., 2000, Enthalpy of solution of carbon dioxide in (water + monoethanoamine, or diethanolamine, or N-methyldiethanolamine) and (water + monoethanolamine + N-methyldiethanolamine) at 298.15 K, J. Chem. Thermodynamics, 32, 1285-1296.

20. Chakma, A. and Meisen, A., 1987, Solubility of CO_2 in Aqueous Methyldiethanolamine and N,N-Bis(hydroxyethyl)piperazine Solutions, Ind.Eng.Chem.Res, 26, 2461-2466.

21. Chiu, L.F. and Li, M.H., 1999, Heat capacity of alkanolamine aqueous solutions, J. Chem. Eng. Data, 44, 1396-1401.

22. Chunxi, L., and Furst, W., 2000, Representation of CO_2 and H_2S solubility in aqueous MDEA solutions using an electrolyte equation of state. Chemical Engineering Science, 55, 2975-2988.

23. Dawodu, O.F. and Meisen, A., 1994, Solubility of Carbon Dioxide in Aqueous Mixture of Alkanolamine, J.Chem.Eng.Data, 39, 548-552.

24. Deshmukh, R.D, and Mather, A.E., 1981, A mathematical model for equilibrium solubility of hydrogen sulfide and carbon dioxide in aqueous alkanolamine solutions, Chemical Engineering Science, 36.

25. Deshmukh, R.D., 1979, A thermodynamic Model for the Solubility of Acid Gases in Treating Solutions, M.Sc. Thesis, The Unversity of Alberta, Canada.

26. Edwards, T.J., Maurer, G., Newman, J., Prausnitz, J. M., 1978, Vapor-liquid equilibria in multicomponent Aqueous Solution of Volatile Weak Electrolytes, AICHE J. 24, 966.

27. Eliott, J.R., and Lira, C.T., 1998, Introductory Chemical Engineering Thermodynamics, Prentice Hall, London.

28. Faramarzi, L., Kontogorgis, G.M., Thomsen, K., Stenby, E.H., 2009, Thermodynamic modeling of the solubility of CO_2 in aqueous alkanolamine solutions using UNIQUAC model Application to monoethanolamine and methyldiethanolamine, Energy Procedia, 1, 861-867

29. Ferrando, N., Lufo, R., Mougin, P., 2006, Coupling activity coefficient models, Henry's constant equation, and equation of state to calculate vapor-liquid and solid-liquid equilibrium data, Chemical Engineering Processing, 45, 773-782

30. Fischer, K. and Gmehling, J., 1996, Further development, status and results of the PSRK method for the prediction of vapor-liquid equilibria and gas solubilities, Fluid Phase Equilibria, 121, 185-206.

31. Fleming, K.B., Spears, M.L., and Bullin, J.A., 2006, Design Alternatives for Sweeteming LPG's and Liquid Hydrocarbons with Amines, Bryan Research and Emingeering, Inc, Technical Papers.

32. Frazier, H.D. and Kohl, A.L., 1950, Selective Absorption of H_2S from Gas Streams, Ind.Eng. Chem., Vol. 42, 2282-2292.

33. Godini, H.R., and Mowla, D., 2008, Selective study of H_2S and CO_2 absorption from gaseous mixture by MEA in packed beds, Chemical Engineering Research and Design, 86, 401-409.

34. Grottoli, M.G., Biardi, G., Pellegrini, L., 1991, A new simulation model for a real trays ansorption column, Computers chem. Eng, 15 (3), 171-179.

35. Haji-Sulaiman, M.Z., Aroua, M.K., Benamor, A., 1998, Analysis of equilibrium data of CO_2 in aqueous solutions of diethanolamine (DEA), methyldiethanolamine (MDEA) and their mixtures using the modified Kent Eisenberg model, Trans IChemE, 76, 961-968.

36. Hansen, H.K., Rasmussen P., Fredenslund A., Schiller M., Gmehling J., 1991, Vapor Liquid Equilibria by UNIFAC Group Gontribution, Revision and Extension 5, Ind. Eng. Chem. Res, 30, 2352-2355.

37. Harvey, A.H., 1996, Semiempirical correlation for Henry's constants ovel large temperature ranges, AIChE Journal, Vol 42 no 5, 1491-1494.

38. Hessen, E.T., Haug-Warberg, T., Svendsen, H.F., 2009, Thermodynamic models for CO_2-H_2O-alkanolamine system, a discussion, Energy Procedia, 971-978.

39. Hoff, K.A., 2003, Modeling and Experimental Study of Carbon Dioxide Absorption in a Membrane Contactor, PhD Thesis, Norwegian University of Science and Technology.

40. Holderbaum, T. and Gmehling, J., 1991, PSRK: A group Contribution Equation of State Based on UNIFAC, Fluid Phase Equilibria, 70, 251-265.

41. Horstmann, Sven., Jabloniec A., Krafczyk J., Fischer K., Gmehling J., 2005, PSRK group contribution equation of state: comprehensive revision and extension IV, including constants and a-function parameters for 1000 components, Fluid Phase Equilibria, 227 , 157-164.

42. Idem, R., Edali, M., Aboudheir, A., 2009, Kinetics Modeling and Simulation of the Experimental Kinetics Data of Carbon Dioxide Absorption into Mixed Aqueous Solutions of MDEA and PZ using Laminar Jet Apparatus with Numerically Solved Absorption-Rate/Kinetic Model, Energy Procedia, 1, 1343-1350.

43. Jakobsen, J.P., Krane, J., Svendsen, H.F., 2005, Liquid-Phase Composition Determintation in CO_2-H_2O-Alkanolamine System: An NMR Study, Ind. Eng. Chem. Res, 44, 9894-9903.

44. Jenab, M.H., Abdi, M. A., Najibi, S. H., Vahidi, M. and Matin, N. S., 2005, Solubility of Carbon Dioxide in Aqueous Mixture of N-Methyldiethanolamine + Piperazine + Sulfolane, J. Chem. Eng. Data, 50, 583-586.

45. Jou, F.Y. Mather, A.U., Otto, F.D., 1982, Solubility of H_2S and CO_2 in Aqueous Methydiethanolamine Solutions, Ind.Eng.Chem.Process.Des, 1982, 539-544.

46. Jou, F.Y. and Mather, A.E., 2006, Solubility of Methane in Methyldiethanolamine. J.Chem. Eng. Data, 51, 1429-1430.

47. Jou, F.Y., Carrol, J.J., Mather, A.E., Otto, F.D., 1993, Solubility of Mixtures of Hydrogen Sulfide and carbon Dioxide in Aqueous N-Methyldiethanolamine Solutions, J.Chem. Eng. Data, 38, 75-77.

48. Jou, F.Y., Otto, F.D., Mather, A.E., 1994, Vapor-Liquid Equilibrium of Carbon Dioxide in Aqueous mixture of Monoethanolamine and Methyldiaethanolamine, Ind.Eng.Chem.Res, 33, 2002-2005.

49. Jou, F.Y., Carrol, J.J., Mather, A.E., Otto, F.D., 1998, Solubility of Methane and Ethane in Aqueous Solutions of Methyldiethanolamine, J.Chem. Eng. Data, 43, 781-784.

50. Kamps, A.P.S., Babalon, A., Jodecke, M., Kuranov, G., Smirnova, N.A., Maurer, G., 2001, Solubility of Single Gases Carbon Dioxide and Hydrogen Sulfide in Aqueous Solutions of N-Methyldiethanolamine at Temperatures from 313 to 393 K and Pressures up to 7.6 MPa: New Experimental Data and Model Extension, Ind. Eng. Chem. Res, 40, 696-706.

51. Kaewsichan, L., Al-Bofersen, O., Yesavage, V.F., Selim, M.S., 2001, Predictions of the solubility of acid gases in monoethanolamine (MEA) and methyldiethanolamine (MDEA) solutions using the electrolyte-UNIQUAC model, Fluid Phase Equilibria, 183-184, 159-171.

52. Khoury, F.M., 2005, Multistage Separation Process. 3rd edition, CRC Press, Florida.

53. Kidnay, A.J., and Parrish, W.R., 2006, Fundamental of Natural Gas Processing, CRC Press, Tailor and Francis Group.

54. Kim, I., Hessen, E.T., Haug-Warberg, T., Svendsen, H.F., 2009, Enthalpies of Absorption of CO_2 in aqueous Alkanolamine Solutions from e-NRTL model, Energy Procedia, 1, 839-835.

55. Kim, I., Hoff, K.A., Hessen, E.T., Haug-Warberg, T., Svendsen, H.F., 2009, Enthalpy of absorption of CO_2 with alkanolamine solutions predicted from reaction equilibrium constant, Chemical Engineering Science, 64, 2027-2038.

56. Kohl, A. L., and Nielsen, R. B, 1997, *Gas Purification*, 5th edition, Gulf Publishing Company, Houston, Texas.

57. Kuranov, G., Rumpf, B., Smirnova, N.A., Maurer, G., 1996, Solubility of Single Gases Carbon Dioxide and Hydrogen Sulfide in Aqueous Solutions of N-Methyldiethanolamine in the Temperature Range 313-413 K at Pressures up to 5 MPa, Ind. Eng. Chem. Res., 35, 1959-1966.

58. Lee, L. J. B., 1996, A Vapor-Liquid Equilibrium Model for Natural Gas Sweetening Process, Ph.D. Dissertation, University of Oklahoma, Norman, Oklahoma.

59. Li, M.H, and Shen, K.P, 1993, Solubility of Hydrogen Sulfide in Aqueous Mixture of Monoethanolamine with N-Methyldiethanolamine, J. Chem. Eng. Data, 38, 105-108

60. Li, M.H.and Shen, K.P., 1993, Calculation of Equilibrium Solubility of Carbon Dioxide in Aqueous Mixtures of Monoethanolamine with Methyldiethanolamine. Fluid Phase Equilibria, 85, 129-140.

61. Li, Y.G, and Mather, A.E, 1994, Correlation and Prediction of Solubility of Carbon Dioxide in a Mixed Alkanolamine Solution, Ind.Eng.Chem.Res, 33, 2006-2015.

62. Loh, H. L., 1987, Simulation of Alkanolamine Sweetening Processes, Ph.D. Dissertation, Oklahoma State University, Oklahoma.

63. Lucka, L., Muller, I., Kenig, E.Y., Gorak, A., 2003, On the modeling and simulation of sour gas absorption by aqueous amine solutions, Chemical Engineering Science, 58, 3571-3578.

64. Maddox, R.N., Morgan, J., 1998, Gas Conditioning and Processing, Volume 4: Gas Treating and Sulfur Recovery, 4th ed, Campbell Petroleum Series, Norman, Oklahoma.

65. Ma'mun, S., Nilsen, R., Svendsen, H.F., 2005, Solubility of Carbon Dioxide in 30 mass % Monoethanolamine and 50 mass % Methyldiethanolamine Solutions, J. Chem. Eng. Data, 50, 630-634.

66. Ma'mun, S., 2005, Selection and charactherization of new absorbents for carbon dioxide capture, PhD Thesis, NTNU.

67. Mandal, B., and Bandyopadhyay, S.S., 2006, Simultaneous Absorption of CO_2 and H_2S into Aqueous Blends of N-Methyldiethanolamine and Diethanolamine, Environ. Sci. Technol., 40, 6076-6084.

68. Manning, Francis S., and Thompson, R., 1991, Oilfield Processing of Petroleum: Natural Gas, Pennwell Books.

69. Mathonat, C., Majer, V., Mather, A.E., Grolier, J.P.E., 1997, Enthalpy of absorption and solubility of CO_2 in aqueous solutions of methyldiethanolamine, Fluid phase Equilibria, 140, 171-182.

70. Matin, N.S., Goharrokhi, M.,Vahidi, M., Jenab, M.H., Abdi, M.A., and Najibi, S.H., 2007, Solubility of CO_2 in Aqueous Solutions of N-Methyldiethanolamine + Piperazine Using Extended Debye-Huckle Model, Journal of Chemical Engineering of Japan, 40, 4.

71. Mofarahi, M., Khojasteh, Y., Khaledi, H., Farahnak, A., 2008, Design of CO_2 absorption plant for recovery of C_2 from flue gases of gas turbine, Energy, 33, 1311-1319.

72. Mortimer, R.G., 2008, Physical Chemistry, 3rd ed, Elsevier Academic Press, Burlington.

73. Nakhaei, G.R., and Modarress, H., 2004, Simplification and application of the mean spherical approximation (MSA) model for 1:1 electrolyte solution, Fluid Phase Equilibria, 216, 301-305.

74. Oscarson, J.L., Dam, R.H., and Izatt, R.M., 1990, Enthalpies of Absorption of hydrogen Sulfide in Aqueous Methyldiethanolamine Solutions, Thermochimica Acta, 170, 235-241.

75. Polasek, J.C., Iglesias-Silva, G.A., Bullin, J.A., 2006, Using Mixed Amine Solutions for Gas Sweetening. Technical Paper, Bryan Research and Engineering Inc, Texas.

76. Poling, B.E. et.al., 2001, The Properties of Gases and Liquids, 5th edition, McGraw-Hill, New York.

77. Poplsteinova, J., et al, 2002, Modeling Vapor-Liquid Equilibrium for Systems H2O-MEA-CO2 and H2O-MDEA-CO2, *Chisa-2002*, Prague, Czech Republic.

78. Jakobsen, J.P., Krane, J., Svendsen, H.F., 2005, Liquid Phase Composition Determination in CO_2-H_2O-Alkanolamine Systems: An NMR Study, Ind. Eng. Chem. Res., 44, 9894-9903.

79. Posey, Mark Leon., 1996, Thermodynamic Model for Acid Gas Loaded Aqueous Alkanolamine Solutions, Ph.D Dissertation, University of Texas at Austin.

80. Prausnitz, J.M., Lichtenthaler, R.N., Azefedo, E.G., 1999, Molecular Thermodynamic of Fluid Phase Equilibria, 3rd edition, Prentice Hall, New Jersey.

81. Prausnitz, J.M. et.al., 1980, Computer Calculations for Multicomponent Vapor-Liquid and Liquid-Liquid Equilibria, Prentice Hall Inc, New Jersey.

82. Rangsunvigit, P., 1998, Vapor-Liquid Equilibrium of Acid Gases in Alkanolamine-Water System, Ph.D. Dissertation, Texas A&M University, Texas.

83. Rinker, E.B., 1997, Acid Gas Treating with Blended Alkanolamines, PhD Dissertation, University of California Santa Barbara.

84. Sadus, R.J., 1999, Simple Equation of State for Hard-Sphere Chains, AICHE Journal, 45, 11, 2454-2457.

85. Sandler S.I., 2006, Chemical, Biochemical, and Engineering Thermodynamics, John Wiley and Sons Inc, New Jersey.

86. Savage, D.W., and Funk, E.W., 1981, Selective Absorption of H_2S and CO_2 into Aqueous Solution of Methyldiethanolamine, AIChE meeting, Houston, Texas.

87. Shen, K.P, and Li, M.H, 1992, Solubility of Carbon Dioxide in Aqueous Mixtures of Monoethanolamine with Methyldiethanolamine, J. Chem. Eng. Data, 37, 96-100.

88. Smith, J.M. et.al., 2005, Introduction to Chemical Engineering Thermodynamics. 7th edition, McGraw Hill, New York.

89. Solbraa, E., 2002, Measurement and Modeling of Absorption of CO_2 into Methyldiethanolamine Solutions at High Pressures, PhD Thesis, Norwegian University of Science and Technology.

90. Thomsen, K., 2005, Modeling electrolyte solutions with the extended universal quasichemical (UNIQUAC) model, Pure Appl. Chem., 77, 3, 531–542

91. Tontiwachwuthikul, P., 1990, New Pilot Plant Technique for Designing Gas Absorber with Chemical Reactions, PhD Dissertation, The University of British Columbia.

92. Triolo, R., Grigera, J.R., Blum, L., 1976, Simple Electrolytes in the Mean Spherical Approximation, The Journal of Physical Chemistry, 80, 17, 1858-1861.

93. Vaz, R. N., 1980, Design of Ethanolamine Sweetening Processes using a Reaction Equilibrium Model, Ph.D. Dissertation, Oklahoma State University, Oklahoma.

94. Vrachnos, A., Voutsas, E., Magoulas, K., Lygeros, A., 2004, Thermodynamic of Acid Gas-MDEA-Water Systems, Ind. Eng. Chem. Res., 43 (11), 2798-2804.

95. Watanasari, T., et al, 1982, Prediction of the thermodynamic properties of Electrolyte solutions using the Mean Spherical Approximation, J. Phys. Chem., 86, 292-294

96. Weiland, R.H., Dingman, J.C., Cronin, D.B., 1997, Heat Capacity of Aqueous Monoethanolamine, Diethanolamine, N-Methyldiethanolamine, and N-Methyldiethanolamine-Based Blends with carbon dioxide, J.Chem.Eng.Data, 1997, 42, 1004-1006.

97. Xu, H.J., Zhang, C.F., Zheng, Z.S., 2002, Solubility of Hydrogen Sulfide and Carbon Dioxide in a Solution of Methyldiethanolamine Mixed with Ethylene Glycol, Ind. Eng. Chem. Res., 2002, 6175-6180.

98. Yarrison, M., 2006, Measurement and modeling of the water content of high pressure sweet and acid natural gas system, Doctoral Thesis, Rice University, Texas.

99. Yaws, Carl.L., 1999, Chemical Properties Handbook, New York, McGraw-Hill.

100. Zarzycki, R. and Chacuk, A., 1993, Absorption. Fundamentals and Applications, Pergamon Press, Oxford.

APPENDIX A

PARAMETERS USED IN THE CALCULATION

Table A.1 Group interaction parameters for Wu-Sandler

a_{mn}						
n\m	CO_2	H_2S	CH_4	H_2O	MDEA-I	CH_2OH
CO_2	0	204.0	0	491.14523	700	700
H_2S	-463.98	0	0.0	514.7971	700.0	700.0
CH_4	0	0.0	0	10753.155	1000	-948.3506
H_2O	269.16452	595.962	-24466.4	0	58.0	-83.88
MDEA-I	700	700.0	1000	6.985	0	-263.518
CH_2OH	700	700.0	1464.286	93.97	352.7907	0
b_{mn}						
n\m	CO_2	H_2S	CH_4	H_2O	MDEA-I	CH_2OH
CO_2	0	-55019.8	0	0	0	0
H_2S	195020	0	0	0	0	0
CH_4	0	0	0	-749169.2371	0	0
H_2O	0	0	17010700	0	6.985007	0
MDEA-I	0	0	0	-78637.4	0	168732.6
CH_2OH	0	0	0	0	-135875.0	0
c_{mn}						
n\m	CO_2	H_2S	CH_4	H_2O	MDEA-I	CH_2OH
CO_2	0	0	0	0	0	0
H_2S	0	0	0	0	0	0
CH_4	0	0	0	72823200	0	0
H_2O	0	0	-2807710000	0	0	0
MDEA-I	0	0	0	0	0	0
CH_2OH	0	0	0	0	0	0

Ref : Lee (1996)

Table A.2 Parameter for water content calculation in methane

T [^{o}C]	A$_1$	A$_2$	A$_3$
30	0.1303	-0.8963	3.5014
40	0.1271	-0.9076	3.7344
50	0.1192	-0.9080	3.9477
60	0.1466	-0.9625	4.1613
70	0.1643	-1.0060	4.3621
80	0.1574	-1.0090	4.5423
90	0.1740	-1.0528	4.7231
100	0.1886	-1.1003	4.8955

Table A.3 Parameter for water content calculation in carbon dioxide

T [^{o}C]	A$_1$	A$_2$	A$_3$
30	0.3403	-1.1539	3.6697
40	0.3115	-1.1640	3.9500
50	0.3279	-1.1477	4.1907
60	0.2682	-1.0738	4.3587
70	0.2198	-1.0039	4.5247

Table A.4 Parameter for water content calculation in hydrogen sulfide

T [^{o}C]	A$_1$	A$_2$	A$_3$
30	0.2986	-0.7136	3.6280
40	0.3294	-0.7720	3.8296
50	0.3204	-0.8014	4.0300
60	0.3306	-0.8218	4.2238
70	0.3597	-0.9095	4.4543

Table A.6 Ionic Size used in MSA model and Born model

Ion	σ in MSA [Angstrom]	σ in Born [Angstrom]
HCO_3^-	$0.57372177 + 5.4569945\ I^{-0.45072176}$	30.0
CO_3^{2-}	$2.8832274 + 9.151789\ I^{-0.42580691}$	30.0
HS^-	$2.2031963 + \dfrac{56.832343}{1 + 56.832343 * 1.9785833 * I} + \dfrac{6.583458}{1 + 6.583458 * 0.17106646 * I}$	25.0
S^{2-}	3.1	12.0
OH^-	3.0	3.0
H_3O^+	3.0	7.0
$MDEAH^+$	$-0.74895748 + \dfrac{20.99086}{1 + 20.99086 * 0.67916318 * I} + \dfrac{5.4487239}{1 + 5.4487239 * 0.014791757 * I}$	25.0
I = ionic strength in mole/L $$I = 0.5\sum_{i}^{n} C_i z_i^2$$ C is ion concentration in mole/L		

Ref : Lee (1996)

APPENDIX B

SIMULATION RESULTS

B.1 Solubility of gas mixture CO_2-H_2S in aqueous MDEA systems

Table B.1 Simulation results for CO_2-H_2S solubility in MDEA-H_2O system

Loading		Data Partial Pressure (kPa)		Calculated Partial Pressure (kPa)	
CO_2	H_2S	CO_2	H_2S	CO_2	H_2S
0.523	0.0769	23.9	3.7	44.97777	4.101484
0.399	0.0678	15.1	2.45	19.28234	2.175206
0.316	0.0784	11	2.51	10.97904	1.88972
0.0813	0.0161	0.976	0.122	0.391912	0.077403
0.0726	0.0356	0.919	0.258	0.380577	0.182192
0.00101	0.448	0.0361	8.38	0.034875	11.2321
0.00061	0.146	0.014	2.07	0.003762	0.849662
0.00044	0.215	0.00621	4.3	0.004703	1.951269
0.00076	0.143	0.0151	1.61	0.004559	0.814433
0.00077	0.104	0.0174	1.06	0.002945	0.419943
0.00129	0.0847	0.0188	0.734	0.003778	0.279931
0.00074	0.0605	0.0144	0.437	0.001304	0.140135
0.00668	0.0535	0.0727	0.348	0.012215	0.127345
0.00819	0.064	0.0796	0.415	0.019585	0.183465
0.00659	0.103	0.12	1.24	0.02752	0.444443
0.00248	0.108	0.0498	1.15	0.010492	0.467622
0.00654	0.36	0.228	10.4	0.167805	6.767861
0.0068	0.49	0.193	12.9	0.308626	15.21735
0.00179	0.699	0.14	48.9	0.192979	47.4979
0.00259	0.811	0.264	76.6	0.484972	91.8174
0.00452	0.873	0.661	97.1	1.215078	138.6273

0.0114	0.873	2.5	98	2.877701	138.8607
0.047	0.266	1.05	5.12	0.912546	4.001117
0.0126	0.746	1.02	59.1	1.605944	62.16524
0.0489	0.815	9.4	86.6	11.06316	116.4848
0.194	0.65	33.8	68.8	41.34254	86.83259
0.516	0.304	70.2	31.8	108.66	39.18211
0.649	0.127	88.8	13.9	114.1653	13.66885
0.758	0.0863	97.4	6.34	201.1128	13.58702
0.588	0.049	33.7	1.21	54.71281	2.921626
0.455	0.0406	18.1	0.644	23.36791	1.416528
0.375	0.0553	9.08	0.587	14.51929	1.502955
0.154	0.16	3.43	2.09	3.250784	2.575799
0.0958	0.341	2.16	7.88	3.304325	8.494784
0.0201	0.715	1.65	53.4	2.300026	53.82683
0.0007	0.882	0.0978	101	0.174141	138.4654
0.00144	0.805	0.154	71.3	0.232328	83.82375
0.00021	0.583	0.0153	27.5	0.01248	23.93489
0.00017	0.303	0.00506	6.51	0.003028	4.238031
0.00118	0.194	0.0279	2.96	0.010949	1.566885
0.00093	0.047	0.0103	0.233	0.001122	0.08472
0.00118	0.0241	0.00559	0.0641	0.000523	0.023228
0.00554	0.0167	0.0227	0.0323	0.002415	0.016024
0.021	0.0166	0.111	0.0401	0.025148	0.030077
0.788	0.0101	101	0.743	163.4489	1.256451
0.0205	0.366	0.719	10.19	0.548443	7.301364
0.0307	0.353	1.099	9.7	0.816271	6.999774
0.0318	0.355	1.207	10.46	0.857656	7.128259
0.0388	0.352	1.618	10.42	1.069348	7.202176
0.0775	0.339	3.271	10.92	2.43501	7.77696
0.0673	0.358	2.824	11.56	2.18108	8.448227
0.0873	0.343	3.417	10.85	2.919076	8.314646
0.102	0.341	4.213	11.25	3.619492	8.710294

0.249	0.355	14.53	16.97	17.79928	16.9864
0.291	0.331	19.09	18.72	22.72536	17.13622
0.31	0.31	20.46	17.46	24.201	16.02195
0.26	0.321	14.88	15.33	17.04644	14.17535
0.226	0.346	13.17	16.68	14.10199	14.63543
0.168	0.338	8.695	13.23	7.901272	11.08872
0.0273	0.2	0.457	2.71	0.326037	1.989744
0.0324	0.197	0.719	3.16	0.394404	1.991262
0.0533	0.204	1.35	3.85	0.78014	2.407143
0.0756	0.236	2.16	5	1.489881	3.591585
0.0908	0.23	2.67	5.14	1.890257	3.668374
0.112	0.214	3.19	4.5	2.424535	3.52806
0.127	0.219	3.95	5.19	3.03924	3.938355
0.164	0.209	5.44	5.47	4.51073	4.240395
0.178	0.193	5.45	4.41	4.8952	3.912415
0.218	0.209	7.81	5.84	7.700524	5.280858
0.252	0.208	9.34	6.01	10.30273	5.980389
0.27	0.177	9.42	4.9	10.58671	4.896019
0.242	0.222	9.51	6.5	10.00203	6.449814
0.237	0.192	7.65	4.91	8.519221	4.922353
0.199	0.149	4.61	3.32	5.029042	2.800769
0.184	0.161	4.17	3.91	4.547483	2.969887
0.594	0.00351	28.7	0.139	47.43502	0.181655
0.591	0.0118	28.9	0.609	48.13136	0.621911
0.612	0.0623	39	4.49	66.92392	4.307841
0.506	0.0836	21.7	4.17	37.8564	4.099286
0.42	0.076	14.3	2.81	21.2731	2.62446
0.539	0.117	31.9	8.12	53.16	7.388479
0.537	0.0947	24.1	4.99	47.96925	5.456883
0.498	0.0752	16.9	2.92	34.88272	3.472472
0.342	0.0473	7.55	1.06	11.1112	1.101432
0.349	0.0584	9.43	1.52	12.21044	1.452088

0.599	0.0865	20.3	3.46	68.33602	6.227773
0.709	0.0702	91.5	7.68	129.5768	7.797233
0.679	0.0525	89.7	5.92	97.67173	4.666594
0.658	0.0435	53.3	3.28	82.1929	3.393483
0.556	0.0369	33.7	2	42.97663	1.858076

B.2 Summary of the stages specification for CO_2 absorption

===
STAGE 1 DATA COMPILATION

Temperature of stage = 334.9815 K

Partial pressure of gas entering stage
    CO2 = 4.5769 bar (or 0.09985 mole fraction)
    CH4 = 48.351 bar (or 0.89865 mole fraction)
    H2O = 0.048678 bar (or 0.001498 mole fraction)

Partial pressure of gas leaving stage
    CO2 = 2.4033 bar (or 0.048961 mole fraction)
    CH4 = 52.3423 bar (or 0.94607 mole fraction)
    H2O = 0.18614 bar (or 0.0049663 mole fraction)

Flow rate gas out = 2463.3272 mole/s
Flow rate gas in = 2594.1784 mole/s

Solvent circulation rate = 2.7795 mole/mole feed gas

Loading of amine solution entering stage
    CO2 = 0.1527 mole/mole amine
    CH4 = 0.01743 mole/mole amine

Loading of amine solution leaving stage
    CO2 = 0.33059 mole/mole amine
    CH4 = 0.018428 mole/mole amine
===

===
STAGE 2 DATA COMPILATION

Temperature of stage = 325.8015 K

Partial pressure of gas entering stage
    CO2 = 2.4033 bar (or 0.048961 mole fraction)
    CH4 = 52.3423 bar (or 0.94607 mole fraction)
    H2O = 0.18614 bar (or 0.0049663 mole fraction)

Partial pressure of gas leaving stage
    CO2 = 0.90058 bar (or 0.018739 mole fraction)
    CH4 = 53.3859 bar (or 0.97771 mole fraction)
    H2O = 0.12875 bar (or 0.0035546 mole fraction)

Flow rate gas out = 2383.3221 mole/s
Flow rate gas in = 2463.3272 mole/s

Solvent circulation rate = 2.8947 mole/mole feed gas

Loading of amine solution entering stage
    CO2 = 0.055111 mole/mole amine
    CH4 = 0.017047 mole/mole amine

Loading of amine solution leaving stage
    CO2 = 0.1527 mole/mole amine
    CH4 = 0.01743 mole/mole amine
===

===
STAGE 3 DATA COMPILATION

Temperature of stage = 317.1415 K

Partial pressure of gas entering stage
    CO_2 = 0.90058 bar (or 0.018739 mole fraction)
    CH_4 = 53.3859 bar (or 0.97771 mole fraction)
    H_2O = 0.12875 bar (or 0.0035546 mole fraction)

Partial pressure of gas leaving stage
    CO_2 = 0.3181 bar (or 0.0067705 mole fraction)
    CH_4 = 53.3865 bar (or 0.99075 mole fraction)
    H_2O = 0.086279 bar (or 0.0024753 mole fraction)

Flow rate gas out = 2351.9147 mole/s
Flow rate gas in = 2383.3221 mole/s

Solvent circulation rate = 2.9787 mole/mole feed gas

Loading of amine solution entering stage
    CO_2 = 0.018184 mole/mole amine
    CH_4 = 0.017022 mole/mole amine

Loading of amine solution leaving stage
    CO_2 = 0.055111 mole/mole amine
    CH_4 = 0.017047 mole/mole amine
===

===
STAGE 4 DATA COMPILATION

Temperature of stage = 312.6715 K

Partial pressure of gas entering stage
    CO_2 = 0.3181 bar (or 0.0067705 mole fraction)
    CH_4 = 53.3865 bar (or 0.99075 mole fraction)
    H_2O = 0.086279 bar (or 0.0024753 mole fraction)

Partial pressure of gas leaving stage
    CO_2 = 0.11147 bar (or 0.0024042 mole fraction)
    CH_4 = 53.2196 bar (or 0.99557 mole fraction)
    H_2O = 0.069158 bar (or 0.0020281 mole fraction)

Flow rate gas out = 2340.5087 mole/s
Flow rate gas in = 2351.9147 mole/s

Solvent circulation rate = 3.0136 mole/mole feed gas

Loading of amine solution entering stage
    CO_2 = 0.0049533 mole/mole amine
    CH_4 = 0.016978 mole/mole amine

Loading of amine solution leaving stage
    CO_2 = 0.018184 mole/mole amine
    CH_4 = 0.017022 mole/mole amine
===

```
=========================================
     STAGE 5 DATA COMPILATION
```

Temperature of stage = 310.9315 K

Partial pressure of gas entering stage
    CO_2 = 0.11147 bar (or 0.0024042 mole fraction)
    CH_4 = 53.2196 bar (or 0.99557 mole fraction)
    H_2O = 0.069158 bar (or 0.0020281 mole fraction)

Partial pressure of gas leaving stage
    CO_2 = 0.039019 bar (or 0.00084886 mole fraction)
    CH_4 = 52.9301 bar (or 0.99727 mole fraction)
    H_2O = 0.063311 bar (or 0.0018769 mole fraction)

Flow rate gas out = 2340.5087 mole/s
Flow rate gas in = 2351.9147 mole/s

Solvent circulation rate = 3.0136 mole/mole feed gas

Loading of amine solution entering stage
    CO_2 = 0.0001 mole/mole amine

Loading of amine solution leaving stage
    CO_2 = 0.0049533 mole/mole amine
    CH_4 = 0.016978 mole/mole amine

B.3 Summary of the stages specification for H_2S absorption

```
==========================================
           STAGE 1 DATA COMPILATION


Temperature of stage = 328.4963 K

Partial pressure of gas entering stage
    H2S = 4.1295 bar  (or 0.099837 mole fraction)
    CH4 = 48.3807 bar  (or 0.89854 mole fraction)
    H2O = 0.051978 bar  (or 0.0016258 mole fraction)

Partial pressure of gas leaving stage
    H2S = 1.6366 bar  (or 0.036721 mole fraction)
    CH4 = 52.6439 bar  (or 0.95949 mole fraction)
    H2O = 0.13792 bar  (or 0.00379 mole fraction)

Flow rate gas out = 2456.8008 mole/s
Flow rate gas in  = 2624.4155 mole/s

Solvent circulation rate = 2.7666 mole/mole feed gas

Loading of amine solution entering stage
    H2S = 0.11265 mole/mole amine
    CH4 = 0.017233 mole/mole amine

Loading of amine solution leaving stage
    H2S = 0.33116 mole/mole amine
    CH4 = 0.018327 mole/mole amine
==========================================
```

```
============================================
           STAGE 2 DATA COMPILATION


Temperature of stage = 319.6163 K

Partial pressure of gas entering stage
    H2S = 1.6366 bar  (or 0.036721 mole fraction)
    CH4 = 52.6439 bar  (or 0.95949 mole fraction)
    H2O = 0.13792 bar  (or 0.00379 mole fraction)

Partial pressure of gas leaving stage
    H2S = 0.58165 bar  (or 0.013343 mole fraction)
    CH4 = 53.3542 bar  (or 0.98392 mole fraction)
    H2O = 0.096335 bar  (or 0.0027356 mole fraction)

Flow rate gas out = 2395.6506 mole/s
Flow rate gas in  = 2456.8008 mole/s

Solvent circulation rate = 2.9305 mole/mole feed gas

Loading of amine solution entering stage
    H2S = 0.03867 mole/mole amine
    CH4 = 0.017053 mole/mole amine

Loading of amine solution leaving stage
    H2S = 0.11265 mole/mole amine
    CH4 = 0.017233 mole/mole amine
============================================
```

==

STAGE 3 DATA COMPILATION

Temperature of stage = 314.4463 K

Partial pressure of gas entering stage
    H_2S = 0.58165 bar (or 0.013343 mole fraction)
    CH_4 = 53.3542 bar (or 0.98392 mole fraction)
    H_2O = 0.096335 bar (or 0.0027356 mole fraction)

Partial pressure of gas leaving stage
    H_2S = 0.20426 bar (or 0.0047594 mole fraction)
    CH_4 = 53.3927 bar (or 0.99304 mole fraction)
    H_2O = 0.075592 bar (or 0.0021961 mole fraction)

Flow rate gas out = 2373.6132 mole/s
Flow rate gas in = 2395.6506 mole/s

Solvent circulation rate = 2.9961 mole/mole feed gas

Loading of amine solution entering stage
    H_2S = 0.012419 mole/mole amine
    CH_4 = 0.017018 mole/mole amine

Loading of amine solution leaving stage
    H_2S = 0.03867 mole/mole amine
    CH_4 = 0.017053 mole/mole amine

==

STAGE 4 DATA COMPILATION

Temperature of stage = 312.2263 K

Partial pressure of gas entering stage
    H_2S = 0.20426 bar (or 0.0047594 mole fraction)
    CH_4 = 53.3927 bar (or 0.99304 mole fraction)
    H_2O = 0.075592 bar (or 0.0021961 mole fraction)

Partial pressure of gas leaving stage
    H_2S = 0.071549 bar (or 0.0016811 mole fraction)
    CH_4 = 53.279 bar (or 0.99633 mole fraction)
    H_2O = 0.067765 bar (or 0.0019909 mole fraction)

Flow rate gas out = 2365.7893 mole/s
Flow rate gas in = 2373.6132 mole/s

Solvent circulation rate = 3.0206 mole/mole feed gas

Loading of amine solution entering stage
    H_2S = 0.0031216 mole/mole amine
    CH_4 = 0.017017 mole/mole amine

Loading of amine solution leaving stage
    H_2S = 0.012419 mole/mole amine
    CH_4 = 0.017018 mole/mole amine

==

```
==============================================
     STAGE 5 DATA COMPILATION


   Temperature of stage = 311.4763 K


   Partial pressure of gas entering stage
       H2S = 0.071549 bar  (or 0.0016811 mole fraction)
       CH4 = 53.279 bar  (or 0.99633 mole fraction)
       H2O = 0.067765 bar  (or 0.0019909 mole fraction)


   Partial pressure of gas leaving stage
       H2S = 0.025114 bar  (or 0.00059325 mole fraction)
       CH4 = 53.061 bar  (or 0.99748 mole fraction)
       H2O = 0.065058 bar  (or 0.001922 mole fraction)


 Flow rate gas out = 2365.7893 mole/s
 Flow rate gas in  = 2373.6132 mole/s


 Solvent circulation rate = 3.0206 mole/mole feed gas


 Loading of amine solution entering stage
       H2S = 0.0001 mole/mole amine


 Loading of amine solution leaving stage
       H2S = 0.0031216 mole/mole amine
       CH4 = 0.017017 mole/mole amine
==============================================
```

B4. Summary of the stages specification for mixture CO_2-H_2S absorption

```
=================================================
         STAGE 1 DATA COMPILATION

  Temperature of stage = 344.2934 K
  Partial pressure of gas entering stage
      CO2 = 3.6301 bar  (or 0.07987 mole fraction)
      H2S = 3.2823 bar  (or 0.07987 mole fraction)
      CH4 = 45.1942 bar  (or 0.83863 mole fraction)
      H2O = 0.051359 bar  (or 0.0016279 mole fraction)
  Partial pressure of gas leaving stage
      CO2 = 3.8029 bar  (or 0.076913 mole fraction)
      H2S = 1.849 bar  (or 0.040368 mole fraction)
      CH4 = 48.5369 bar  (or 0.87585 mole fraction)
      H2O = 0.26158 bar  (or 0.0068695 mole fraction)
  Flow rate gas out = 2539.885 mole/s
  Flow rate gas in  = 2650.5948 mole/s
  Solvent circulation rate = 2.849 mole/mole feed gas
  Loading of amine solution entering stage
      CO2 = 0.23766 mole/mole amine
      H2S = 0.12635 mole/mole amine
      CH4 = 0.03022 mole/mole amine
  Loading of amine solution leaving stage
      CO2 = 0.25922 mole/mole amine
      H2S = 0.26371 mole/mole amine
      CH4 = 0.028105 mole/mole amine
=================================================
```

```
=================================================
         STAGE 2 DATA COMPILATION

  Temperature of stage = 340.3634 K
  Partial pressure of gas entering stage
      CO2 = 3.8029 bar  (or 0.076913 mole fraction)
      H2S = 1.849 bar  (or 0.040368 mole fraction)
      CH4 = 48.5369 bar  (or 0.87585 mole fraction)
      H2O = 0.26158 bar  (or 0.0068695 mole fraction)
  Partial pressure of gas leaving stage
      CO2 = 2.2607 bar  (or 0.04588 mole fraction)
      H2S = 0.80016 bar  (or 0.017513 mole fraction)
      CH4 = 51.3983 bar  (or 0.93045 mole fraction)
      H2O = 0.23385 bar  (or 0.0061557 mole fraction)
  Flow rate gas out = 2392.0266 mole/s
  Flow rate gas in  = 2539.885 mole/s
  Solvent circulation rate = 2.915 mole/mole feed gas
  Loading of amine solution entering stage
      CO2 = 0.13002 mole/mole amine
      H2S = 0.050105 mole/mole amine
      CH4 = 0.031613 mole/mole amine
  Loading of amine solution leaving stage
      CO2 = 0.23766 mole/mole amine
      H2S = 0.12635 mole/mole amine
      CH4 = 0.03022 mole/mole amine
=================================================
```

===

STAGE 3 DATA COMPILATION

Temperature of stage = 327.2534 K
Partial pressure of gas entering stage
    CO_2 = 2.2607 bar (or 0.04588 mole fraction)
    H_2S = 0.80016 bar (or 0.017513 mole fraction)
    CH_4 = 51.3983 bar (or 0.93045 mole fraction)
    H_2O = 0.23385 bar (or 0.0061557 mole fraction)
Partial pressure of gas leaving stage
    CO_2 = 0.8583 bar (or 0.01789 mole fraction)
    H_2S = 0.29202 bar (or 0.0065875 mole fraction)
    CH_4 = 52.8591 bar (or 0.97176 mole fraction)
    H_2O = 0.13675 bar (or 0.0037665 mole fraction)
Flow rate gas out = 2291.4044 mole/s
Flow rate gas in = 2392.0266 mole/s
Solvent circulation rate = 3.0531 mole/mole feed gas
Loading of amine solution entering stage
    CO_2 = 0.043563 mole/mole amine
    H_2S = 0.01641 mole/mole amine
    CH_4 = 0.032899 mole/mole amine
Loading of amine solution leaving stage
    CO_2 = 0.13002 mole/mole amine
    H_2S = 0.050105 mole/mole amine
    CH_4 = 0.031613 mole/mole amine

===

STAGE 4 DATA COMPILATION

Temperature of stage = 316.8934 K
Partial pressure of gas entering stage
    CO_2 = 0.8583 bar (or 0.01789 mole fraction)
    H_2S = 0.29202 bar (or 0.0065875 mole fraction)
    CH_4 = 52.8591 bar (or 0.97176 mole fraction)
    H_2O = 0.13675 bar (or 0.0037665 mole fraction)
Partial pressure of gas leaving stage
    CO_2 = 0.30277 bar (or 0.0064757 mole fraction)
    H_2S = 0.10294 bar (or 0.0023921 mole fraction)
    CH_4 = 52.9986 bar (or 0.98868 mole fraction)
    H_2O = 0.085018 bar (or 0.0024489 mole fraction)
Flow rate gas out = 2252.8508 mole/s
Flow rate gas in = 2291.4044 mole/s
Solvent circulation rate = 3.1704 mole/mole feed gas
Loading of amine solution entering stage
    CO_2 = 0.010363 mole/mole amine
    H_2S = 0.0042058 mole/mole amine
    CH_4 = 0.03374 mole/mole amine
Loading of amine solution leaving stage
    CO_2 = 0.043563 mole/mole amine
    H_2S = 0.01641 mole/mole amine
    CH_4 = 0.032899 mole/mole amine

===

===
    STAGE 5 DATA COMPILATION

Temperature of stage = 312.2134 K
Partial pressure of gas entering stage
    CO_2 = 0.30277 bar (or 0.0064757 mole fraction)
    H_2S = 0.10294 bar (or 0.0023921 mole fraction)
    CH_4 = 52.9986 bar (or 0.98868 mole fraction)
    H_2O = 0.085018 bar (or 0.0024489 mole fraction)
Partial pressure of gas leaving stage
    CO_2 = 0.10602 bar (or 0.0022981 mole fraction)
    H_2S = 0.03607 bar (or 0.00085102 mole fraction)
    CH_4 = 52.9116 bar (or 0.99486 mole fraction)
    H_2O = 0.067544 bar (or 0.0019901 mole fraction)
Flow rate gas out = 2252.8508 mole/s
Flow rate gas in = 2291.4044 mole/s
Solvent circulation rate = 3.1704 mole/mole feed gas
Loading of amine solution entering stage
    CO_2 = 0.0001 mole/mole amine
    H_2S = 0.0001 mole/mole amine
Loading of amine solution leaving stage
    CO_2 = 0.010363 mole/mole amine
    H_2S = 0.0042058 mole/mole amine
    CH_4 = 0.03374 mole/mole amine
===

APPENDIX C

SAMPLE OF MATLAB CODE

CO_2 solubility calculation

Main Matlab M-file Routine

```
clc
clear all
T = 40+273.15;
cw = 1000/18; % mol/L
K1 = exp(132.899-13445.9/T-22.4773*log(T));
K2 = 1/cw*exp(231.465-12092.1/T-36.7816*log(T));
K3 = exp(216.049-12431.7/T-35.4819*log(T));
K4 = exp(-46.086-4756.9/T+6.4268*log(T)); % by posey
Kc1 = K3/K4;
Kabs = K2/K4;
%1=H2O
%2=MDEA
massfrac = [1-0.2354605 0.2354605]; % T = 40
%massfrac = [1-0.239318 0.239318]; % T = 70
%massfrac = [1-0.244695 0.244695]; % T = 100
ys = input('ys = '); %0.1;
% ======== cons_water calculation ==========
%----------Density of aqueous MDEA ------
MR = [18.02 119.2];
density = densityMDEAalghawas(T,massfrac);
density = density*1000; % in kg/m3
mass_solvent = 1000; % g
volume_solvent = mass_solvent/density; % L
mol_MDEA = massfrac(2)*mass_solvent/MR(2);
mol_H2O = massfrac(1)*mass_solvent/MR(1);
cons_MDEA = mol_MDEA/volume_solvent
cons_water = mol_H2O/volume_solvent;

%==========================================
m = cons_MDEA; % concentrasi MDEA total mol/L
cacing(1) = (Kc1*m+m*ys-m*sqrt(Kc1^2+6*Kc1*ys+ys^2-
4*Kc1^2*ys+4*Kc1^2*ys^2-4*Kc1*ys^2))/(2*(Kc1-1));
cacing(2) = (Kc1*m+m*ys+m*sqrt(Kc1^2+6*Kc1*ys+ys^2-
4*Kc1^2*ys+4*Kc1^2*ys^2-4*Kc1*ys^2))/(2*(Kc1-1));

mys = m*ys;
mymin = m*(1-ys);
if cacing(1)>=0 & cacing(1)<=mys & cacing(1)<=mymin
    jawab = cacing(1);
else if cacing(2)>=0 & cacing(2)<=mys & cacing(2)<=mymin
    jawab = cacing(2);
    end
end
B1 = m*(1-ys)-jawab;
B2 = m*ys+jawab;
B3 = m*ys-jawab;
B4 = jawab;
```

```
jawab;

C1 = (cons_water-2*B3-3*B4+B2)/(1+2*B2*K4/B1); % newest set
A = B2*B3/B1/C1/Kabs;
C2 = K4*B2*C1/B1;
%C2 = K3*B3*C1/B4;
C3 = K1*C1^2/C2;


cons(1) = A;
cons(2) = C1;
cons(3) = B1;
cons(4) = C3;
cons(5) = C2;
cons(6) = B3;
cons(7) = B4;
cons(8) = B2;
cons';


for i = 1:8
    moli(i) = cons(i)*volume_solvent;
end
moli;
mol_tot = sum(moli);
xt(1) = moli(1)/mol_tot;
xt(2) = moli(2)/mol_tot;
xt(3) = moli(3)/mol_tot;
xt(4) = moli(4)/mol_tot;
xt(5) = moli(5)/mol_tot;
xt(6) = moli(6)/mol_tot;
xt(7) = moli(7)/mol_tot;
xt(8) = moli(8)/mol_tot;
format long g

x_tot = sum(xt);
gamma= GAMMA_ELECGC(xt,T,mol_tot,volume_solvent,massfrac);
gammai = gamma;

Kc1app = Kc1/(gammai(8)*gammai(7)/(gammai(3)*gammai(6)));
Kabsapp = Kabs/(gammai(8)*gammai(6)/(gammai(1)*gammai(3)*gammai(2)));
K1app = K1/(gammai(5)*gammai(4)/(gammai(2)*gammai(2)));
K2app = K2/(gammai(6)*gammai(5)/(gammai(1)*gammai(2)*gammai(2)));
K3app = K3/(gammai(7)*gammai(5)/(gammai(6)*gammai(2)));
K4app = K4/(gammai(5)*gammai(3)/(gammai(2)*gammai(8)));

cacing(1) = (Kc1app*m+m*ys-m*sqrt(Kc1app^2+6*Kc1app*ys+ys^2-
4*Kc1app^2*ys+4*Kc1app^2*ys^2-4*Kc1app*ys^2))/(2*(Kc1app-1));
cacing(2) = (Kc1app*m+m*ys+m*sqrt(Kc1app^2+6*Kc1app*ys+ys^2-
4*Kc1app^2*ys+4*Kc1app^2*ys^2-4*Kc1app*ys^2))/(2*(Kc1app-1));

if cacing(1)>=0 & cacing(1)<=mys & cacing(1)<=mymin
    jawab = cacing(1);
else if cacing(2)>=0 & cacing(2)<=mys & cacing(2)<=mymin
    jawab = cacing(2);
    end
end
B1 = m*(1-ys)-jawab;
B2 = m*ys+jawab;
B3 = m*ys-jawab;
B4 = jawab;
```

```
C1 = (cons_water-2*B3-3*B4+B2)/(1+2*B2*K4app/B1); % newest set
A = B2*B3/B1/C1/Kabsapp;
C2 = K4app*B2*C1/B1;
C3 = K1app*C1^2/C2;

cons(1) = A;
cons(2) = C1;
cons(3) = B1;
cons(4) = C3;
cons(5) = C2;
cons(6) = B3;
cons(7) = B4;
cons(8) = B2;
cons';
for i = 1:8
    moli(i) = cons(i)*volume_solvent;
end
moli;
mol_tot = sum(moli);
xt_old = xt';
xt(1) = moli(1)/mol_tot;
xt(2) = moli(2)/mol_tot;
xt(3) = moli(3)/mol_tot;
xt(4) = moli(4)/mol_tot;
xt(5) = moli(5)/mol_tot;
xt(6) = moli(6)/mol_tot;
xt(7) = moli(7)/mol_tot;
xt(8) = moli(8)/mol_tot;
format long g
xt';

tolerance = 1e-10;
deltax = abs(xt_old(1)-xt(1))+abs(xt_old(2)-xt(2))+abs(xt_old(3)-
xt(3))+abs(xt_old(4)-xt(4))+abs(xt_old(5)-xt(5))+abs(xt_old(6)-
xt(6))+abs(xt_old(7)-xt(7))+abs(xt_old(8)-xt(8));

while deltax > tolerance
    x_tot = sum(xt);
    gamma = GAMMA_ELECGC(xt,T,mol_tot,volume_solvent,massfrac);
    gammai = gamma;
    Kc1app = Kc1/(gammai(8)*gammai(7)/(gammai(3)*gammai(6)));
    Kabsapp =
Kabs/(gammai(8)*gammai(6)/(gammai(1)*gammai(3)*gammai(2)));
    K1app = K1/(gammai(5)*gammai(4)/(gammai(2)*gammai(2)));
    K2app = K2/(gammai(6)*gammai(5)/(gammai(1)*gammai(2)*gammai(2)));
    K3app = K3/(gammai(7)*gammai(5)/(gammai(6)*gammai(2)));
    K4app = K4/(gammai(5)*gammai(3)/(gammai(2)*gammai(8)));

    cacing(1) = (Kc1app*m+m*ys-m*sqrt(Kc1app^2+6*Kc1app*ys+ys^2-
        4*Kc1app^2*ys+4*Kc1app^2*ys^2-4*Kc1app*ys^2))/(2*(Kc1app-1));
    cacing(2) = (Kc1app*m+m*ys+m*sqrt(Kc1app^2+6*Kc1app*ys+ys^2-
        4*Kc1app^2*ys+4*Kc1app^2*ys^2-4*Kc1app*ys^2))/(2*(Kc1app-1));

    if cacing(1)>=0 & cacing(1)<=mys & cacing(1)<=mymin
        jawab = cacing(1);
    else if cacing(2)>=0 & cacing(2)<=mys & cacing(2)<=mymin
        jawab = cacing(2);
        end
    end
    B1 = m*(1-ys)-jawab;
```

```matlab
        B2 = m*ys+jawab;
        B3 = m*ys-jawab;
        B4 = jawab;


        C1 = (cons_water-2*B3-3*B4+B2)/(1+2*B2*K4app/B1); % newest set
        A = B2*B3/B1/C1/Kabsapp;
        C2 = K4app*B2*C1/B1;
        C3 = K1app*C1^2/C2;


        cons(1) = A;
        cons(2) = C1;
        cons(3) = B1;
        cons(4) = C3;
        cons(5) = C2;
        cons(6) = B3;
        cons(7) = B4;
        cons(8) = B2;
        cons';
        for i = 1:8
            moli(i) = cons(i)*volume_solvent;
        end
        moli;
        mol_tot = sum(moli);
        xt_old = xt';
        xt(1) = moli(1)/mol_tot;
        xt(2) = moli(2)/mol_tot;
        xt(3) = moli(3)/mol_tot;
        xt(4) = moli(4)/mol_tot;
        xt(5) = moli(5)/mol_tot;
        xt(6) = moli(6)/mol_tot;
        xt(7) = moli(7)/mol_tot;
        xt(8) = moli(8)/mol_tot;
        format long g
        xt';
        deltax = abs(xt_old(1)-xt(1))+abs(xt_old(2)-xt(2))+abs(xt_old(3)-
                xt(3))+abs(xt_old(4)-xt(4))+abs(xt_old(5)-
                xt(5))+abs(xt_old(6)-xt(6))+abs(xt_old(7)-
                xt(7))+abs(xt_old(8)-xt(8));
    end

xt';
loading = (ys*m+A)/m;
[H_CO2 H_CH4] = HENRY_NG_water_MDEA2(T);
fug_gas = [1 1];
poynting_solute = [1 1];
poynting_solvent = [1 1];
Ppar(1) = xt(1)*gammai(1)*H_CO2*poynting_solute(1);
Ppar(2) = xt(2)*gammai(2)*poynting_solvent(1); % bar
P = Ppar(1)/fug_gas(1)+Ppar(2)/fug_gas(2);
y_gas = [Ppar(1)/P/fug_gas(1) Ppar(2)/P/fug_gas(2)]
Pold=P;
fug_gas = PR_NG_MDEA_CO2_H2O(y_gas,P,T)
poynting_solute = poynting_solute_MDEA(T,P);
poynting_solvent = poynting_solvent_MDEA(T,P);
Ppar(1) = xt(1)*gammai(1)*H_CO2*poynting_solute(1);
Ppar(2) = xt(2)*gammai(2)*poynting_solvent(1) % bar;
P = Ppar(1)/fug_gas(1)+Ppar(2)/fug_gas(2)
y_gas = [Ppar(1)/P/fug_gas(1) Ppar(2)/P/fug_gas(2)];
delta = (Pold-P)/(P);

while abs(delta) > 0.001
```

```
        Pold=P;
        fug_gas = PR_NG_MDEA_CO2_H2O(y_gas,P,T);
        poynting_solute = poynting_solute_MDEA(T,P);
        poynting_solvent = poynting_solvent_MDEA(T,P);
        Ppar(1) = xt(1)*gammai(1)*H_CO2*poynting_solute(1);
        Ppar(2) = xt(2)*gammai(2)*poynting_solvent(1); % bar
        P = Ppar(1)/fug_gas(1)+Ppar(2)/fug_gas(2);
        y_gas = [Ppar(1)/P/fug_gas(1) Ppar(2)/P/fug_gas(2)];
        delta = (Pold-P)/(P)
end
CS(1) = Ppar(1)*100;
CS(2) = loading;
CS(3) = ys;
CS'
```

M-file densityMDEAalghawas

```
function density_MDEA = densityMDEAalghawas(T,massfrac)
wMDEA = massfrac(2);
T;
Kd1 = 0.715929+0.395951*wMDEA+0.927974*wMDEA^2-0.794931*wMDEA^3;
Kd2 = 2.13799e-3-1.98173e-3*wMDEA-3.87553e-3*wMDEA^2+3.04228e-3*wMDEA^3;
Kd3 = -4.00972e-6+3.07038e-6*wMDEA+3.58483e-6*wMDEA^2-2.70947e-
6*wMDEA^3;
density_MDEA = Kd1+Kd2*T+Kd3*T^2; %in kg/L
```

M-file GAMMA_ELECGC

```
function gamma = GAMMA_ELECGC(xi,T,mol_tot,volume_solvent,massfrac)
% System CO2-H2O-MDEA
%=======================
% 1 = CO2
% 2 = H2O
% 3 = MDEA
%========================================================================
% Main group    m    subgroup    k     Rk      Qk     vk(1) vk(2) vk(3)
%    CO2        56     CO2        56   1.3000   1.120   1     0     0
%    H2O        7      H2O        16   0.9200   1.400   0     1     0
%    MDEA-I                            2.5353   2.020   0     0     1
%    CH2OH                             1.2044   1.124   0     0     2
%========================================================================

Rk = [1.3000;0.92;2.5353;1.2044];
Qk = [1.12;1.4;2.02;1.124];
v = [1 0 0 0 ;0 1 0 0;0 0 1 2];

r = v*Rk;
q = v*Qk;
v=v';
for i = 1:3;
    for k = 1:4;
        e(k,i) = v(k,i)*Qk(k)/q(i);
    end
end

a_nm = [0 491.14523 700 700;269.16452 0 58.0 -83.88;700 6.985 0
    -263.518;700 93.97 352.7907 0];
```

123

```
b_nm = [0 0 0 0;0 0 6.985007 0;0 -78637.4 0 168732.6;0 0 -135875.0 0];
c_nm = [0 0 0 0;0 0 0 0;0 0 0 0;0 0 0 0];
R = 8.314;
for m = 1:4
    for k = 1:4
        tao(m,k) = exp(-(a_nm(m,k)+b_nm(m,k)/T+c_nm(m,k)/T^2)/(R*T));
    end
end

beta = e'*tao;

teta1=(xi(1)*q(1)*e(1,1)+xi(2)*q(2)*e(1,2)+xi(3)*q(3)*e(1,3))/(xi(1)*q(1
      )+ xi(2)*q(2)+xi(3)*q(3));
teta2=(xi(1)*q(1)*e(2,1)+xi(2)*q(2)*e(2,2)+xi(3)*q(3)*e(2,3))/(xi(1)*q(1
      )+ xi(2)*q(2)+xi(3)*q(3));
teta3=(xi(1)*q(1)*e(3,1)+xi(2)*q(2)*e(3,2)+xi(3)*q(3)*e(3,3))/(xi(1)*q(1
      )+ xi(2)*q(2)+xi(3)*q(3));
teta4=(xi(1)*q(1)*e(4,1)+xi(2)*q(2)*e(4,2)+xi(3)*q(3)*e(4,3))/(xi(1)*q(1
      )+ xi(2)*q(2)+xi(3)*q(3));

s1 = teta1*tao(1,1)+teta2*tao(2,1)+teta3*tao(3,1)+teta4*tao(4,1);
s2 = teta1*tao(1,2)+teta2*tao(2,2)+teta3*tao(3,2)+teta4*tao(4,2);
s3 = teta1*tao(1,3)+teta2*tao(2,3)+teta3*tao(3,3)+teta4*tao(4,3);
s4 = teta1*tao(1,4)+teta2*tao(2,4)+teta3*tao(3,4)+teta4*tao(4,4);

Ji(1) = r(1)/(r(1)*xi(1)+r(2)*xi(2)+r(3)*xi(3));
Ji(2) = r(2)/(r(1)*xi(1)+r(2)*xi(2)+r(3)*xi(3));
Ji(3) = r(3)/(r(1)*xi(1)+r(2)*xi(2)+r(3)*xi(3));

Li(1) = q(1)/(q(1)*xi(1)+q(2)*xi(2)+q(3)*xi(3));
Li(2) = q(2)/(q(1)*xi(1)+q(2)*xi(2)+q(3)*xi(3));
Li(3) = q(3)/(q(1)*xi(1)+q(2)*xi(2)+q(3)*xi(3));

lngamma_C(1) = 1-Ji(1)+log(Ji(1))-5*q(1)*(1-
Ji(1)/Li(1)+log(Ji(1)/Li(1)));
lngamma_C(2) = 1-Ji(2)+log(Ji(2))-5*q(2)*(1-
Ji(2)/Li(2)+log(Ji(2)/Li(2)));
lngamma_C(3) = 1-Ji(3)+log(Ji(3))-5*q(3)*(1-
Ji(3)/Li(3)+log(Ji(3)/Li(3)));

lngammaR(1) = q(1)*(1-((teta1*beta(1,1)/s1-
      e(1,1)*log(beta(1,1)/s1))+(teta2*beta(1,2)/s2-
      e(2,1)*log(beta(1,2)/s2))+(teta3*beta(1,3)/s3-
      e(3,1)*log(beta(1,3)/s3))+(teta4*beta(1,4)/s4-
      e(4,1)*log(beta(1,4)/s4))));
lngammaR(2) = q(2)*(1-((teta1*beta(2,1)/s1-
      e(1,2)*log(beta(2,1)/s1))+(teta2*beta(2,2)/s2-
      e(2,2)*log(beta(2,2)/s2))+(teta3*beta(2,3)/s3-
      e(3,2)*log(beta(2,3)/s3))+(teta4*beta(2,4)/s4-
      e(4,2)*log(beta(2,4)/s4))));
lngammaR(3) = q(3)*(1-((teta1*beta(3,1)/s1-
      e(1,3)*log(beta(3,1)/s1))+(teta2*beta(3,2)/s2-
      e(2,3)*log(beta(3,2)/s2))+(teta3*beta(3,3)/s3-
      e(3,3)*log(beta(3,3)/s3))+(teta4*beta(3,4)/s4-
      e(4,3)*log(beta(3,4)/s4))));

xsatu(2) = xi(2)/(xi(2)+xi(3));
xsatu(3) = xi(3)/(xi(2)+xi(3));
xsatu = [1e-20 xsatu(2) xsatu(3)];
```

```matlab
teta1satu=(xsatu(1)*q(1)*e(1,1)+xsatu(2)*q(2)*e(1,2)+xsatu(3)*q(3)*e(1,3
        ))/(xsatu(1)*q(1)+xsatu(2)*q(2)+xsatu(3)*q(3));
teta2satu=(xsatu(1)*q(1)*e(2,1)+xsatu(2)*q(2)*e(2,2)+xsatu(3)*q(3)*e(2,3
        ))/(xsatu(1)*q(1)+xsatu(2)*q(2)+xsatu(3)*q(3));
teta3satu=(xsatu(1)*q(1)*e(3,1)+xsatu(2)*q(2)*e(3,2)+xsatu(3)*q(3)*e(3,3
        ))/(xsatu(1)*q(1)+xsatu(2)*q(2)+xsatu(3)*q(3));
teta4satu=(xsatu(1)*q(1)*e(4,1)+xsatu(2)*q(2)*e(4,2)+xsatu(3)*q(3)*e(4,3
        ))/(xsatu(1)*q(1)+xsatu(2)*q(2)+xsatu(3)*q(3));

s1satu=teta1satu*tao(1,1)+teta2satu*tao(2,1)+teta3satu*tao(3,1)+teta4sat
        u*tao(4,1);
s2satu=teta1satu*tao(1,2)+teta2satu*tao(2,2)+teta3satu*tao(3,2)+teta4sat
        u*tao(4,2);
s3satu=teta1satu*tao(1,3)+teta2satu*tao(2,3)+teta3satu*tao(3,3)+teta4sat
        u*tao(4,3);
s4satu=teta1satu*tao(1,4)+teta2satu*tao(2,4)+teta3satu*tao(3,4)+teta4sat
        u*tao(4,4);

Jisatu(1) = r(1)/(r(1)*xsatu(1)+r(2)*xsatu(2)+r(3)*xsatu(3));
Lisatu(1) = q(1)/(q(1)*xsatu(1)+q(2)*xsatu(2)+q(3)*xsatu(3));

lngammaCin(1)=1-Jisatu(1)+log(Jisatu(1))-5*q(1)*(1-
        Jisatu(1)/Lisatu(1)+log(Jisatu(1)/Lisatu(1)));
lngammaRin(1)=q(1)*(1-((teta1satu*beta(1,1)/s1satu-
        e(1,1)*log(beta(1,1)/s1satu))+(teta2satu*beta(1,2)/s2satu-
        e(2,1)*log(beta(1,2)/s2satu))+(teta3satu*beta(1,3)/s3satu-
        e(3,1)*log(beta(1,3)/s3satu))+(teta4satu*beta(1,4)/s4satu-
        e(4,1)*log(beta(1,4)/s4satu))));

gamma_net(1) = exp(lngamma_C(1)+lngammaR(1)-lngammaCin(1)-
lngammaRin(1));
gamma_net(2) = exp(lngamma_C(2)+lngammaR(2));
gamma_net(3) = exp(lngamma_C(3)+lngammaR(3));
gamma_net;

zi = [-1 1 -1 -2 1];
mol = xi.*mol_tot;
C = mol./volume_solvent;


%=======================
% ion:
% 1 = OH-
% 2 = H3O+
% 3 = HCO3-
% 4 = CO3-2
% 5 = MDEAH+
%===============================================================
% MSA
%---------------------------------------------------------------
% input : ion concentration [mol/L]
%         temperature [K]

k_Boltz = 1.38045e-23;  %[J/K]
e_charge = 1.60206e-19; %[coulomb]
Nl = 6.02214178e23;      %[/mol] avogadro number

% dielectric calculation
MR = [18.02 119.2];
n_dens = C.*Nl;
```

```matlab
moltotal = 1;
totalmass = 0;
diel(2) = 24.74+8989.3*(1/T-1/273.15);
Tc = T-273.15;
deltaT = Tc-25;
diel(1) = 78.54*(1-0.0046*deltaT+8.8e-6*deltaT^2);
diel = diel*1e-12;
dielectric = massfrac(1)*diel(1)+massfrac(2)*diel(2);

% ionic strength calculation
Ion_str=1/2*(C(1+3)*(zi(1))^2+C(2+3)*(zi(2))^2+C(3+3)*(zi(3))^2+C(4+3)*(
    zi(4))^2+C(5+3)*(zi(5))^2);

% ionic size calculation (in Angstrom)
Ion_size_Born = [3.0e-10 7.0e-10 30e-10 30e-10 25e-10];
Ion_size = [3.0e-10 3.0e-10 (0.57372177+5.4569945*Ion_str^-
0.45072176)*1e-10 (2.8832274+9.151789*Ion_str^-0.42580691)*1e-10 (-
0.74895748+20.99086/(1+20.99086*0.67916318*Ion_str)+5.4487239/(1+5.44872
39*0.014790757*Ion_str))*1e-10];
%----------------------------------------------------


alffa = 4*pi*e_charge^2/(dielectric*k_Boltz*T);
kappa=alffa*(n_dens(1+3)*(zi(1))^2+n_dens(2+3)*(zi(2))^2+n_dens(3+3)*(zi
    (3))^2+n_dens(4+3)*(zi(4))^2+n_dens(5+3)*(zi(5))^2)^.5;
tato = kappa/2;
%----------------------------------------------------
tolen = 1e-20;
delta_tato = 10;
while delta_tato > tolen
    curl_3 =
pi/6*(n_dens(1+3)*(Ion_size(1))^3+n_dens(2+3)*(Ion_size(2))^3+n_dens(3+3
)*(Ion_size(3))^3+n_dens(4+3)*(Ion_size(4))^3+n_dens(5+3)*(Ion_size(5))^
3);
    delta = 1-curl_3;
    sumforomega = 0;
    for i = 1:5

sumforomega=sumforomega+n_dens(i+3)*(Ion_size(i))^3/(1+tato*Ion_size(i))
;
    end
    omega = 1+pi/(2*delta)*sumforomega;
    sumforPn = 0;
    for i = 1:5

sumforPn=sumforPn+n_dens(i+3)*Ion_size(i)*zi(i)/(1+tato*Ion_size(i));
    end
    Pn = 1/omega*sumforPn;
    sumfortato = 0;
    for i =1:5
        sumfortato=sumfortato+n_dens(i+3)*((zi(i)-
            (pi/2/delta*(Ion_size(i))^2*Pn))/(1+tato*Ion_size(i)))^2;
    end
    tatoold = tato;
    tato = sqrt(alffa^2/4*sumfortato);
    delta_tato = abs((tatoold-tato)/tatoold);
end
%----------------------------------------------------
for i = 1:5
    ai(i) = alffa^2*(zi(i)-
        (pi/2/delta)*(Ion_size(i))^2*Pn)/(2*tato*(1+tato*Ion_size(i)
        )));
```

126

```
        Mi(i) = (2*tato*ai(i)/alffa^2-zi(i))/Ion_size(i);
        ln_gamma_MSA(i) = zi(i)*e_charge^2*Mi(i)/(dielectric*k_Boltz*T)-
                Pn*Ion_size(i)/(4*delta)*(tato*ai(i)+pi/12/delta*alffa^2*Pn*
                Ion_size(i)^2);
end
gamma_MSA = exp(ln_gamma_MSA);
%=====================================================================
% Hard Sphere
curl_0=pi/6*(n_dens(1+3)*(Ion_size(1))^0+n_dens(2+3)*(Ion_size(2))^0+n_d
        ens(3+3)*(Ion_size(3))^0+n_dens(4+3)*(Ion_size(4))^0+n_dens(5+3)*
        (Ion_size(5))^0);
curl_1=pi/6*(n_dens(1+3)*(Ion_size(1))+n_dens(2+3)*(Ion_size(2))+n_dens(
        3+3)*(Ion_size(3))+n_dens(4+3)*(Ion_size(4))+n_dens(5+3)*(Ion_siz
        e(5)));
curl_2=pi/6*(n_dens(1+3)*(Ion_size(1))^2+n_dens(2+3)*(Ion_size(2))^2+n_d
        ens(3+3)*(Ion_size(3))^2+n_dens(4+3)*(Ion_size(4))^2+n_dens(5+3)*
        (Ion_size(5))^2);
curl_3=pi/6*(n_dens(1+3)*(Ion_size(1))^3+n_dens(2+3)*(Ion_size(2))^3+n_d
        ens(3+3)*(Ion_size(3))^3+n_dens(4+3)*(Ion_size(4))^3+n_dens(5+3)*
        (Ion_size(5))^3);
delta = 1-curl_3;
for i = 1:5
    ln_gamma_HS(i)=-
                    log(delta)+((Ion_size(i))^3*curl_0+3*(Ion_size(i))^2*
                    curl_1+3*Ion_size(i)*curl_2)/delta+(3*(Ion_size(i))^3
                    *curl_1*curl_2+9/2*(Ion_size(i))^2*curl_2^2)/delta^2+
                    3*(Ion_size(i))^3*curl_2^3/delta^3;
end
gamma_HS = exp(ln_gamma_HS);
%=====================================================================
% BORN
for i = 1:5
    ln_gamma_Born(i) =
                    e_charge^2/2/k_Boltz/T*(zi(i))^2/Ion_size_Born(i)
                    *(1/dielectric-1/diel(1))*1e-2;
end
T;
gamma_Born = exp(ln_gamma_Born);
for i =1:5
    gamma_ion(i) = gamma_MSA(i)*gamma_HS(i)*gamma_Born(i);
end
gamma_ion;

for i = 4:8
    gamma(i) = gamma_ion(i-3);
end

sum_net = n_dens(1)+n_dens(2)+n_dens(3);
sum_ion = n_dens(4)+n_dens(5)+n_dens(6)+n_dens(7)+n_dens(8);

b = [4.282e5 3.049e5 18.16e5];
for i=1:3
    HS_dia(i) = (b(i)*3/(2*pi*Nl))^(1/3);
    pack_factor(i) = pi*n_dens(i)*(HS_dia(i))^3/6;
    Z_HS(i) = (1+pack_factor(i)+(pack_factor(i))^2-
(pack_factor(i))^3)/(1-pack_factor(i))^3;
end
for i = 1:3
    ln_gamma_GD(i) = 1/sum_net*(tato/3/pi+alffa^2/8*(Pn/delta)^2-
Z_HS(i)*sum_ion);
    gamma_GD(i) = exp(ln_gamma_GD(i));
```

127

```
end

for i = 1:3
    gamma(i) = gamma_net(i)*gamma_GD(i);
end
gamma;
```

M-file HENRY_NG_water_MDEA2

```
function [H_CO2 H_CH4] = HENRY_NG_water_MDEA2(T)
% 1 = CO2
% 2 = CH4
% 3 = H2O
ln_H_T(1) = 110.034525-6789.04/T-11.4519*log(T)-0.010454*T; % in Pa
H_CO2 = exp(ln_H_T(1)); % in Pa
H_CO2 = H_CO2/1e5;

A2 = 0.1305;
B2 = 7.8879e3;
C2 = -1.4196e6;
ln_H_T(2) = A2+B2/T+C2/T^2; % in bar
H_CH4 = exp(ln_H_T(2)); % in bar
```

M-file poynting_solvent_MDEA

```
function poynting_solvent = poynting_solvent_MDEA(T,P)
D1 = [72.55 26.137];
D2 = [-7206.7 -7588.5];
D5 = [-7.1385 0];
D6 = [4.046e-6 0];
D7 = [2 0];
P = P*1e5; %Pa
for i = 1:1
    v_sat = [18.0 115.779]; %cm3/mol
    v_sat(i) = v_sat(i)/1e6; %m3/mol
    ln_P_sat(i) = 16.5362-3985.44/(T-38.9974); %kPa
    P_sat(i) = exp(ln_P_sat(i))*1000; % Pa
    P_satb(i) = P_sat(i)/1e5; % bar

    poynting_solvent(i) = P_satb(i)*exp(v_sat(i)*(P-P_sat(i))/8.314/T);
end
```

M-file poynting_solute_MDEA

```
function poynting_solute = poynting_solute_MDEA(T,P)
%1 = CO2
%2 = H2S
%3 = CH4
a = [74.31498 78.70247 80.1504];
b = [-0.309091 -0.32458 -0.32459];
c = [5.7e-4 6.0e-4 6.102e-4];
D1 = [72.55];
D2 = [-7206.7];
D5 = [-7.1385];
```

```
D6 = [4.046e-6];
D7 = [2];
P = P*1e5; %Pa
for i = 1:3
    v_inf(i) = a(i)+b(i)*T+c(i)*T^2; %cm3/mol
    v_inf(i) = v_inf(i)/1e6; %m3/mol
    ln_P_sat_w = D1+D2/T+D5*log(T)+D6*T^(D7); %Pa
    P_sat_w = exp(ln_P_sat_w); % Pa
    poynting_solute(i) = exp(v_inf(i)*(P-P_sat_w)/8.324/T);
end
```

M-file PR_NG_MDEA_CO2_H2O

```
function fug_coeff_v = PR_NG_MDEA_CO2_H2O(y,P,T)

% System CO2-H2O
% 1 = CO2
% 2 = H2O

Tc = [304.19 647.13]; % [K]
Pc = [73.82e5 220.55e5]; % [pa]
w = [0.228 0.345];
R = 8.314; % [J/mol K] or [m3 Pa/mol K]
P = P*1e5;
for i = 1:2
    Tr(i) = T/Tc(i);
    k(i) = 0.37464+1.54226*w(i)-0.26992*w(i)^2;
    alfa(i) = (1+k(i)*(1-sqrt(Tr(i))))^2;
    a_i(i) = 0.45724*R^2*Tc(i)^2/Pc(i)*alfa(i);
    b_i(i) = 0.077796*R*Tc(i)/Pc(i);
    A(i) = a_i(i)*P/(R^2*T^2);
    B(i) = b_i(i)*P/(R*T);
end
mij = 1.224-0.0044*T+3.251e-5*T^2;
for i = 1:2
    for j = 1:2
        Al(i,j) = sqrt(A(i)*A(j));
    end
end
Al;
A_mix = y*Al*y';
B_mix = y*B';

z1 = 1;
z2 = -(1-B_mix);
z3 = A_mix-3*B_mix^2-2*B_mix;
z4 = -(A_mix*B_mix-B_mix^2-B_mix^3);

zroot = roots([z1 z2 z3 z4]);
zroot = real(zroot);
z = max(zroot);
fug_coeff_v(1) = exp(-log(z-B_mix)+B(1)/B_mix*(z-1)-
        A_mix/(2*B_mix*sqrt(2))*(log((z+(1+sqrt(2))*B_mix)/(z+(1-
        sqrt(2))*B_mix)))*(2*(y(1)*Al(1,1)+y(2)*Al(1,2))/A_mix-
        B(1)/B_mix));
fug_coeff_v(2) = exp(-log(z-B_mix)+B(2)/B_mix*(z-1)-
        A_mix/(2*B_mix*sqrt(2))*(log((z+(1+sqrt(2))*B_mix)/(z+(1-
        sqrt(2))*B_mix)))*(2*(y(1)*Al(2,1)+y(2)*Al(2,2))/A_mix-
        B(2)/B_mix));
```